ME571/GEOL571 GEOLOGY AND ECONOMICS OF STRATEGIC AND CRITICAL MINERALS COMMODITIES: REE

Virginia T. McLemore

ASSIGNMENT

- Midterm due March 19, 2013 by e-mail ginger@nmbg.nmt.edu
- Castor, S.B., 2008, The Mountain Pass rare-earth carbonatite and associated ultrapotassic rocks, California: The Canadian Mineralogist, v. 46, p. 779-806, http://canmin.geoscienceworld.org/content/46/4/779.full.pdf+html?sid=180ae325-acd5-4226-9a02-175f7a865e17
- Long, K.R., van Gosen, B.S., Foley, N.K. and Cordier, D., 2010, The principle rare earth elements deposits of the United States—A summary of domestic deposits and a global perspective: U.S. Geological Survey, Scientific Investigations Report 2010-5220, 104 p., http://pubs.usgs.gov/sir/2010/5220/ (accessed 5/1/12).
- Mariano and Mariano, 2012, Rare earth mining and exploration in North America: Elements, v. 8, 369-376, http://elements.geoscienceworld.org/content/8/5/369.full.pdf+html?sid=605ebd04-9070-4994-9bce-b1cdd79f349d

Eldorado faces more Greek protests

Anthony Halley | **March 5, 2013**

Thousands in the northern, historic Greek region of Thrace were out in the streets today to protest Vancouver-based Eldorado Gold's Perama Hill mining project.

The protest comes just two weeks after a violent attack on an Eldorado mine site in Halkidiki.

Click here to see photos of today's protest.

About Perama Hill:

The Perama Hill gold project is a late-stage development project in Thrace, Greece. The property consists of two mining titles covering an area of 1,897.5 ha, and two mining exploration licenses covering an area of 1,762.7 ha.

Processing of the Environmental Impact Assessment (EIA) application through the Greek Ministry of Environment (MoE) continues with approval anticipated during the first quarter of 2013.

Estimated development capital is $189 million. Upon receipt of all permits and licenses Eldorado will make a construction decision. Production is expected in 2015.

TYPES OF REE DEPOSITS

TYPES OF REE DEPOSITS

- Alkaline/peralkaline Igneous Rocks
- Carbonatites
- Pegmatites
- Iron oxide Cu-Au (REE)
  - Magnetite ore bodies
- Porphyry Mo
- Metamorphic/ metasomatic
- Paleoplacer/placer/ beach sands
- Colluvial REE
- Residual
  - Stratiform phosphate residual
  - Ion adsorption clays/laterite/bauxite
- REE-Th-U Hydrothermal Veins
- Unconformity uranium deposits
- Quartz-pebble conglomerate deposits
- Collapse breccia pipes
- Sea floor muds
- Other REE-Bearing Deposits

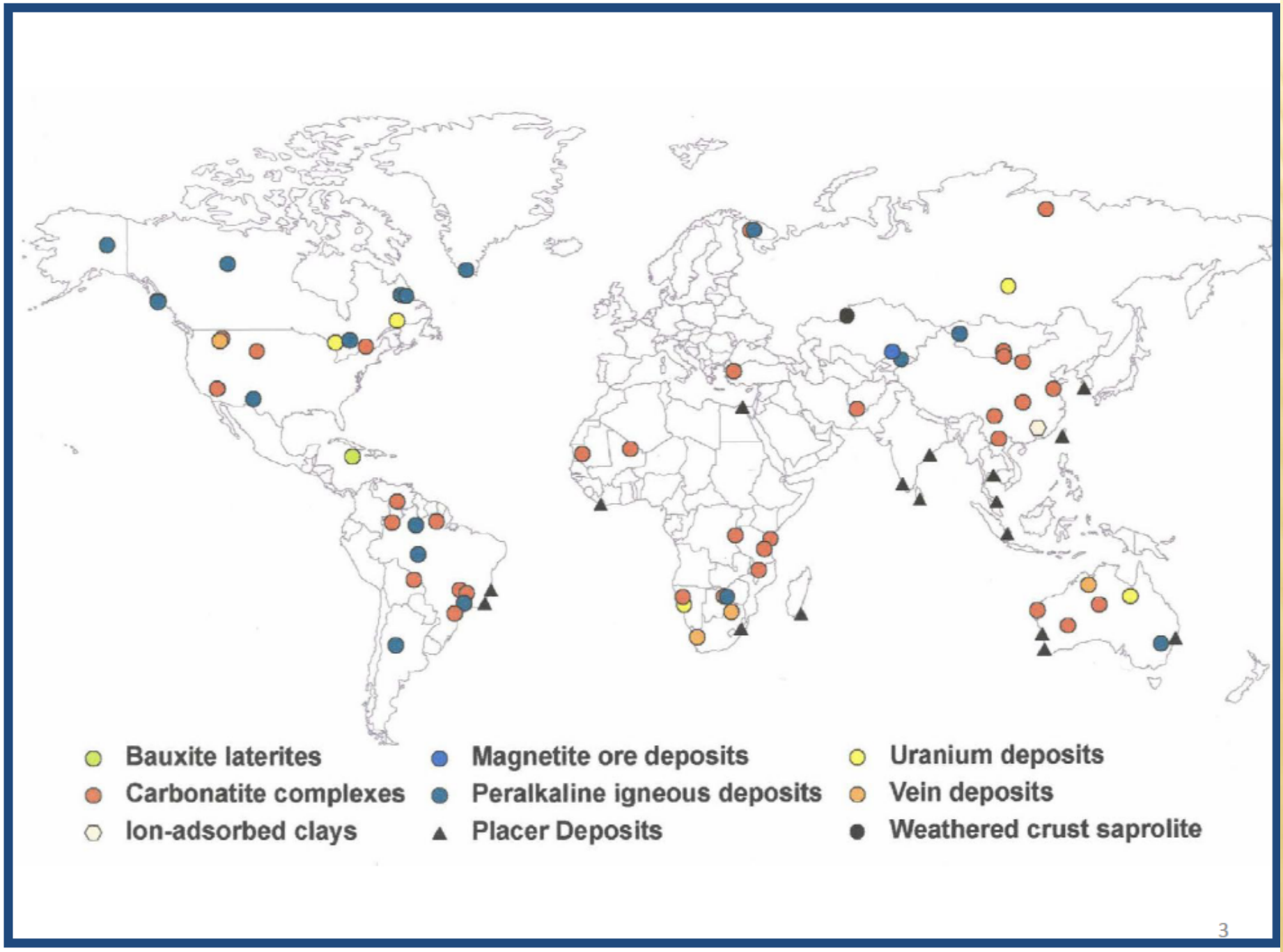

http://www.adimb.com.br/simexmin2012/wp-content/themes/simexmin/palestras/06terras/VII_1_Mariano.pdf

PEGMATITES

>551 pegmatites

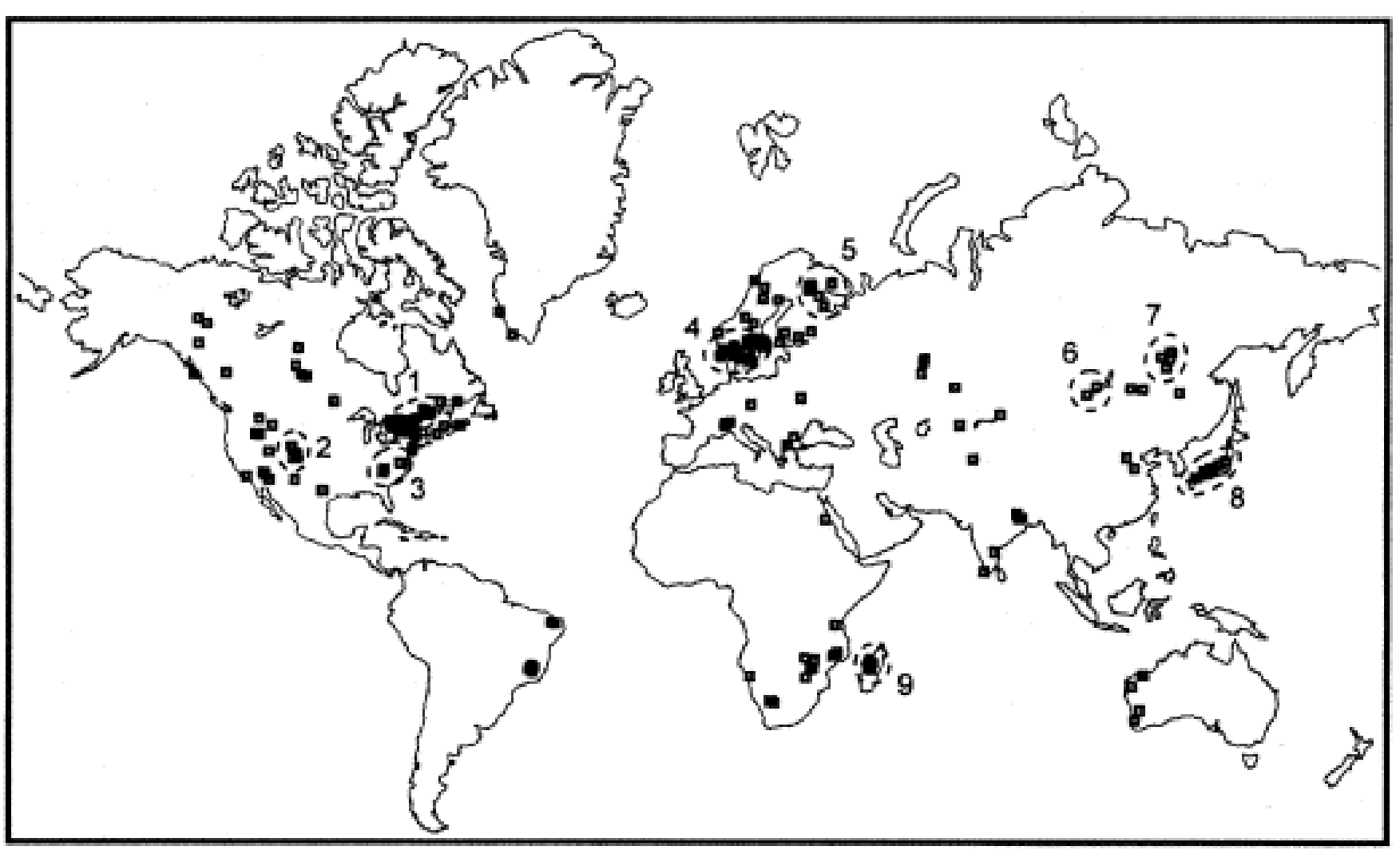

PEGMATITES

- “an essentially igneous rock, commonly of granitic composition, that is distinguished from other igneous rocks by its extremely coarse but variable grain-size, or by an abundance of crystals with skeletal, graphic, or other strongly directional growth-habits.” (London, 2008)
- Products of magmatic differentiation, residual parts of the magma
- Increased volatiles and incompatible elements (large ionic radii)

PEGMATITES

- Dikes, sills, veins, irregular masses
- In part due to slow cooling
- Grade into aplites, which formed if the magma losses suddenly the volatiles and only small crystals grow
- mostly due to large volumes of gases (volatiles =H20, Cl, F)
  - Make it difficult for crystals to form=fewer crystals
  - Makes the normally sticky granitic magma more viscous, which allows for elements to move around
  - Volatiles separate as bubbles surrounded by normal liquid magma and crystals can form from both

TYPES

- Acidic pegmatites or granitic pegmatites
- Syenitic pegmatites (Na rich with little quartz)
- Basic and ultrabasic (feldspar, olivine, amphibole, biotite)

Table 1: The three petrogenetic families of rare element pegmatites, based on geochemical criteria, and different crustal sources of rare elements (adapted from Cerny, 1993; Cerny and Ercit, 2005). Peralkaline pegmatites are not included in this schema.

Family	*Dominant Pegmatite Subclasses*	*Geochemical Signature*	*Pegmatite Bulk Composition*	*Associated Granites Bulk Composition*	*Source Lithologies*
LCT	REL-Li MI-Li	**Li**,Rb, **Cs**,Be,Sn,Ga **Ta** > Nb(B,P,F)	peraluminous	mostly late orogenic; S,I or mixed S+I types	undepleted upper-to middle-crust supracrustals and basement gneisses
NYF	REL-REE MI-REE	**Nb** > Ta,Ti, **Y**,Sc,REE, Zr,U,Th, **F**	subaluminous-metaluminous (to subalkaline)	mostly anorogenic; A and (I) types	depleted middle to lower crustal granulites, or undepleted juvenile granitoids
Mixed	"Cross-bred" LCT and NYF	mixed	(metaluminous to) moderately peraluminous	(postorogenic to) anorogenic; mixed geochemical signature	Mixed protoliths; or assimilation of supracrustals by A(or I) type granites

Definitions: peraluminous A/CNK>1; subaluminous A/CNK~1; metaluminous A/CNK<1 and A/NK>1; subalkaline A/NK~1, where A = molecular Al_2O_3, CNK = Ca_2O + Na_2O + K_2O, and NK = Na_2O + K_2O
REL = Rare element pegmatite class, MI = miarolitic pegmatite class

Table 2: Summary of characteristic differences between LCT and NYF petrogenetic pegmatite family endmembers (adapted from Vanstone, 2010).

	LCT (***L***ithium-***C***aesium-***T***antalum)	**NYF** (***N***iobium-***Y***ttrium-***F***luorine)
Relationship to source granites	• Pegmatitic granite phase is required for pegmatite development. • Typically forms part of regional zonation pattern	• No pegmatitic granite phase • Mostly lack of regional zonation patterns
Chemical signature	• Ta > Nb • (Very) low REE contents • Enriched in boron and alkali elements. • Sn content can equal Ta content. • U and Th levels tend to be low.	• Nb > Ta • Enriched in the light and heavy rare earth elements (REE's). • Sn is not commonly enriched. • May be enriched in U and Th.
Mineralogy	• Fluorite is rare (F bound in topaz, lepidolite, amblygonite) • Lithium and phosphate minerals are common. • Tourmaline is common • Generally simple Ta-Nb oxides ± Sn without essential REE • Beryl can be present	• Fluorite is common • Lithium and phosphate minerals are rare • Tourmaline is relatively rare; restricted compositional range • Complex oxides of Nb, Ta and REE's, viz., euxenite, fergusonite, samarskite, aeschynite mineral groups • Beryl can be present.
Western Australian pegmatite examples*	Wodgina district, Pilbara Craton Tabba Tabba field, Pilbara Craton Greenbushes field, Yilgarn Craton Londonderry district, Yilgarn Craton	Cooglegong district, Pilbara Craton Abydos district, Pilbara Craton Mukinbudin district, Yilgarn Craton Fraser Range group, Albany Fraser Orogen

*Principal references for examples: Sweetapple and Collins (2002); Jacobsen et al. (2007)

Figure 1. World map showing the locations of LCT pegmatite deposits or districts, including smaller districts in the United States. The symbols are color-coded by age. Giant deposits are represented by larger symbols.

USGS OF13-1008

Blocky Potassium Feldspar at southeast contact of pegmatite

Lithian muscovite veins cutting blocky potassium feldspar white beryl to right of scale card

http://www.nwopa.net/symposium/nwomms2010/05_PegmatitesRedLake.pdf

White albite veins in quartz-spodumene zone

SQUI (spodumene-quartz intergrowth) with blocky blue potassium feldspar

http://www.nwopa.net/symposium/nwomms2010/05_PegmatitesRedLake.pdf

PEGMATITES

coarse-grained igneous rocks, lenses, or veins with granitic composition, contains essential quartz and feldspar, and represent the last and most hydrous phase of crystallizing magmas

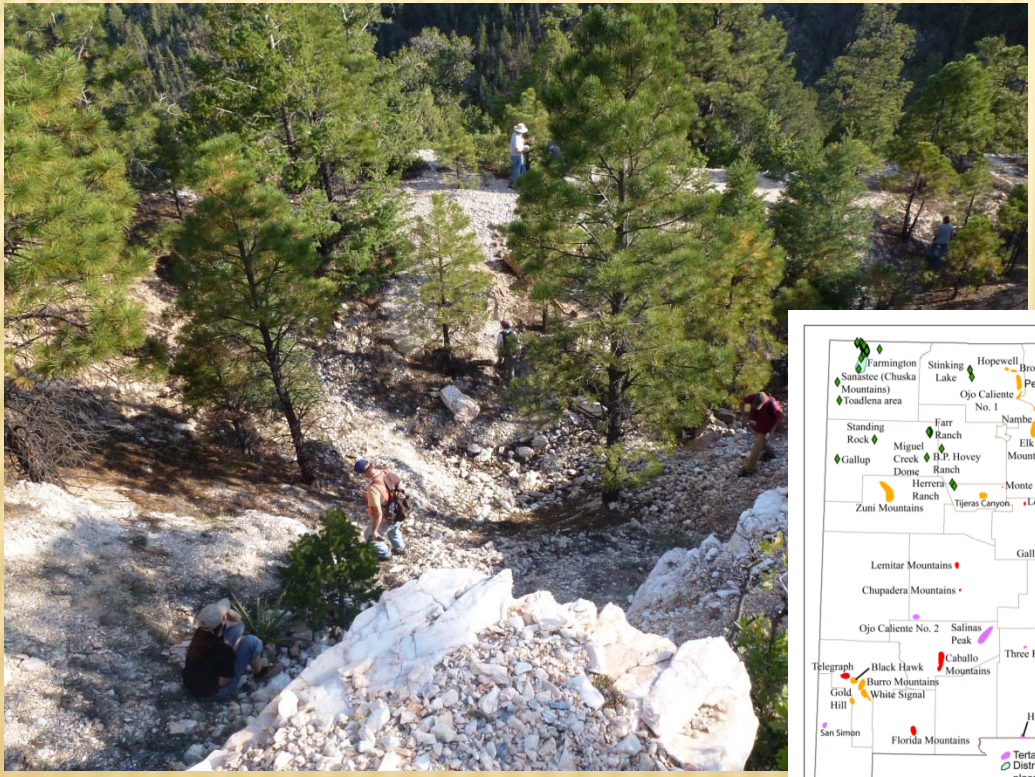

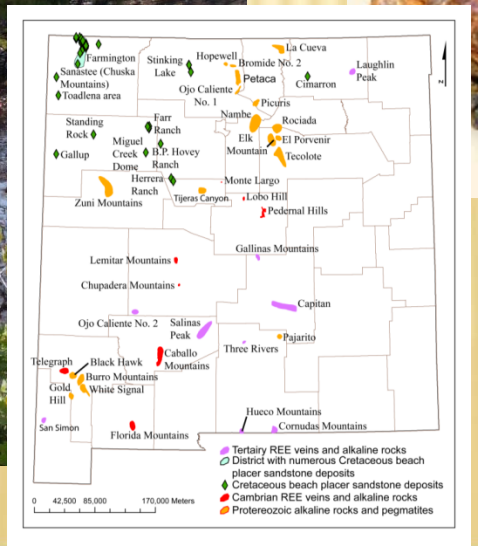

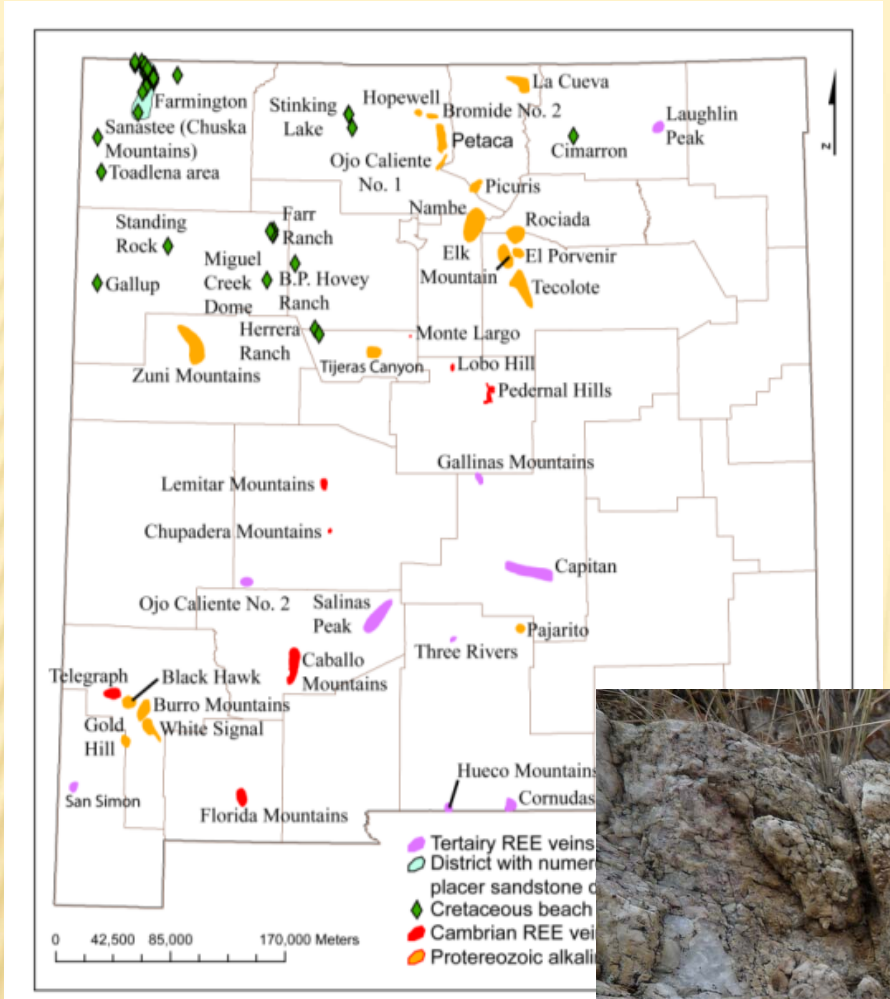

PEGMATITES

- Petaca
- Burro
- Mountains

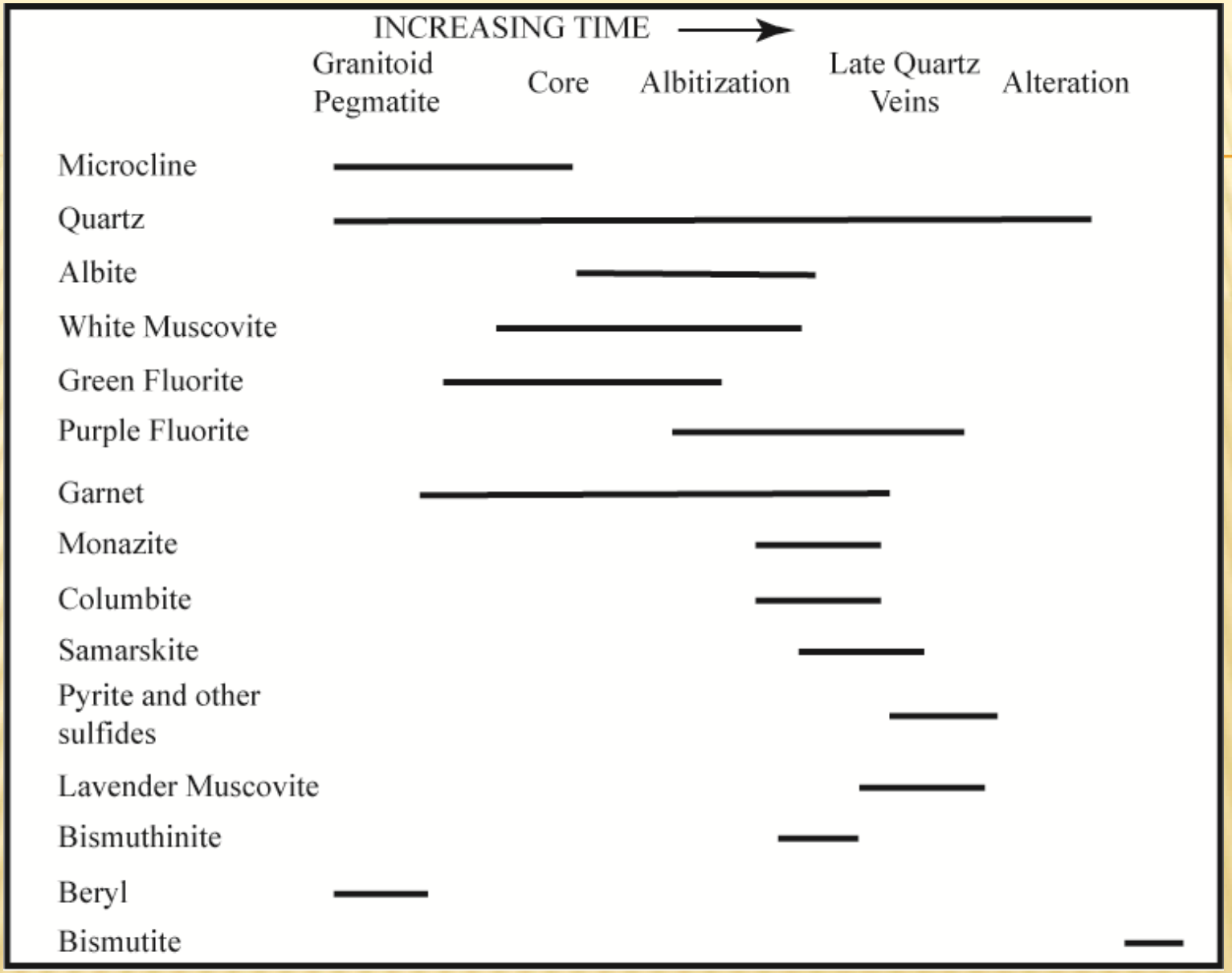

PARAGENESIS, GLOBE PEGMATITE (PETACA)

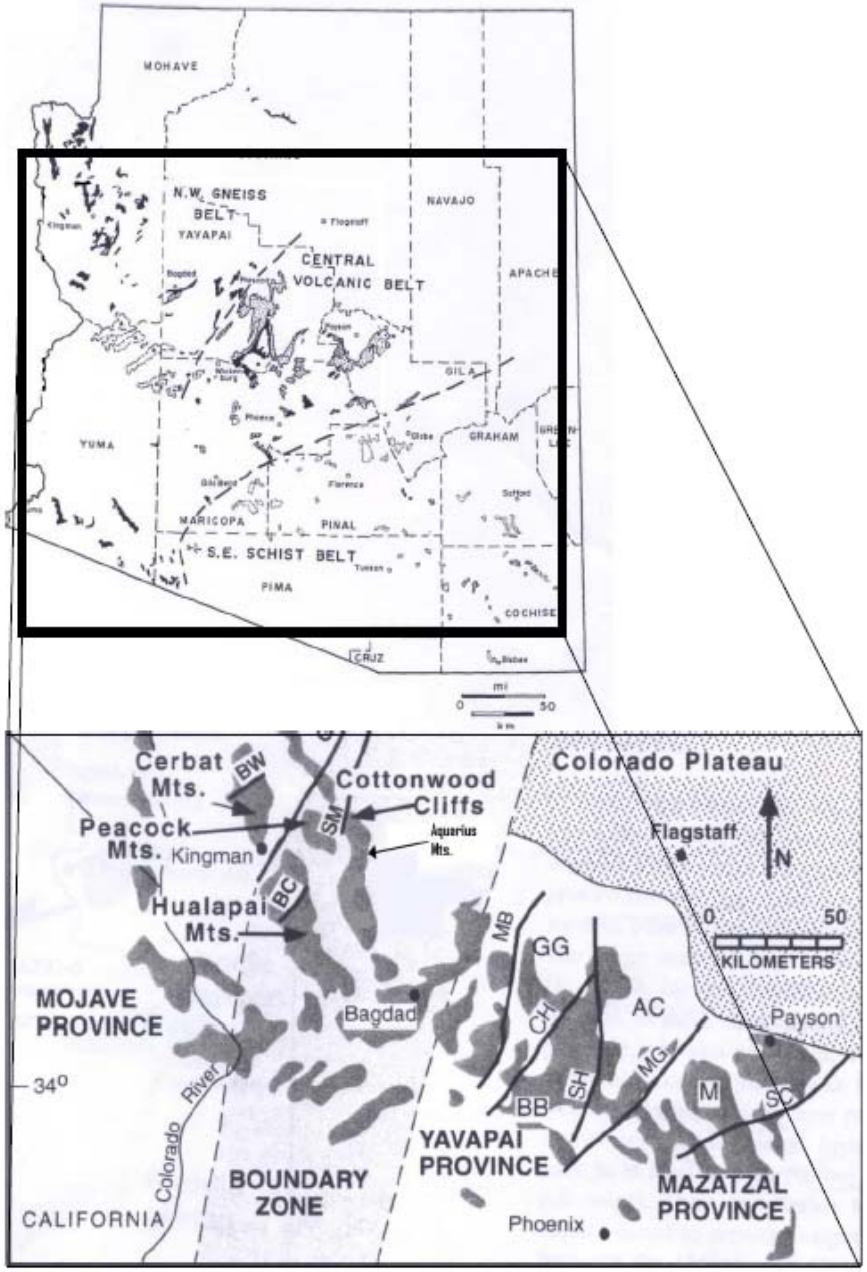

Figure 1a. Arizona state map, modified from Anderson (1989), with study area pulled out, modified from Duebendorfer (2001)

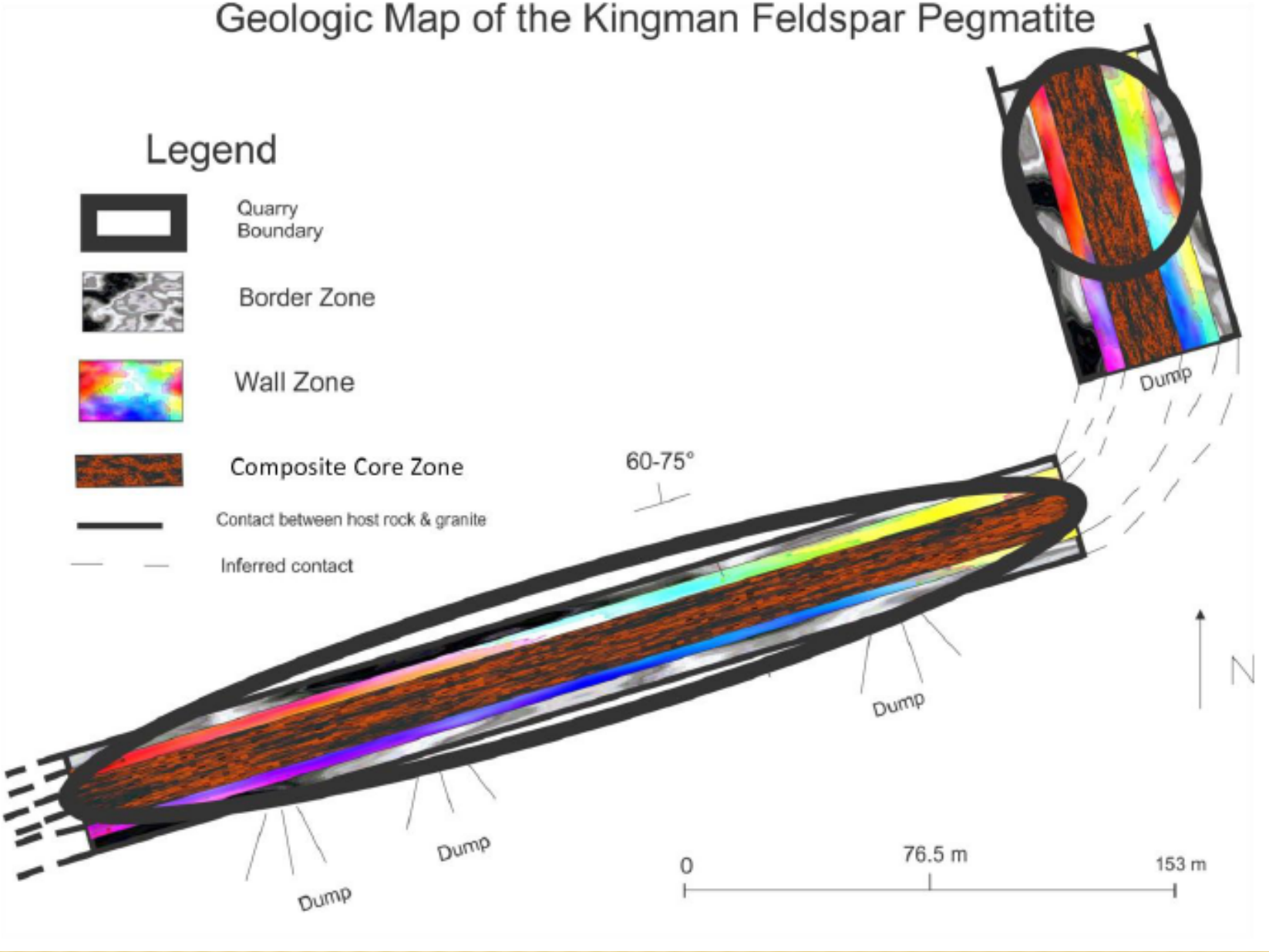

Figure 3. Idealized geologic map of the Kingman Feldspar

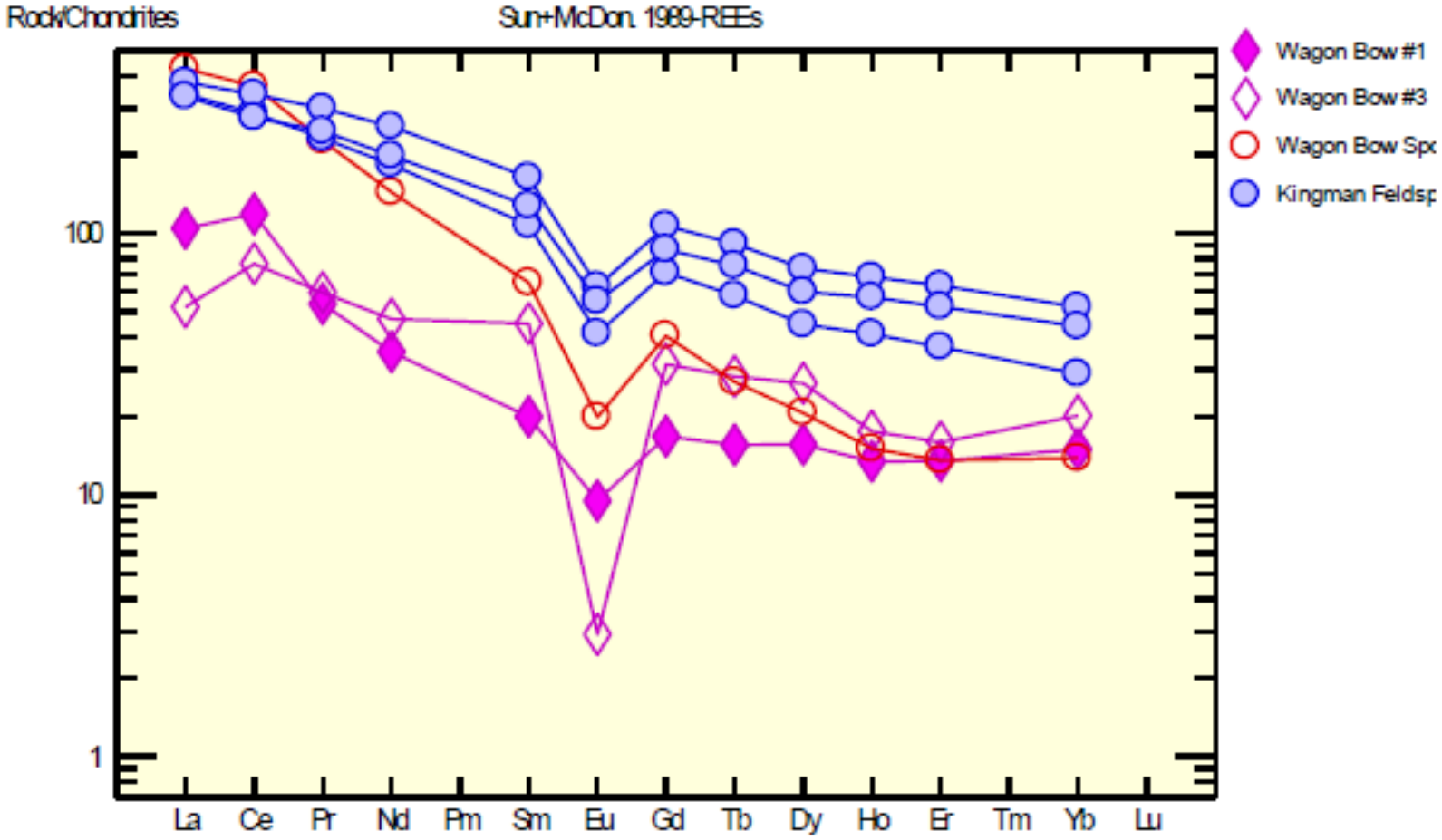

Figure 47. Chondrite diagram showing LREE enrichment trend and negative Eu anomaly, noticeably in the Wagon Bow #3 granite.

http://scholarworks.uno.edu/cgi/viewcontent.cgi?article=2263&context=td

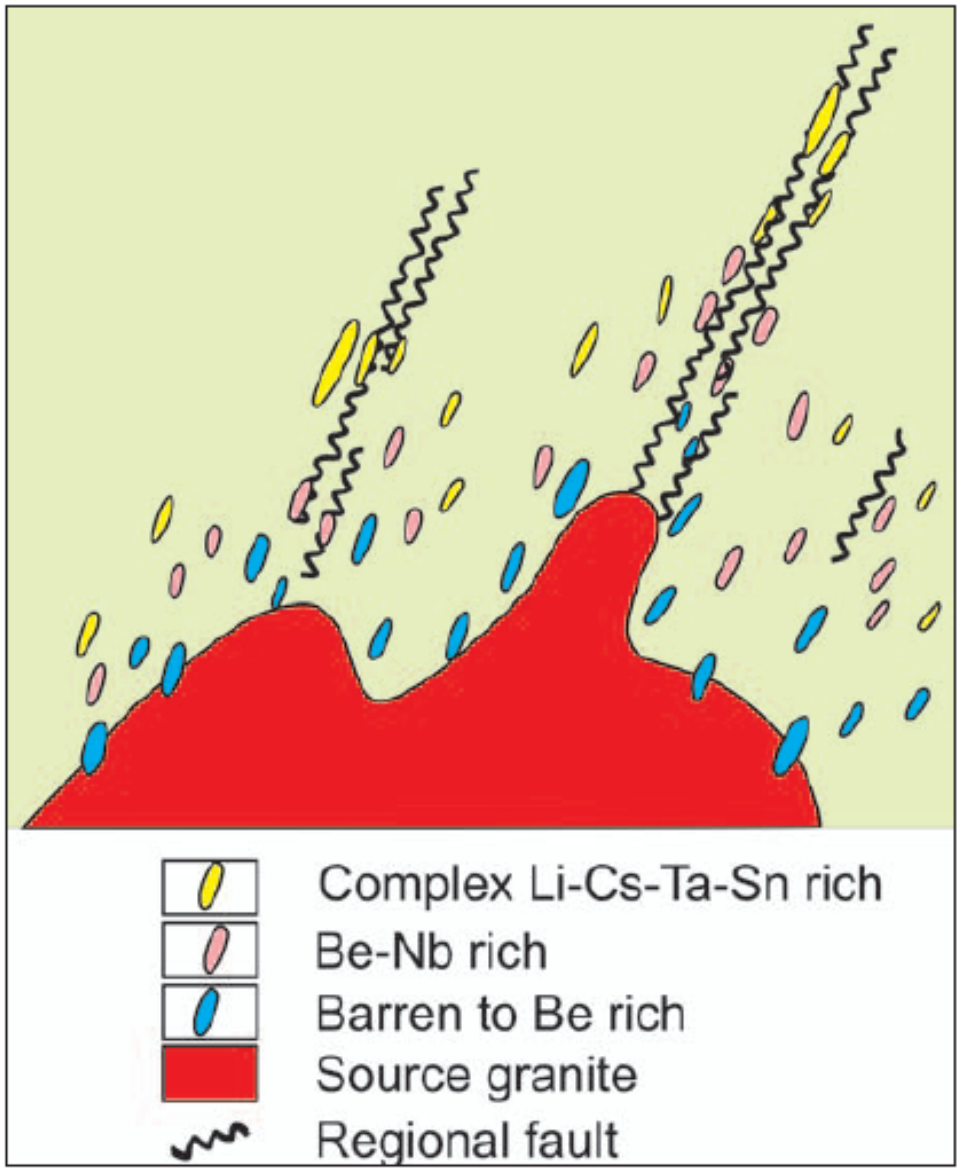

FIGURE 1 Idealized zoned pegmatite field around a source granite. The maximum distance of pegmatites from the source granite is on the order of kilometers or, at most, tens of kilometers. MODIFIED FROM ČERNÝ (1989)

http://web.mit.edu/12.000/www/m2016/pdf/pegmatites_strategic_metals.pdf

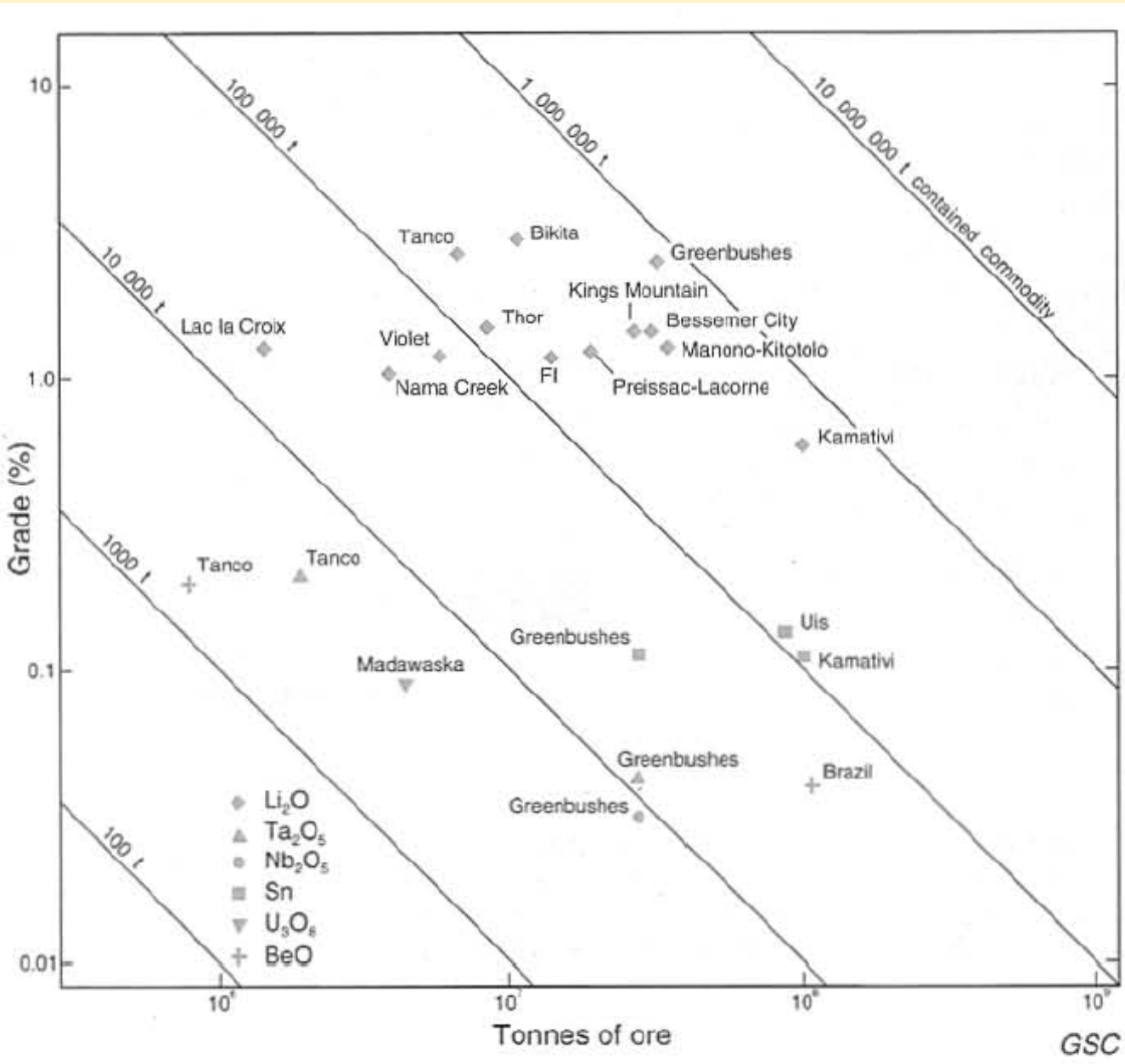

Figure 21-2. Grade versus tonnage diagram for pegmatite deposits (data are from Table 21-2).

SINCLAIR, 1996

IRON OXIDE-COPPER-GOLD (IOCG) DEPOSITS

IRON OXIDE-COPPER-GOLD (IOCG) DEPOSITS

wide spectrum of S-deficient low-Ti magnetite and/or hematite ore bodies of hydrothermal origin where breccias, veins, disseminations and massive lenses with polymetallic enrichments (Cu, Au, Ag, U, REE, Bi, Co, Nb, P) are genetically associated with, but either proximal or distal to largescale continental, A- to I-type magmatism, alkaline-carbonatite stocks, and crustal-scale fault zones and splays (Corriveau)

IRON OXIDE-COPPER-GOLD (IOCG) DEPOSITS

- Known as
  - Olympic Dam deposit
  - hematite-rich granite breccia
  - Metasomatic skarns
  - Magmatic magnetite-hematite bodies
  - Magnetite ore bodies
- Enriched in Fe, Cu, U, Au, Ag, REE s (mainly La and Ce) and F
- hydraulic fracturing, tectonic faulting, chemical corrosion, and gravity collapse

IRON OXIDE-COPPER-GOLD (IOCG) DEPOSITS

- at the margins of large igneous bodies which intrude into sedimentary strata
- form pipe-like, mantle-like or extensive breccia-vein sheets
- associated with distal zones of particular large-scale igneous events

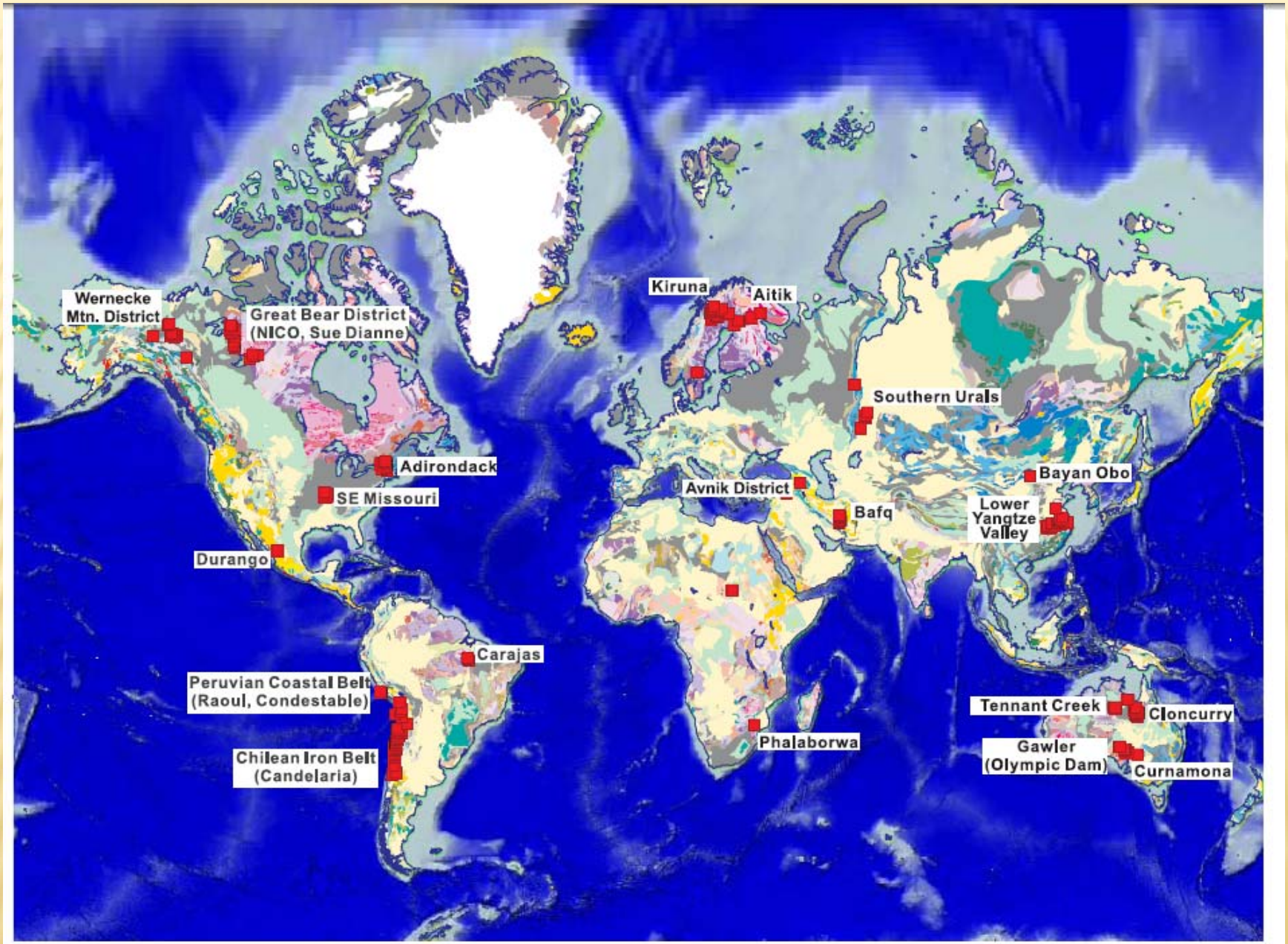

Fig. 1. Distribution of IOCG districts and important deposits worldwide (red dots). Australia: Gawler (Olympic Dam, Acropolis, Moonta, Oak Dam,

http://kenanaonline.com/files/0040/40858/deposit_synthesis.iocg.corriveau.pdf

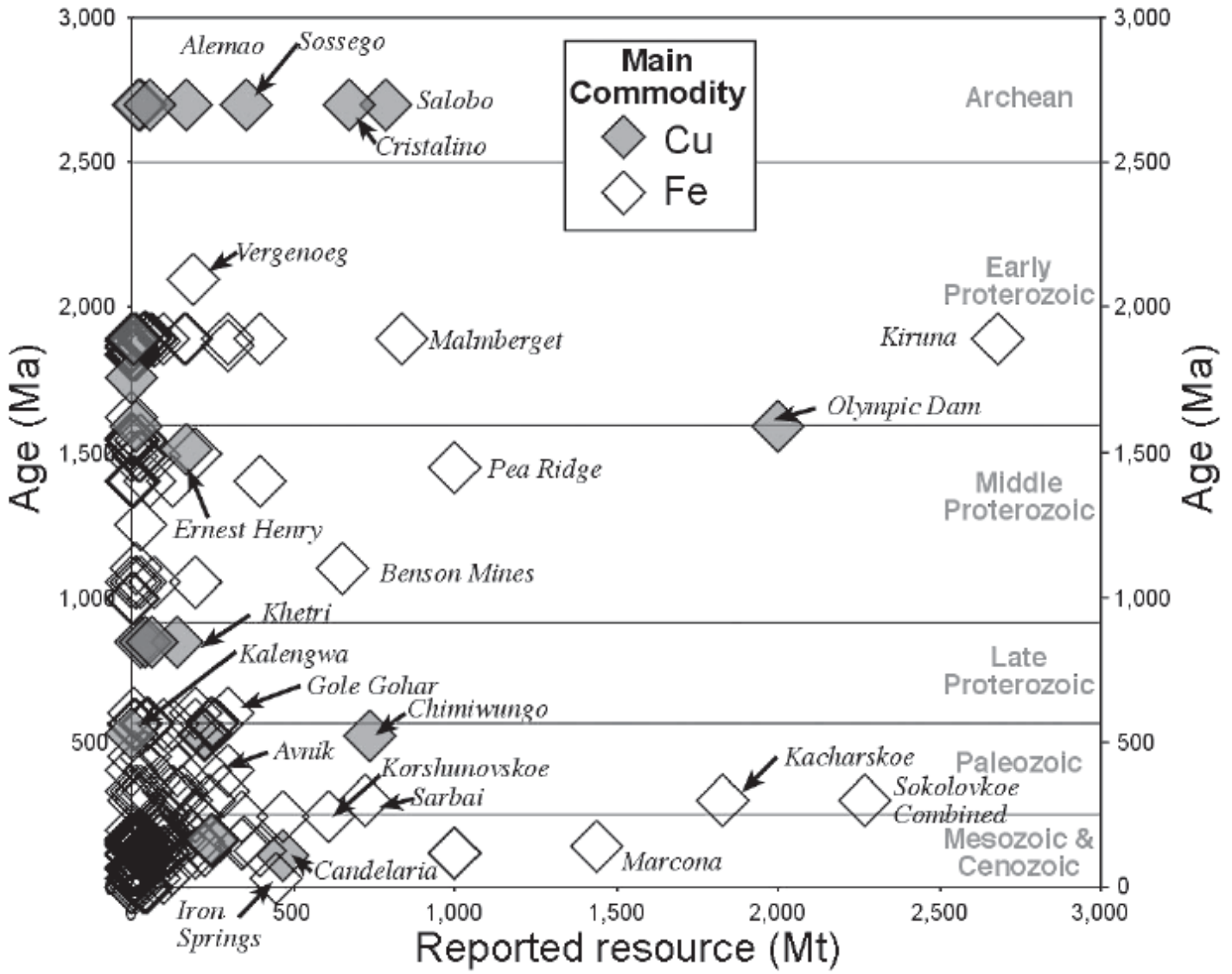

FIG. 2. Age distribution of IOCG deposits and Fe oxide deposits (mainly magnetite-apatite and Fe skarn; cf. Barton and Johnson, 1996), divided on the basis of the main commodity recovered (Cu or Fe). Ages for provinces are summarized in Table A1; deposit data are derived from publicly available data (D.A. Johnson and M.D. Barton, unpub. compilation).

http://www.unige.ch/sciences/terre/mineral/publications/onlinepub/williams_ironoxidecoppergold_seg05.pdf

Table 1. Size and Grade of Selected IOCG Deposits

Deposit	Tonnes ($\times 10^6$)	Commodity	Grade	Associated Metals	Mineralization Styles
		Magmatic End-Member IOCG			
Lightning Creek[1]	–	Cu (%) Au (g/t)	minor minor	–	Qz-Mt ± Py ± chalcopyrite veins
Eloise[2]	3.2	Cu (%) Au (g/t) Ag (g/t)	5.8 1.5 19	Co, Ni, Zn, As, Bi	Veins, stockwork veins, massive sulfide
		Hybrid Magmatic–Non-Magmatic IOCG			
Olympic Dam[3]	2320	Cu (%) Au (g/t) Ag (g/t) U_3O_8 (kg/t)	1.3 0.5 2.9 0.4	Co, REE (dominantly La and Ce), Ni, As	Disseminations, veinlets, and fragments within breccia zones, primarily within breccia matrix
Aitik[4]	800	Cu (%) Au (g/t) Ag (g/t)	0.3 0.2 2	Mo	Disseminations and veins
Candelaria[5]	470	Cu (%) Au (g/t) Ag (g/t)	.95 .22 3.1	Zn, Mo, As, LREE	Vein, breccia-hosted, mantos, overprints Mt replacement bodies
Salobo[6]	450	Cu (%) Au (g/t)	1.15 0.5	Ag, U, Co, Mo, F, LREE	Lenses, veins
Ernest Henry[7]	166	Cu (%) Au (g/t)	1.1 0.54	Co, Mo, U, REE, F, Mn, As, Ba	In breccia
		Non-Magmatic End-Member IOCG			
Wernecke Breccia[8]	Slab: 20	Cu (%)	0.35	U, Co, Mo	Disseminations, veins, breccia infill
Tennant Creek[9]	West Peko: 3.2 Eldorado: 0.0292	Cu (%) Au (g/t)	4 20.8	Bi	Massive and vein mineralization overprinting ironstone
Redbank[10]	Bluff: 2 Sandy Flat: 1.5	Cu (%) Cu (5)	1.66 2	Pb, Zn, REE	Breccia infill, veins, disseminations

http://www.sfu.ca/~dthorkel/linked/hunt%20et%20al.,%20rev%20iocg_s%202007.pdf

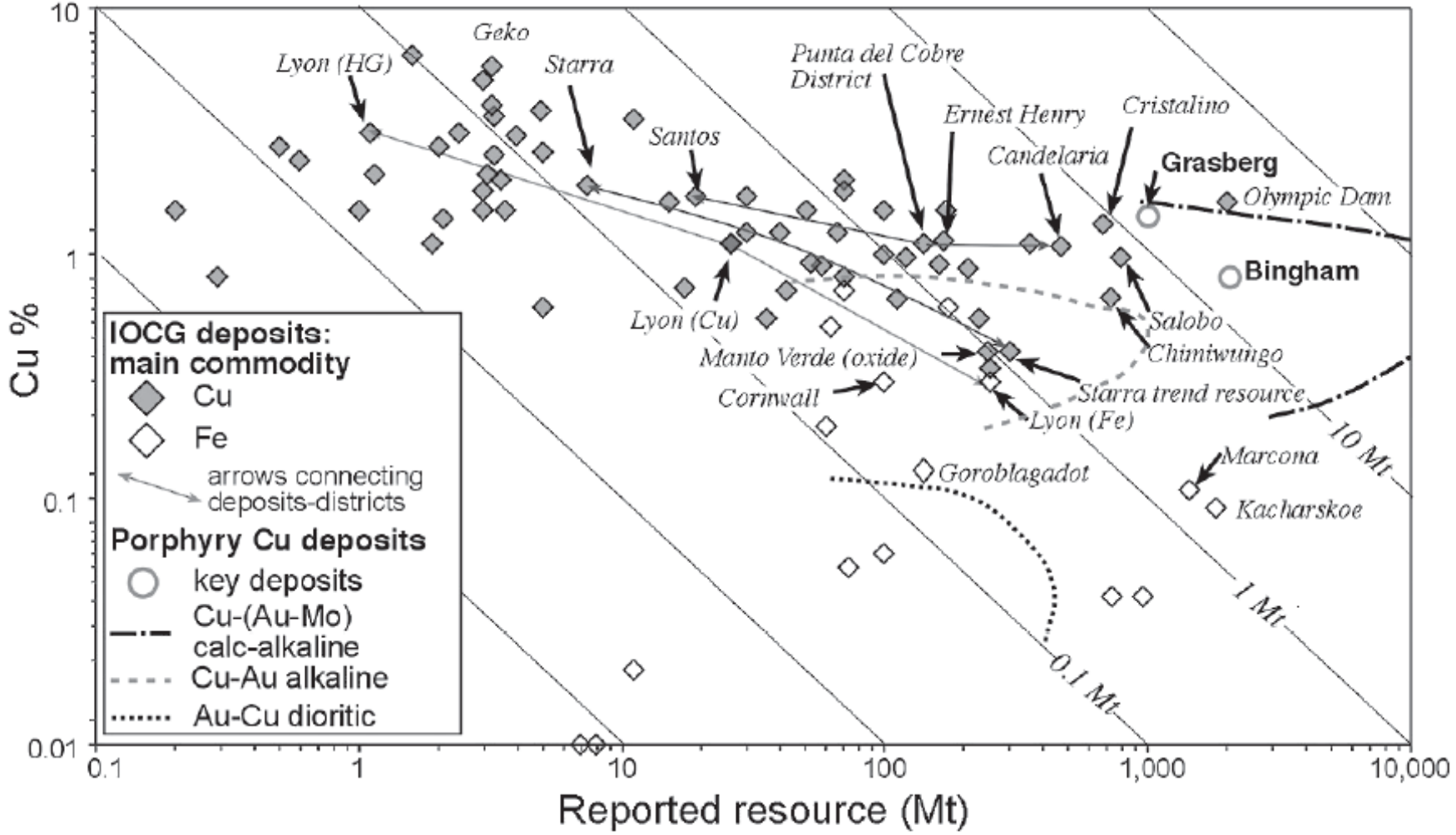

FIG. 3. Grade-tonnage data showing Cu grades for Fe oxide (mainly magnetite-apatite and skarn) and Fe oxide-Cu–rich hydrothermal systems (D.A. Johnson and M.D. Barton, unpub. compilation). Note the arrows connecting various resource categories (deposits and ore types) within the same districts. These data are skewed by the principal commodity produced and by the scarcity of representative Cu data for Fe-producing deposits. Also shown are fields for several types of porphyry Cu-Au–rich systems (modified from Seedorff et al., 2005).

http://www.unige.ch/sciences/terre/mineral/publications/onlinepub/williams_ironoxidecoppergold_seg05.pdf

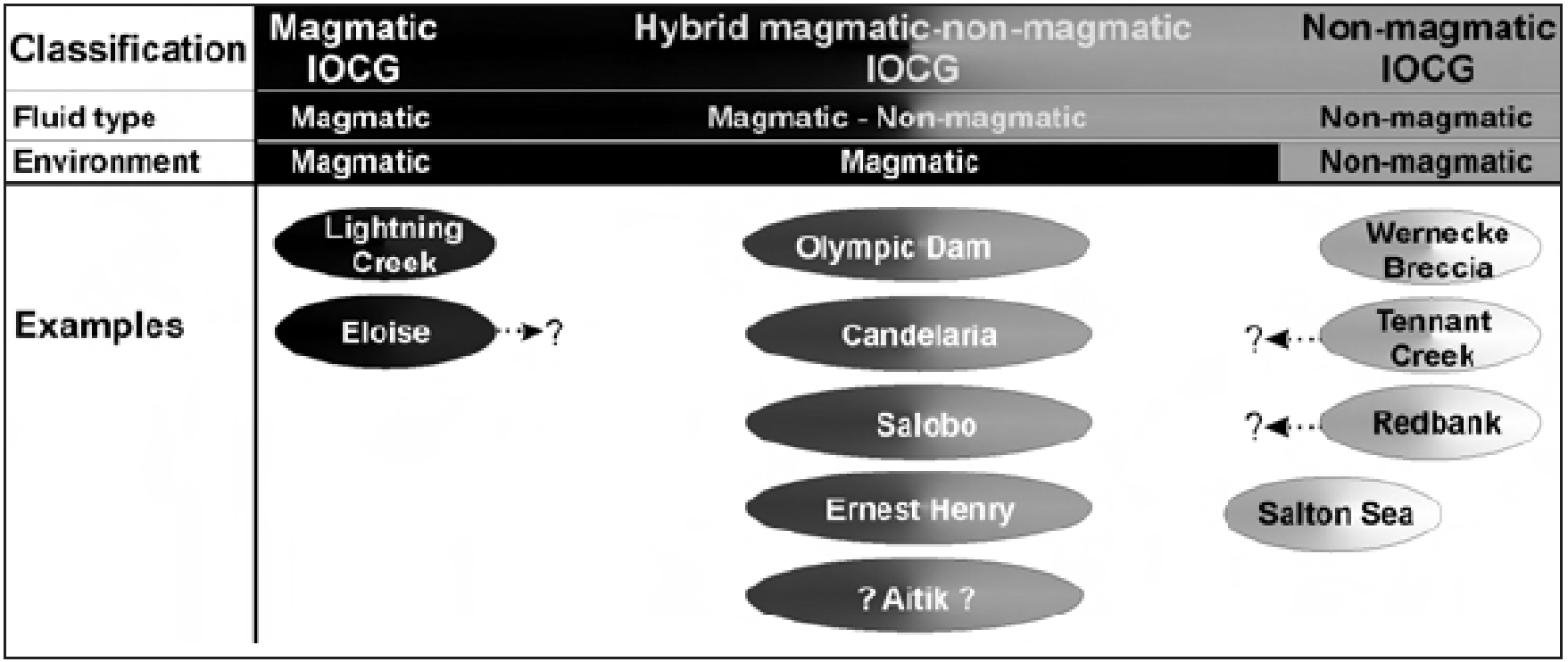

Fig. 7. Suggested classification of IOCG systems into magmatic and non-magmatic end members, with hybrid IOCG systems in between. Also shown are examples for each IOCG category. See text for discussion and references.

http://www.sfu.ca/~dthorkel/linked/hunt%20et%20al.,%20rev%20iocg_s%202007.pdf

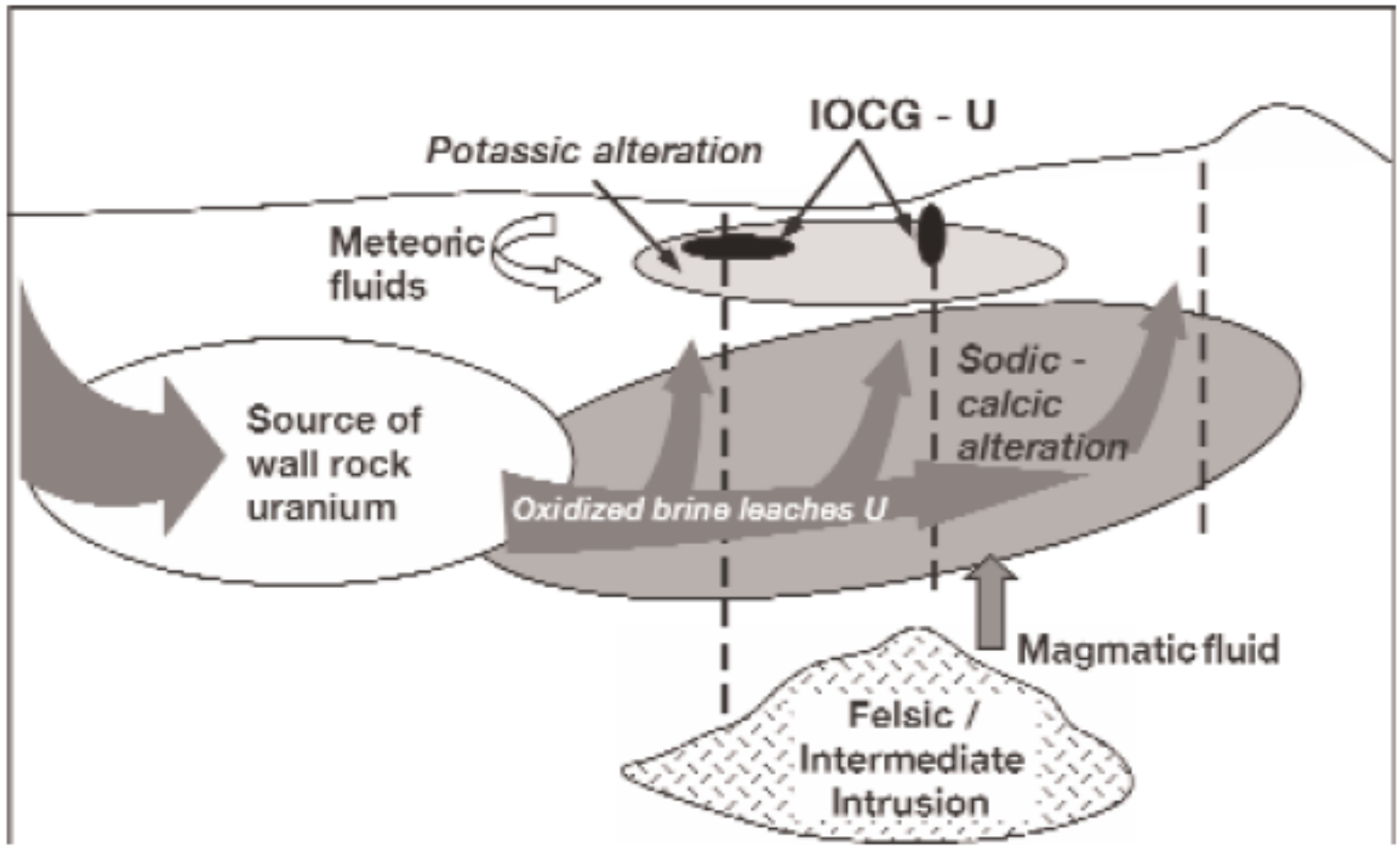

FIG. 2. Schematic model for the formation of uranium-rich IOCG deposits. In this model, uranium-rich IOCG deposits probably require a rich source of wall-rock uranium within the host-rock sequence altered as part of the IOCG system. Additional uranium could also be contributed by magmatic or meteoric fluids.

HITZMAN AND VALENTA, 2005, *ECONOMIC GEOLOGY*, V. 100, PP. 1657–1661

OLYMPIC DAM DEPOSIT IN AUSTRALIA

OLYMPIC DAM DEPOSIT IN AUSTRALIA

- Discovered 1975
- production for Cu 1988
- Underground mine, BHP Billiton
- Measured resource of 650 million tons (Mt) of 500 g/t U_3O_8 (425 ppm U), 1.5 percent Cu, and 0.5 g/t Au
- Total resource approximately 3.8 billion tons of 400 g/t U_3O_8 (339 ppm U), 1.1 percent Cu, and 0.5 g/t Au.

Hitzman and Valenta, 2005, *Economic Geology,* v. 100, pp. 1657–1661

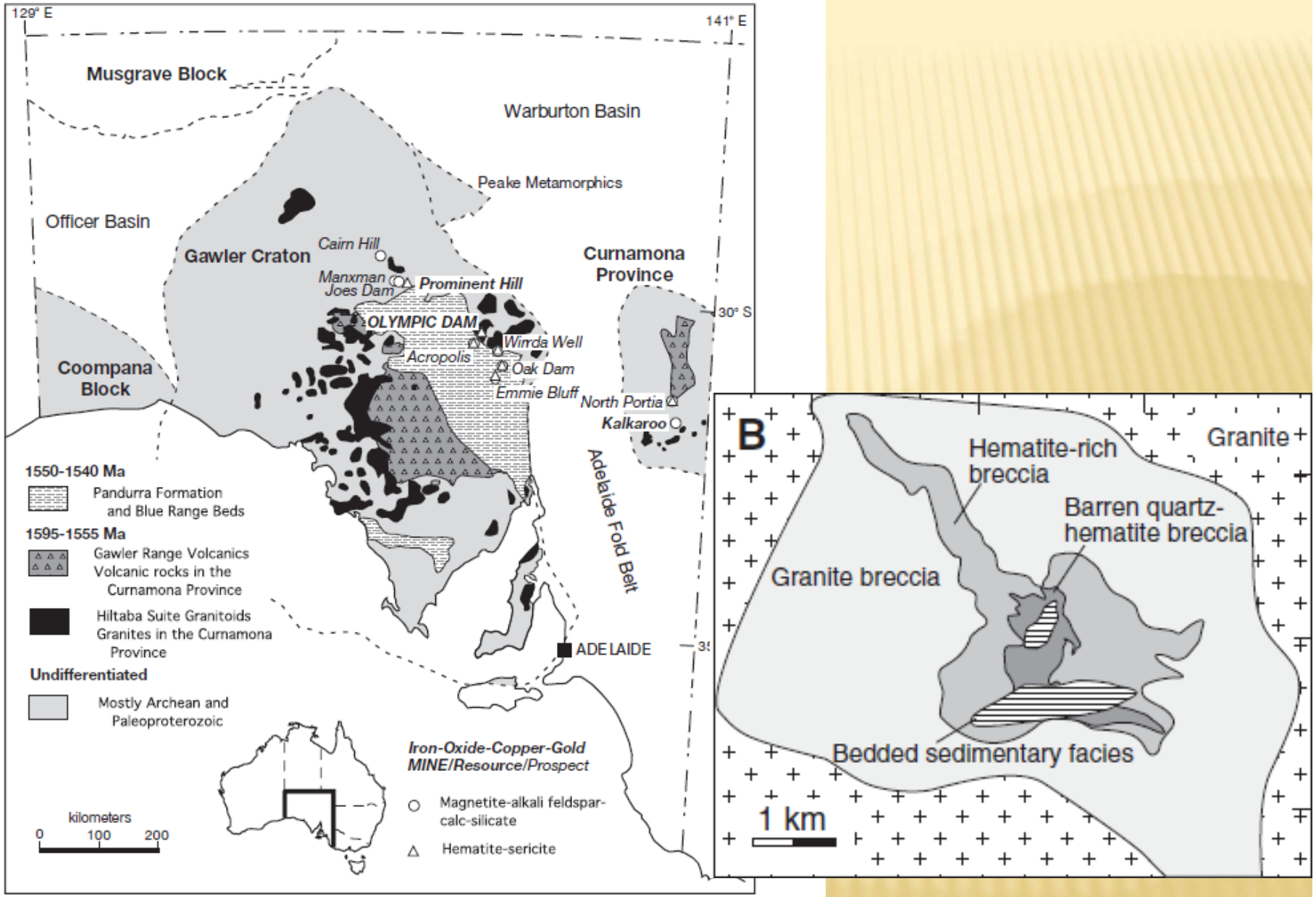

FIG. 10. Simplified geology of South Australia, showing the distribution of IOCG deposits and 1595 to 1555 Ma igneous rocks (adapted from Flint et al., 1993, with additional information from Williams and Skirrow, 2000, and Skirrow et al., 2002). Neoproterozoic and younger cover has been omitted in the cratonic areas. Note that the Gawler Range Volcanics are known to persist extensively under the Pandurra Formation and host several IOCG occurrences south of Olympic Dam, including Acropolis and part of the Emmie Bluff prospect.

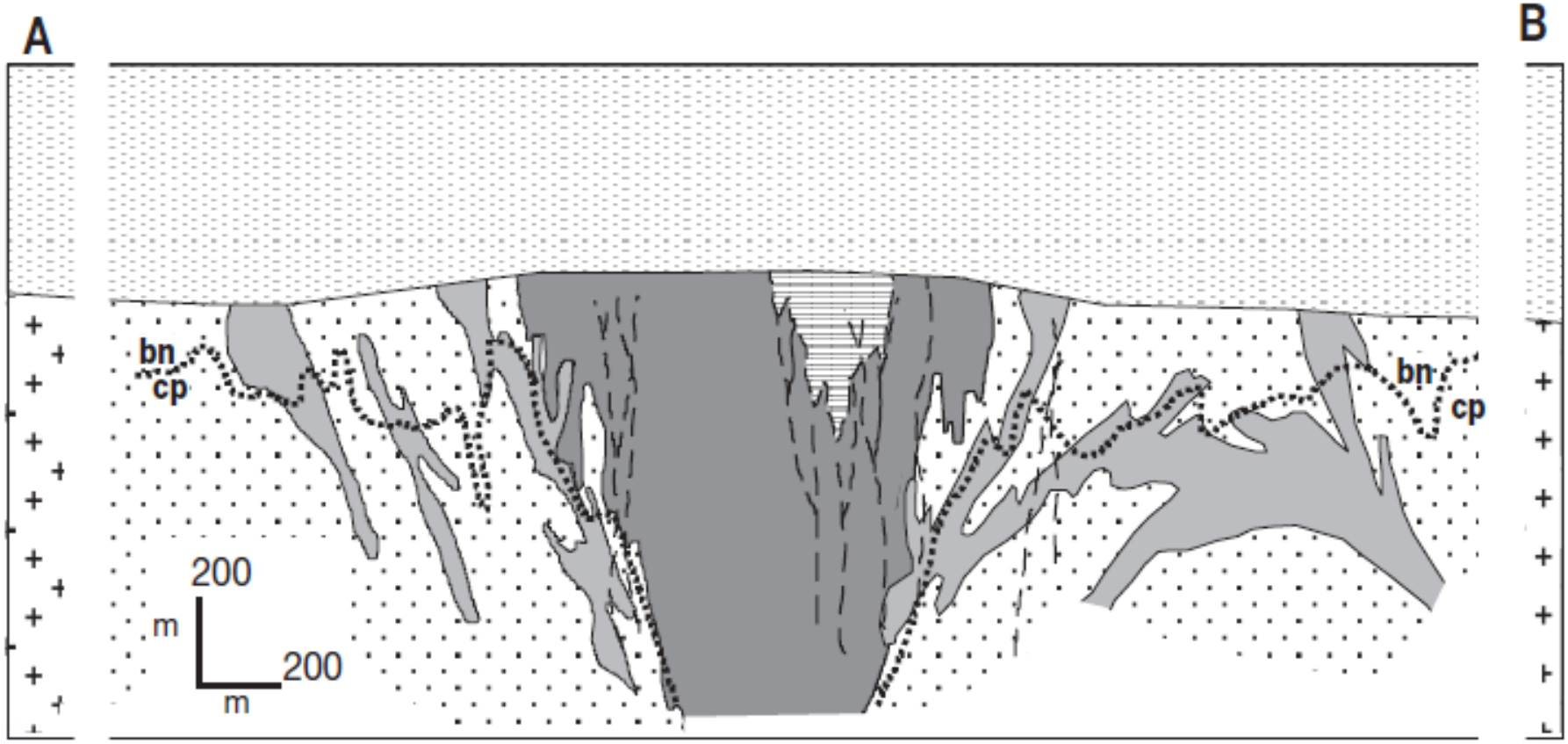

FIG. 11. (a). Geology and ore distribution at around 400 m below land surface at Olympic Dam (adapted and simplified from Reynolds, 2000). (b). Olympic Dam cross section, showing generalized geologic relationships and location of the bornite-chalcopyrite interface (adapted and simplified from Reeve et al., 1990).

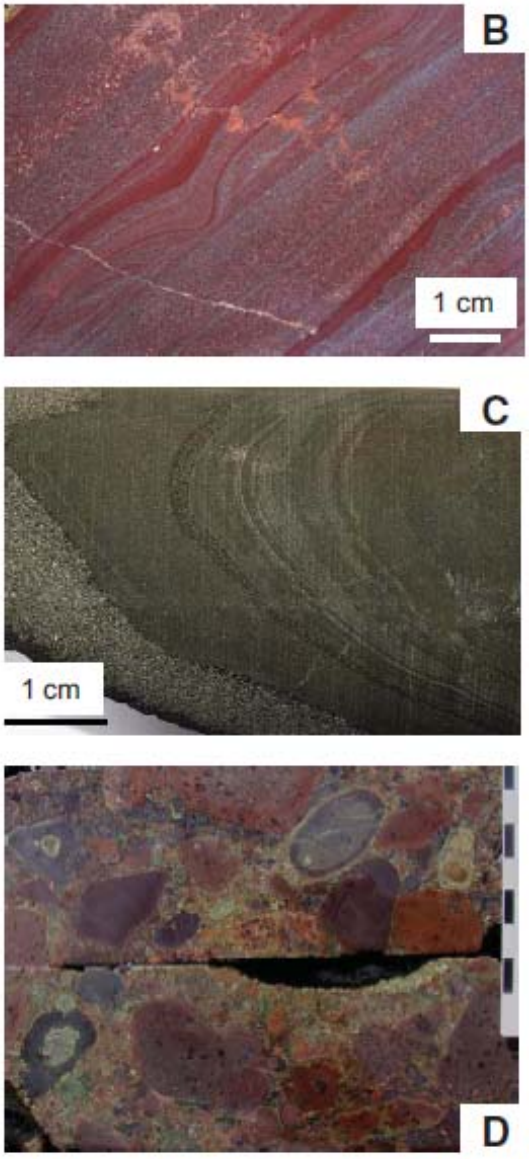

Figure 2. A: Clast of laminated hematite-rich sandstone in hematite-rich breccia, RD3008, 722.2 m. B: Laminated hematite-rich mudstone and sandstone in bedded sedimentary facies, RD3287, 355.3 m. C: Laminated chlorite-rich mudstone and sandstone, RD1989, 422.1 m. D: Polymictic volcanic conglomerate, RD3449, 414 m. Scale bar increments are in centimeters.

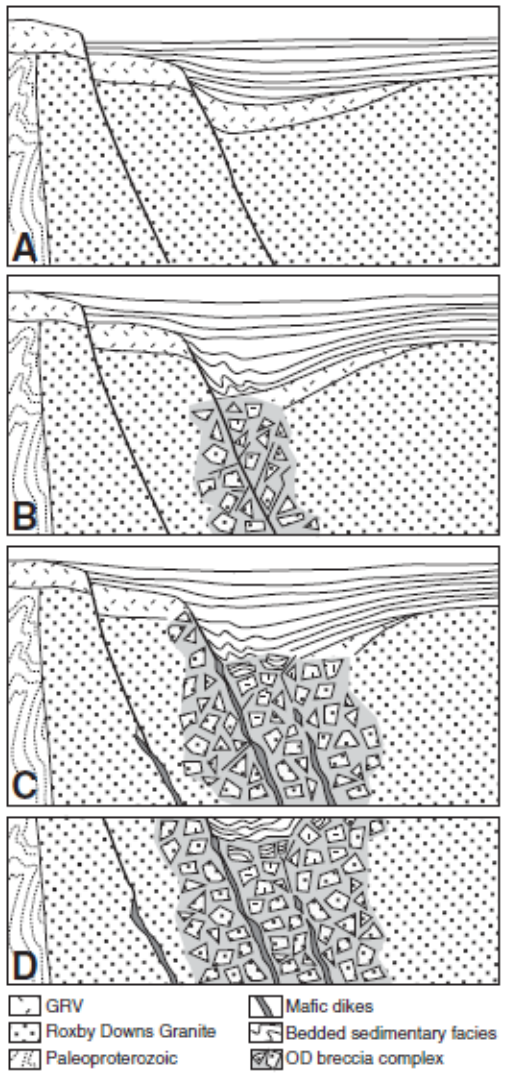

Figure 4. A: Bedded sedimentary facies accumulated in fault-bound basin above Mesoproterozoic granite and lavas. B: Fault-controlled subsurface fragmentation of Roxby Downs Granite, Gawler Range Volcanics (GRV) lavas, and bedded sedimentary facies formed Olympic Dam (OD) breccia complex. C: Mafic dikes intruded granite and breccia complex along faults. D: Erosion unroofed breccia complex, removing almost all traces of bedded sedimentary facies.

- Sedimentary basin
- Brecciation, mineralization
- Intrusion of mafic dikes
- erosion

http://eprints.utas.edu.au/11461/1/Geology_OD1.pdf

POTENTIAL IN SW US

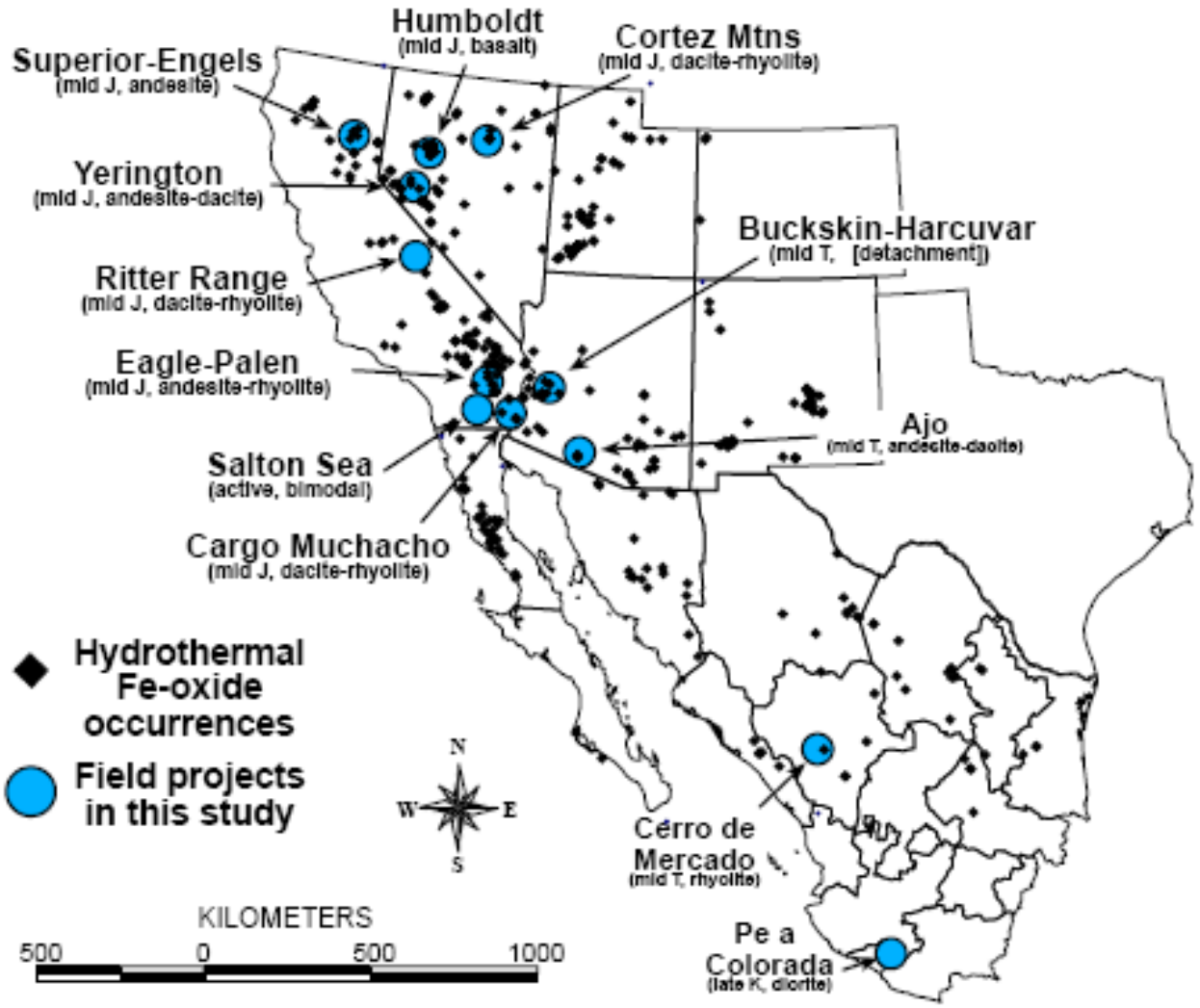

Figure 1. Distribution of Fe-oxide-rich hydrothermal systems of Phanerozoic age in southwestern North America. Most belong to one of three episodes: Jurassic (western U.S., northern Mexico), Laramide (Late Cretaceous - Paleocene; western Mexico), Oligocene-Early

Barton et al, 2000

PEA RIDGE, MISSOURI

PEA RIDGE

- 60 mi SW St. Louis, underground mine
- 1950s—Bethlehem Steel and St. Joseph Lead Co. began developing
- 1964—Meramec Mining Co began production
- 1981—sold to Fluor Corp.
- 1990—sold again
- 2001--bankrupt
- 2001—Upland Wings bought the mine
- 2011—Pea Ridge Resources, Inc. formed and continued development

MINERALOGY

- Magnetite
- Hematite
- Monazite
- Xenotime
- Allanite
- Cassiterite
- Pyrite
- Apatite
- Feldspar
- Quartz
- Actinolite

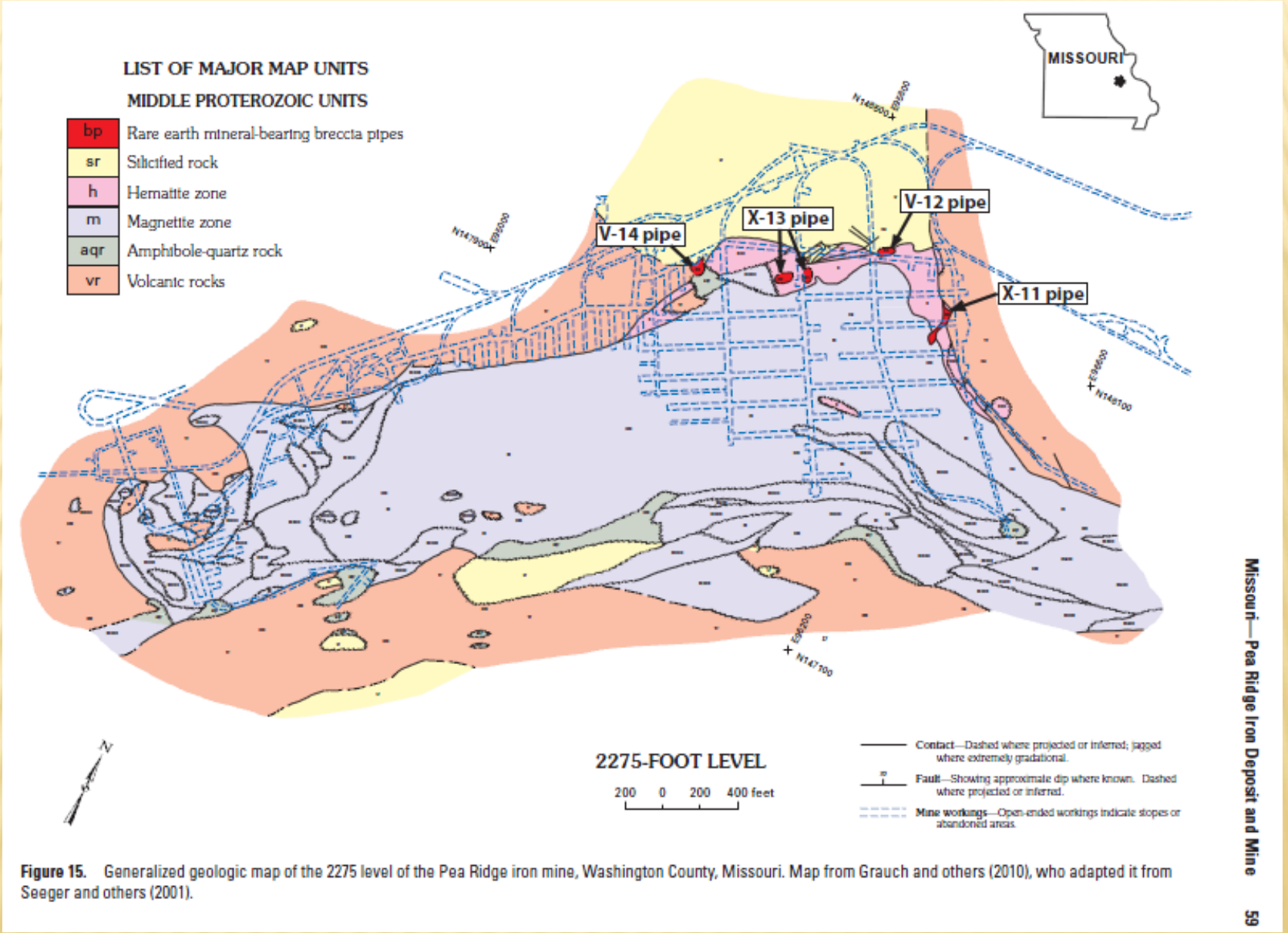

Figure 15. Generalized geologic map of the 2275 level of the Pea Ridge iron mine, Washington County, Missouri. Map from Grauch and others (2010), who adapted it from Seeger and others (2001).

http://pubs.usgs.gov/sir/2010/5220/

FORMATION

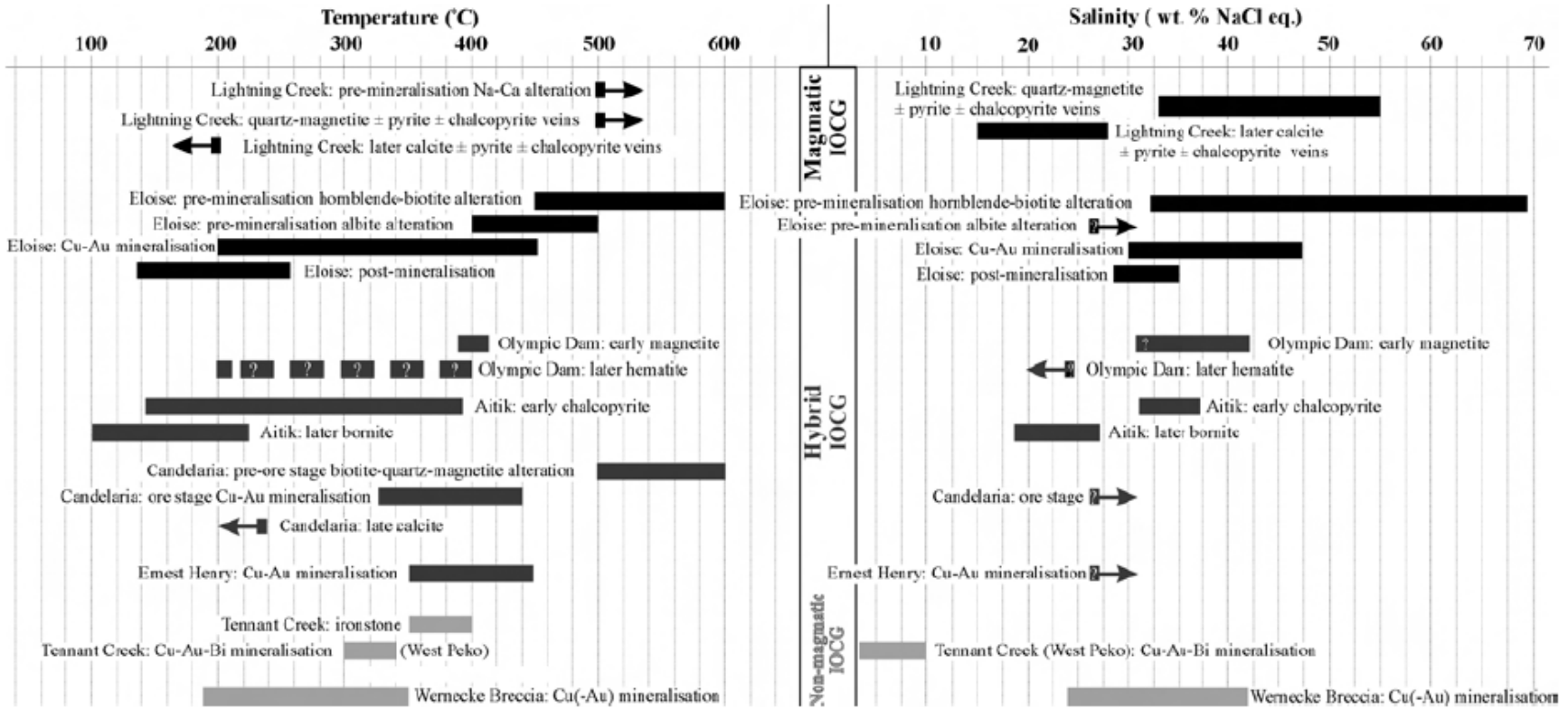

Fig. 5. Fluid temperature and salinity data for selected IOCG deposits and prospects. References as in Table 1.

http://www.sfu.ca/~dthorkel/linked/hunt%20et%20al.,%20rev%20iocg_s%202007.pdf

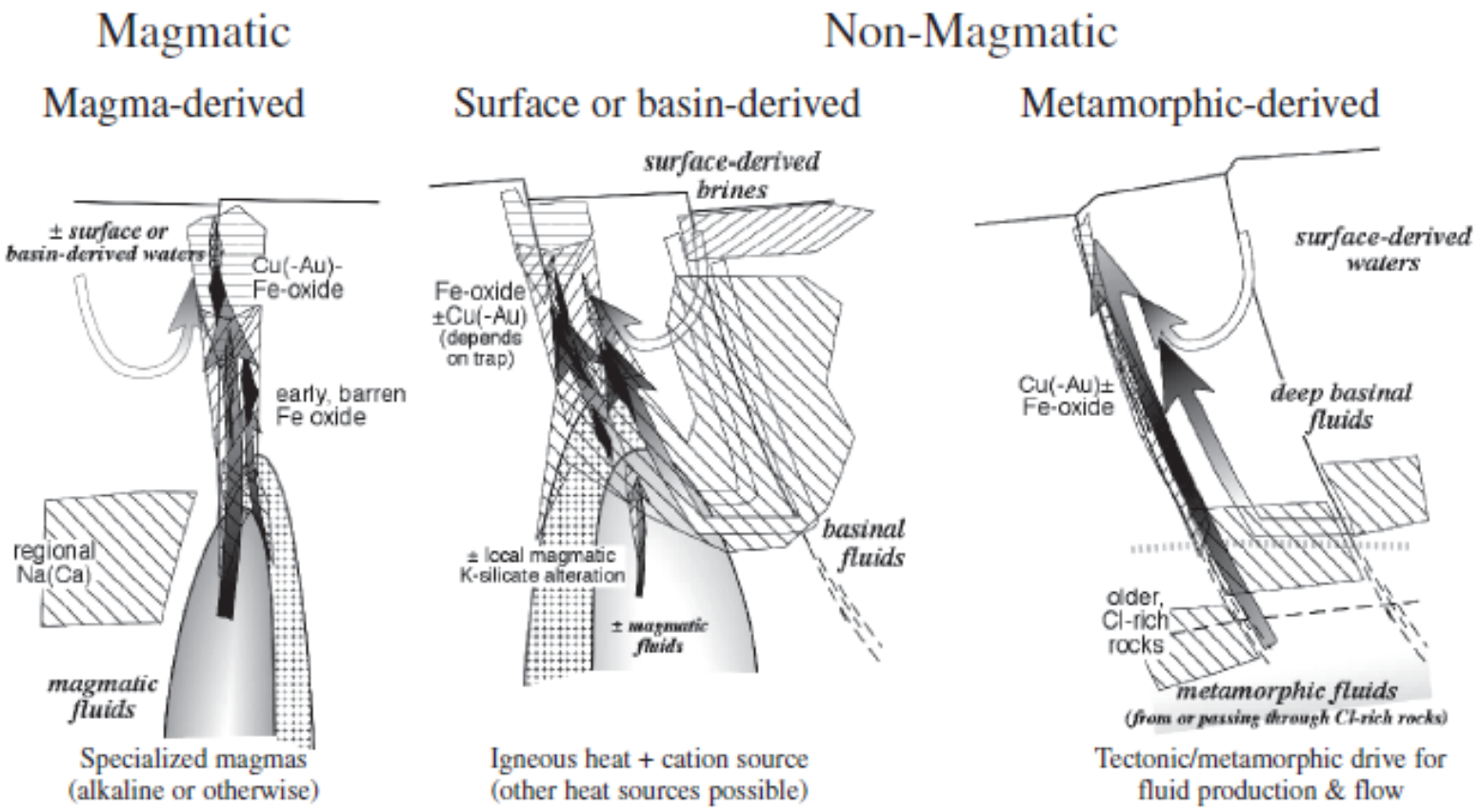

FIG. 18. Schematic illustration of flow paths and hydrothermal features for alternative models for IOCG deposits. See Table 2 for synopsis of characteristics. Shading of arrows indicates predicted quartz precipitation (veining) for a variety of paths in different quartz-saturated rocks that provides a useful first-order indication of flow (from Barton and Johnson, 2004).

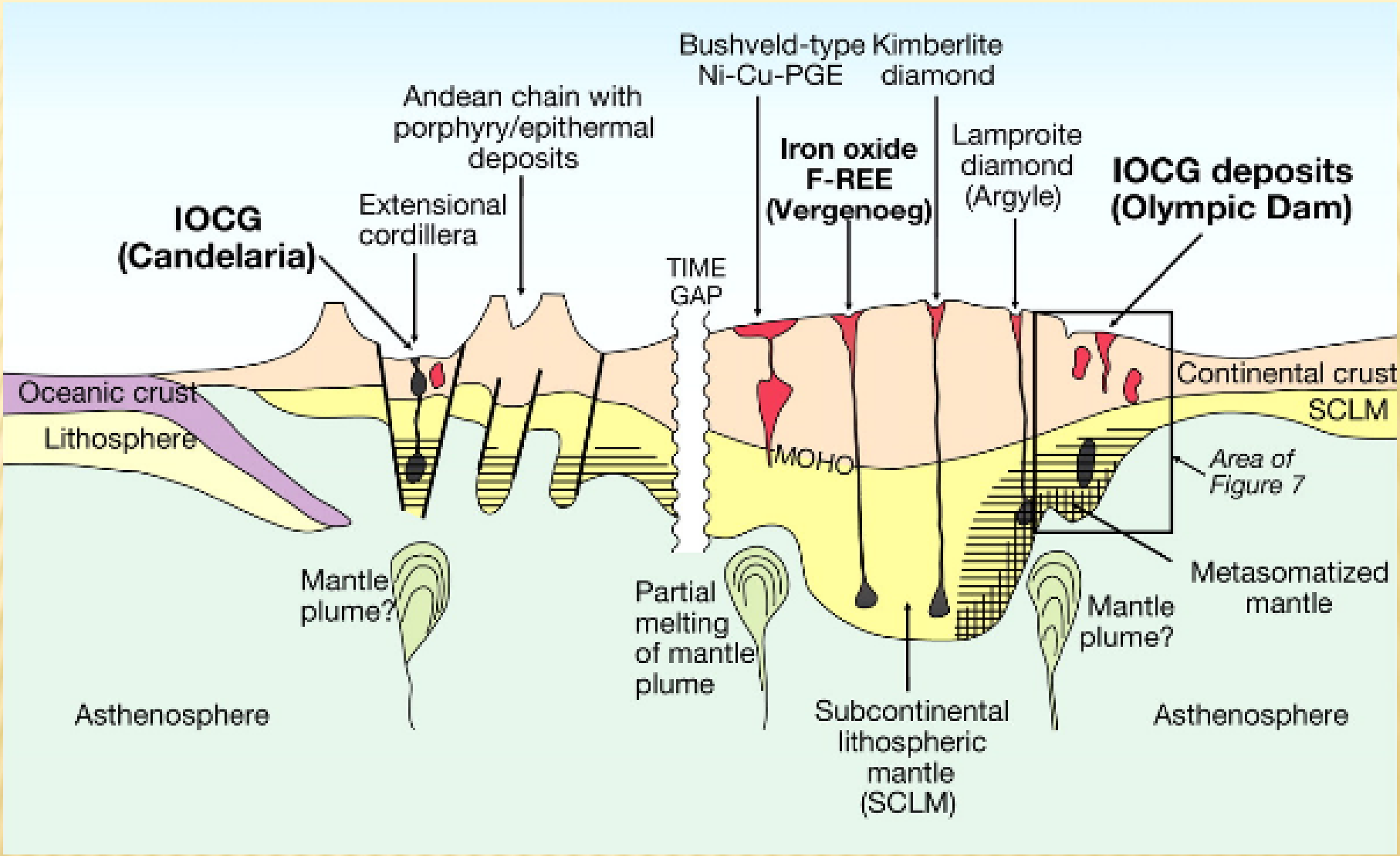
Bushveld-type Ni-Cu-PGE
Kimberlite diamond
Andean chain with porphyry/epithermal deposits
Iron oxide F-REE (Vergenoeg)
Lamproite diamond (Argyle)
IOCG deposits (Olympic Dam)
IOCG (Candelaria)
Extensional cordillera
TIME GAP
Oceanic crust
Lithosphere
MOHO
Continental crust
SCLM
Area of Figure 7
Mantle plume?
Partial melting of mantle plume
Metasomatized mantle
Mantle plume?
Asthenosphere
Subcontinental lithospheric mantle (SCLM)
Asthenosphere

PALEOPLACER/PLACER/ BEACH SANDS

PALEOPLACER/PLACER/ BEACH SANDS

- Monazite-bearing placers
- Heavy mineral placers
- Beach placers
- fluviatile placers
- eluvial or lag deposits

HEAVY MINERALS SANDS

- accumulations of heavy, resistant minerals (i.e. high specific gravity) that form on upper regions of beaches or in long-shore bars in a marginal-marine environment
- Currently mined in Virginia and Florida
  - Ilmenite 20-70%
  - Zirocn trace-20%
  - Rutile, leucoxene trace-30%
  - Garnet, starolite, kyanite trace-50%
  - Monazite trace-15%
- Monazite not being produced because of concerns about Th, U

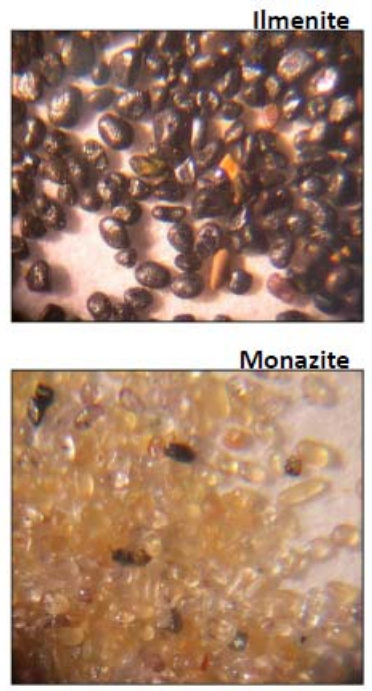

Iluka Concord Mine, Virginia

USGS
science for a changing world

Australia

Heavy Mineral Sand Deposits

Small quantities of monazite-(Ce) are sometimes recovered as a by-product

USGS

- Central Idaho stream placers
- North and South Carolina stream placers
- Virginia, Georgia, and Florida beach placers

Monazite-bearing Stream and Beach Placer Deposits

USGS

Monazite-bearing Stream and Beach Placer Deposits

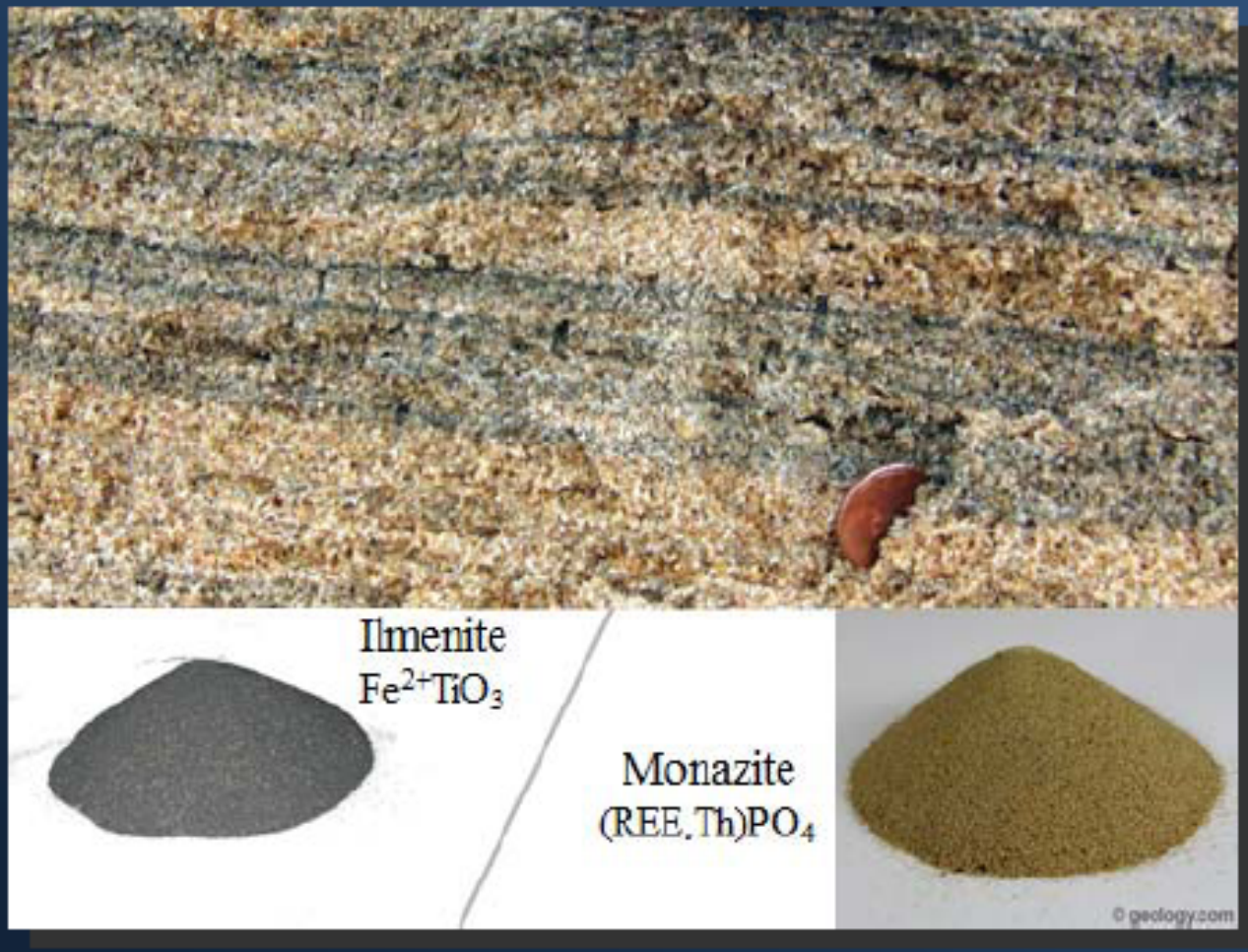

USGS

RIVER PLACERS

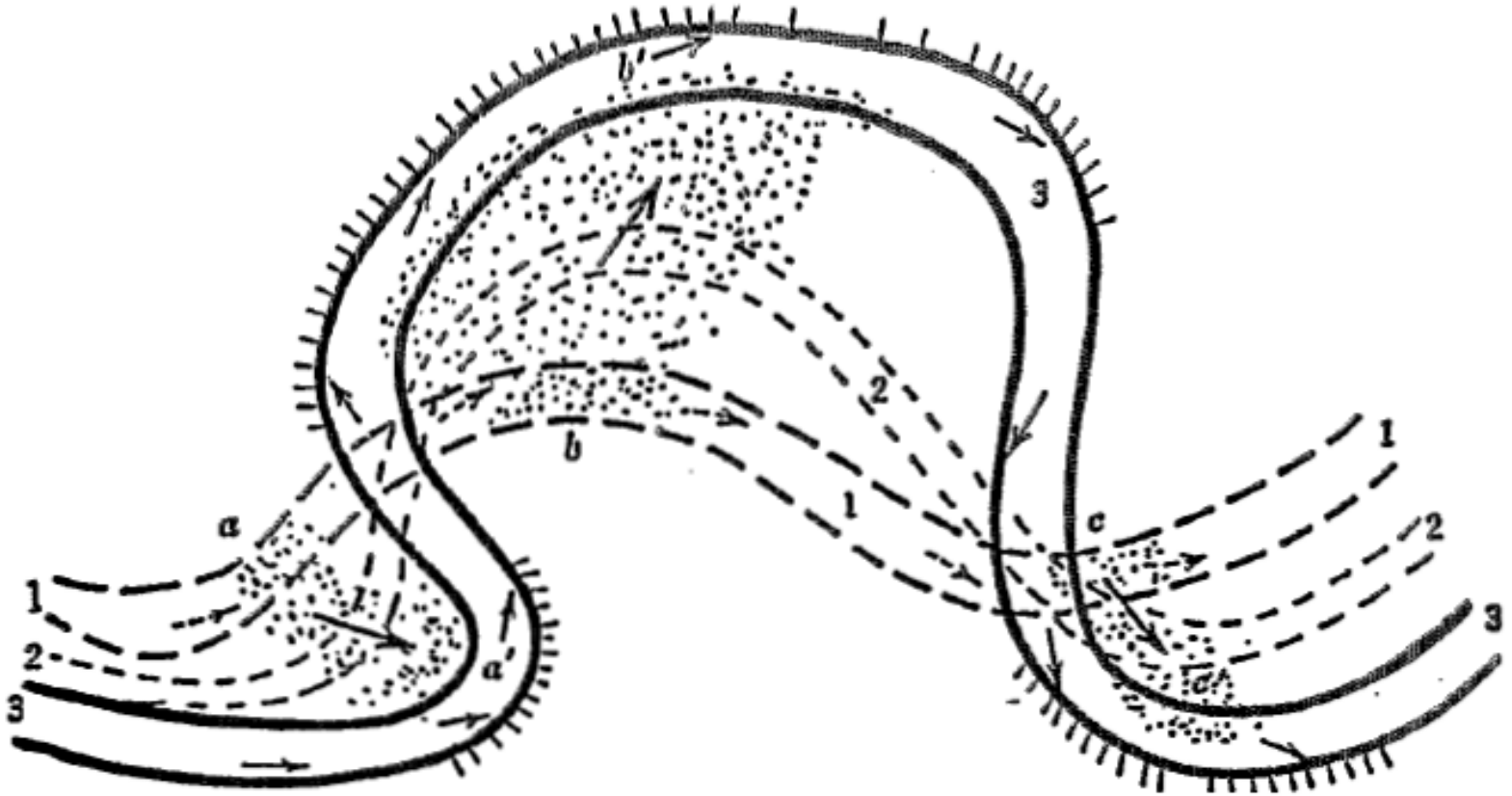

Fig. 4: The meandering of rivers and the location of gold deposition.

RIVER PLACERS

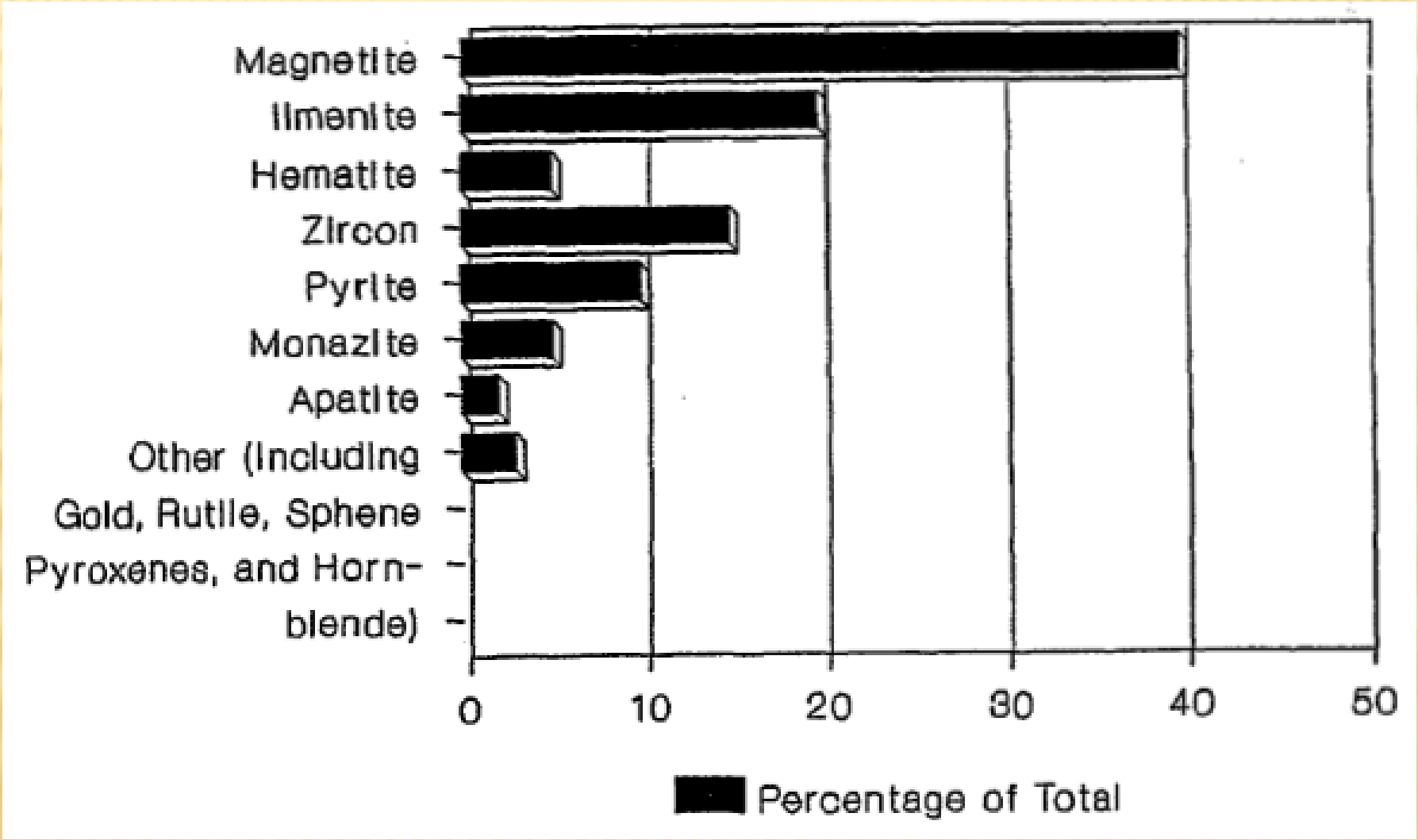

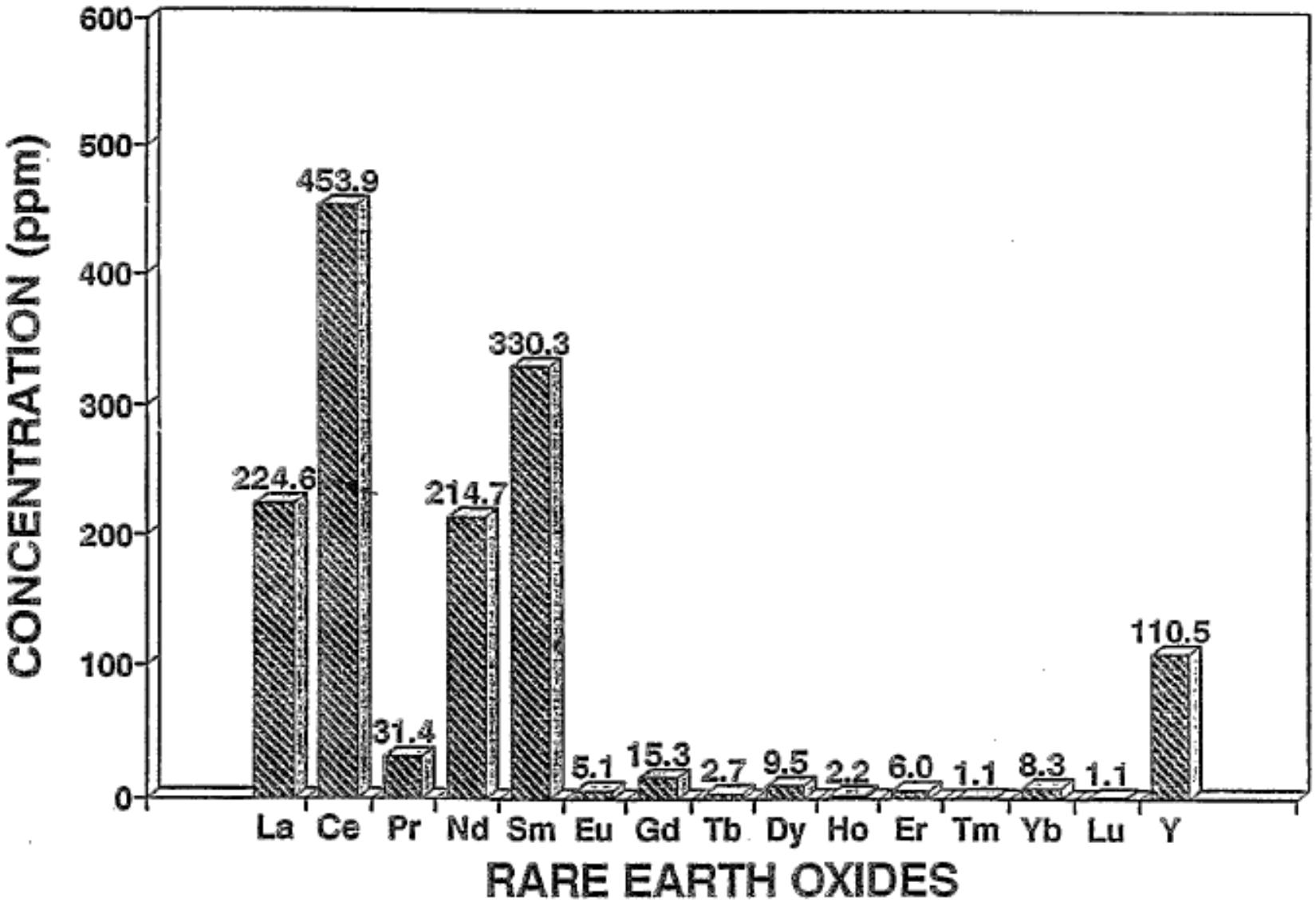

Fig. 7: Rare earth oxides in heavy mineral sand (Typical Urubama).

PALEOBEACH PLACERS

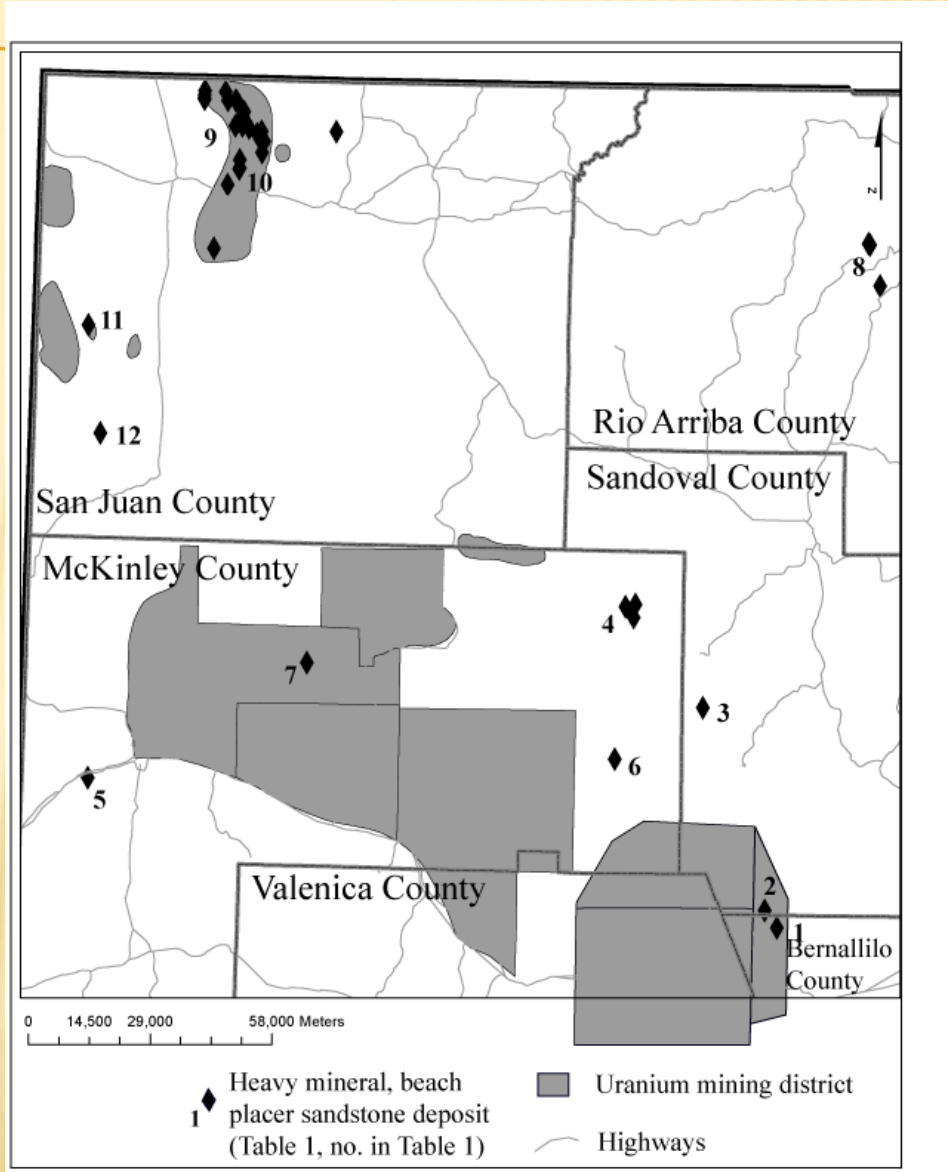

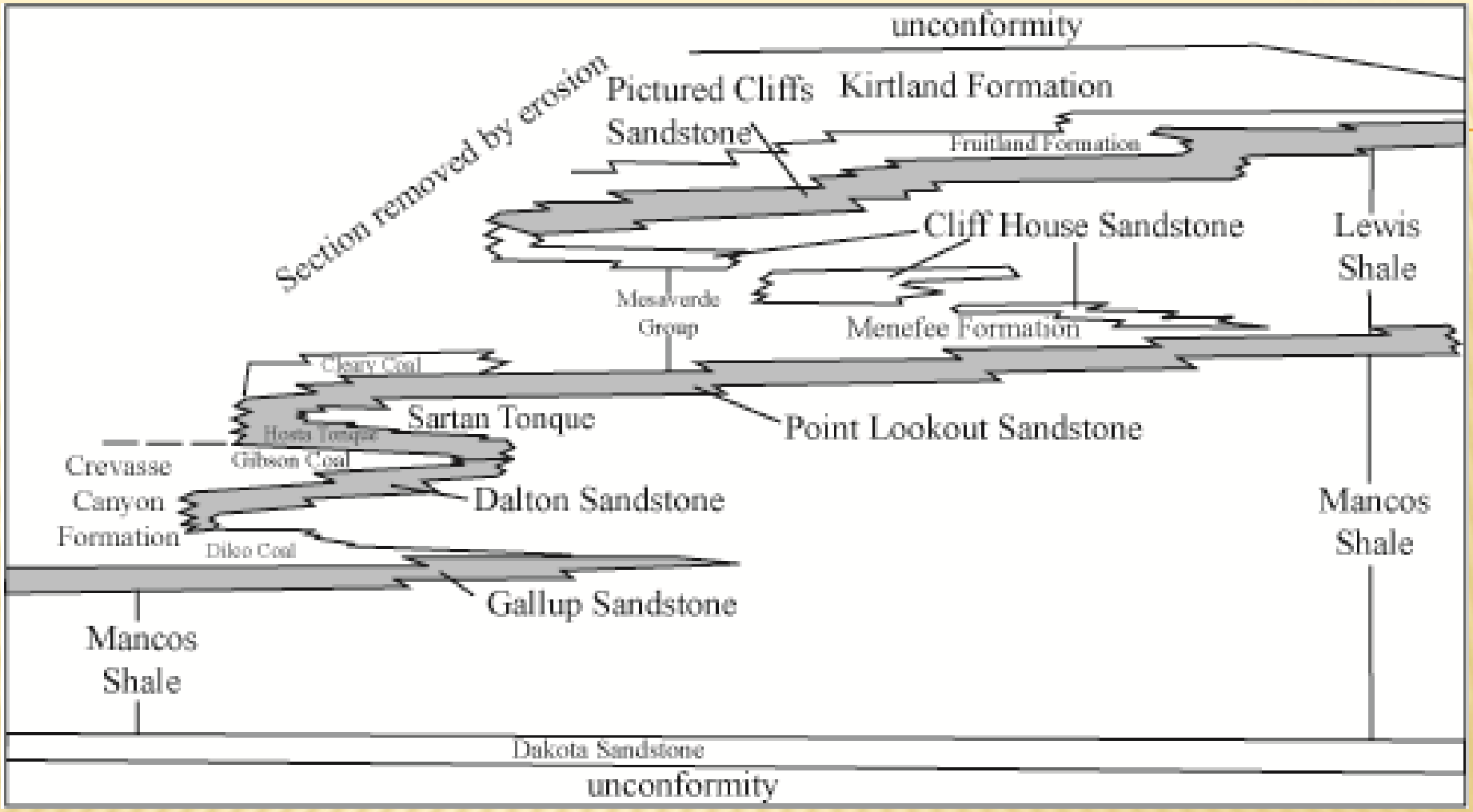

GRAY-SHADED SANDSTONE UNITS ARE HOSTS OF KNOWN BEACH-PLACER SANDSTONE DEPOSITS IN THE SAN JUAN BASIN

Sanostee deposit, San Juan County

SANOSTEE

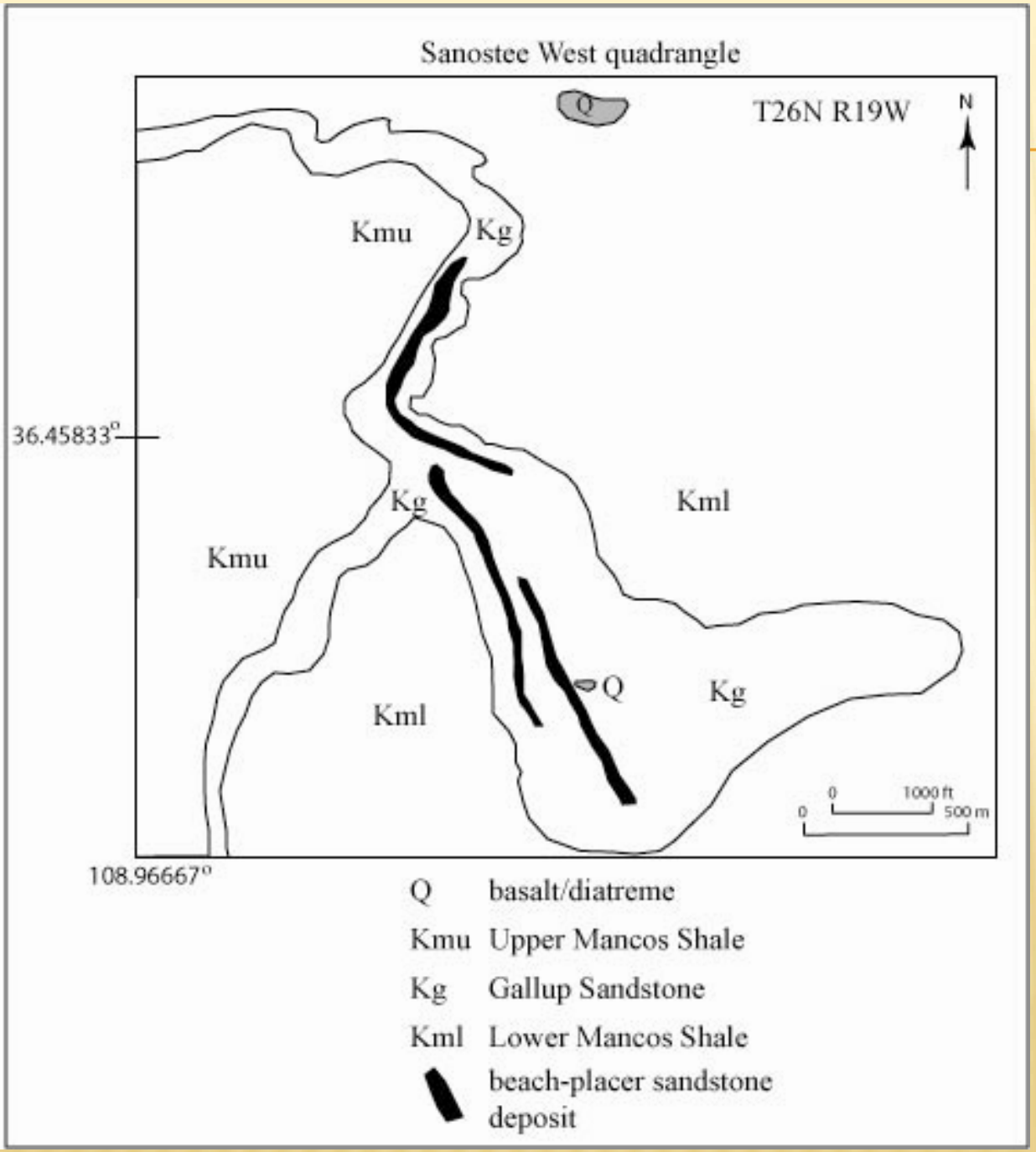
Sanostee West quadrangle
T26N R19W
N
Q
Kmu
Kg
Kml
Kg
Kmu
Kml
Q
Kg
36.45833°
108.96667°
0
1000 ft
0
500 m
Q basalt/diatreme
Kmu Upper Mancos Shale
Kg Gallup Sandstone
Kml Lower Mancos Shale
beach-placer sandstone deposit

REE IN BEACH PLACER DEPOSITS

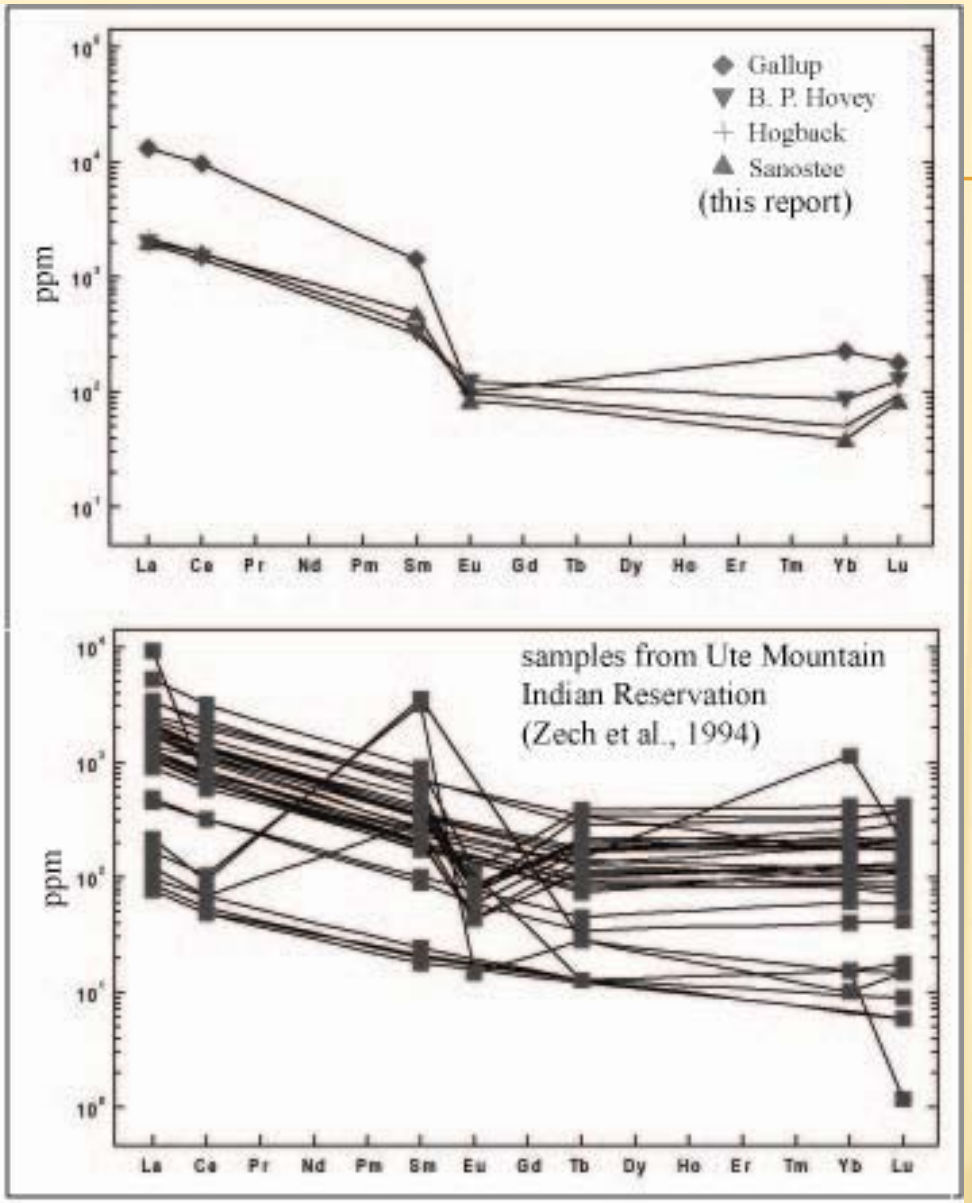

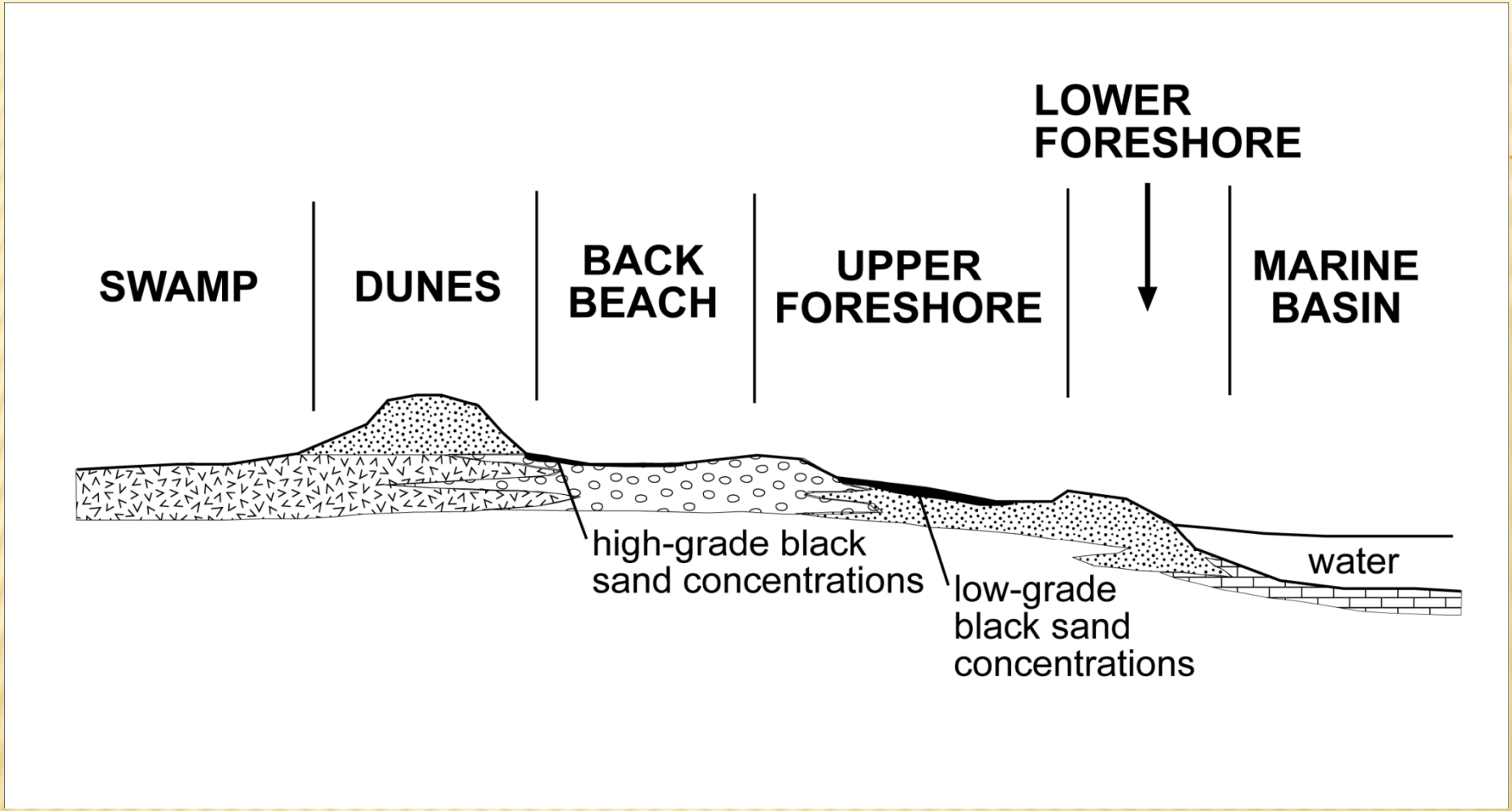

IDEALIZED CROSS-SECTION OF FORMATION

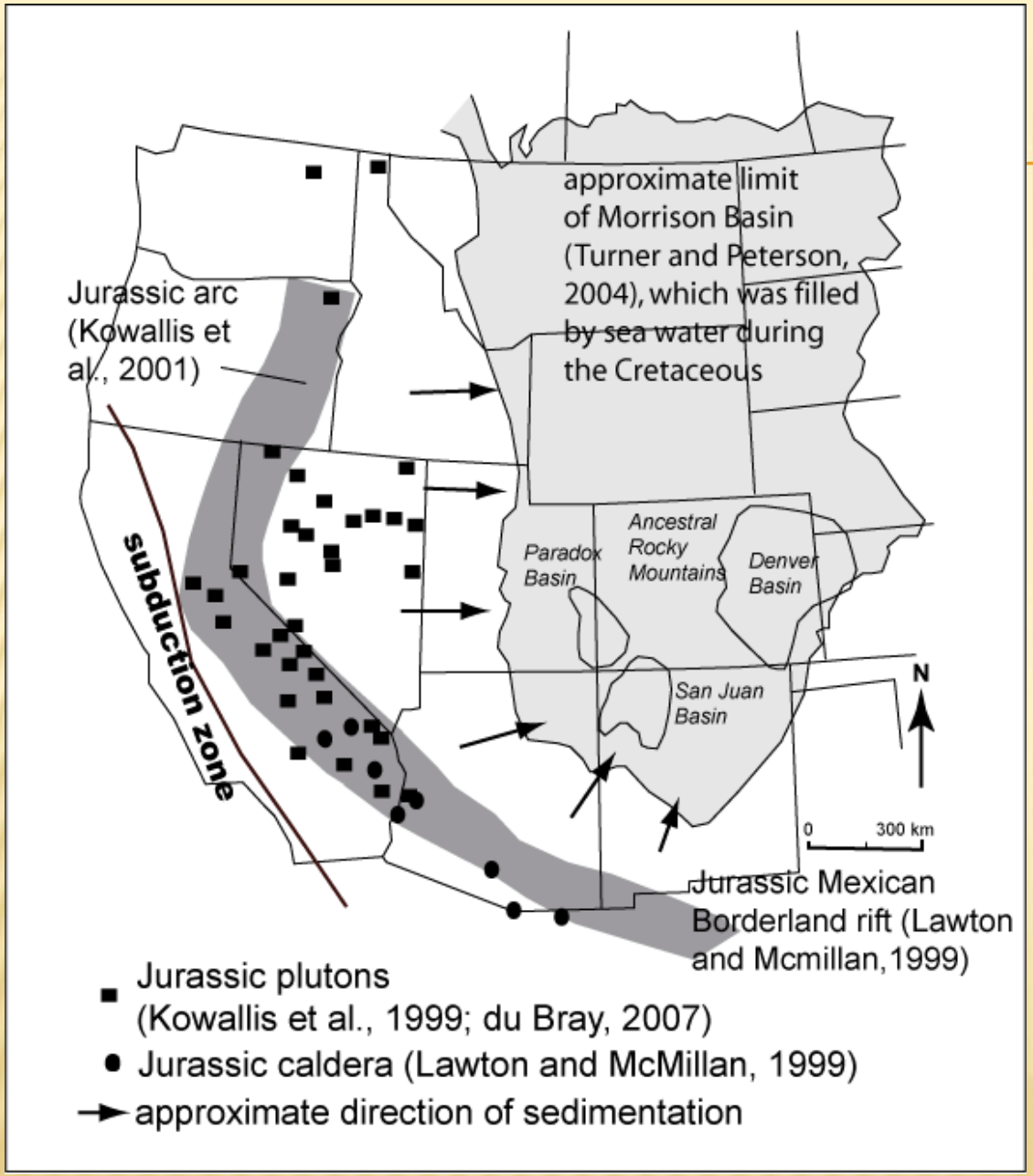

JURASSIC ARC PROVIDED A HIGHLAND CONSISTING OF GRANITIC ROCKS THAT COULD HAVE BEEN A SOURCE

PORPHYRY Mo DEPOSITS

PORPHYRY Mo DEPOSITS

- Climax-type
- Low F

CLIMAX-TYPE

- Rare
- pluton-related deposits associated with rare-metal granites
- Mo, F, Li, Rb, Cs, Sn, Ta, Nb, REE, Be
- calc-alkaline I-type, peraluminous S-type, or peralkaline
- Closely associated with alkaline-related mineral deposits

GEOCHEMISTRY

- Rb >250 ppm, Rb >250 ppm, F>2000 ppm
- Ta>2 ppm, Sr<100 ppm, Nb>50 ppm
- enriched in Be, Cs, Li, Sn, Th, W, U, REE

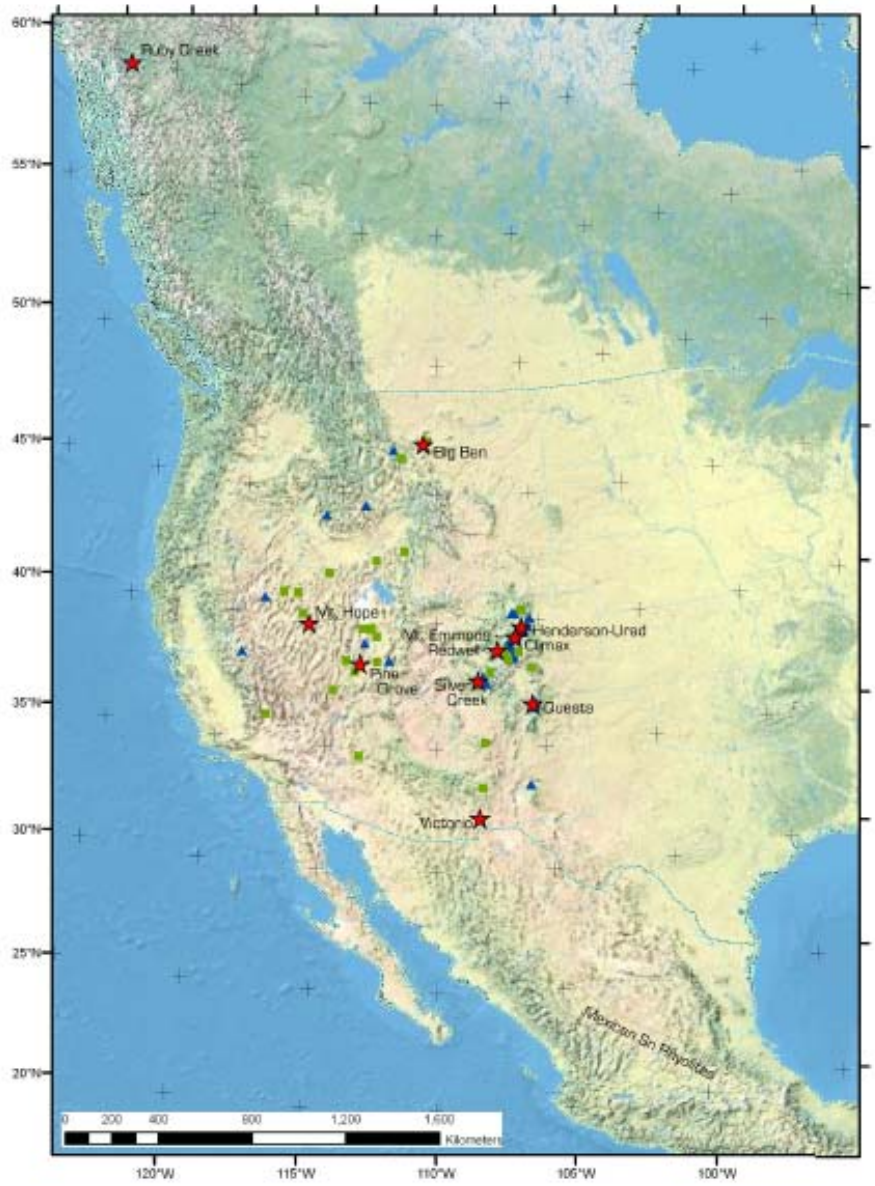

Figure 1. Location of Climax-type porphyry molybdenum deposits, prospects, and igneous centers with Climax-like compositions. Only the deposits (red stars) are labeled. Prospects are shown as blue triangles; igneous centers as green squares.

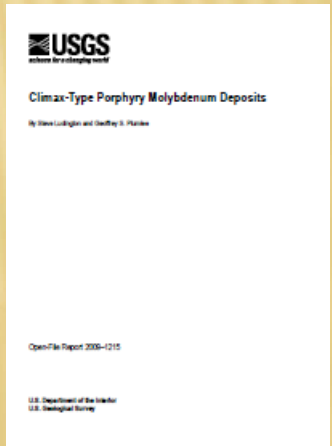
USGS

Climax-Type Porphyry Molybdenum Deposits

By Steve Ludington and Geoffrey S. Plumlee

Open-File Report 2009–1215

U.S. Department of the Interior
U.S. Geological Survey

Table 1. Climax-type Porphyry Molybdenum Deposits.

Deposit	Age (Ma)	Longitude	Latitude	Contained Mo (t)*	Primary reference
Climax, Colorado	33–24	-106.171	39.369	1,790,000	Wallace and others, 1968
Henderson, Colorado	30–27	–105.841	39.758	1,070,000	Shannon and others, 2004
Urad, Colorado	29	–105.835	39.760	29,100	Not available
Mt. Emmons, Colorado	17	–107.051	38.884	344,000	Thomas and Galey, 1982
Redwell Basin, Colorado	17	–107.057	38.890	18,400	Sharp, 1978
Silver Creek, Colorado	5	–108.008	37.698	124,000	Cameron and others, 1986
Questa, New Mexico	25	–105.508	36.717	442,000	Ishihara, 1967
Log Cabin, New Mexico	25	–105.570	36.688	53,400	Not available
Victorio, New Mexico	35	–108.103	32.180	112,000	McLemore and others, 2000
Pine Grove, Utah	23	–113.607	38.336	192,000	Keith and others, 1986
Mt. Hope, Nevada	38–26	–116.186	39.795	460,000	Westra and Riedell, 1995
Big Ben, Montana	51	–110.710	46.975	104,000	Johnson, 1964
Ruby Creek, British Columbia	84	–133.403	59.709	208,000	Pinsent and Christopher, 1995

*Molybdenum tonnage from Gregory Spanski, 2009, written commun.

FORMATION

- very high temperatures, 400° C to >600° C
- Fluid inclusions are hypersaline and contain both halite and sylvite daughter minerals
- Alteration potassic, sericitic, and propylitic, and the potassic zone
- F- and Cl-rich hydrothermal fluid separated from the crystallizing apex of the pluton and moved primarily upward (contained Mo, W, other metals)
- This fluid evolved compositionally as it cooled and moved upward

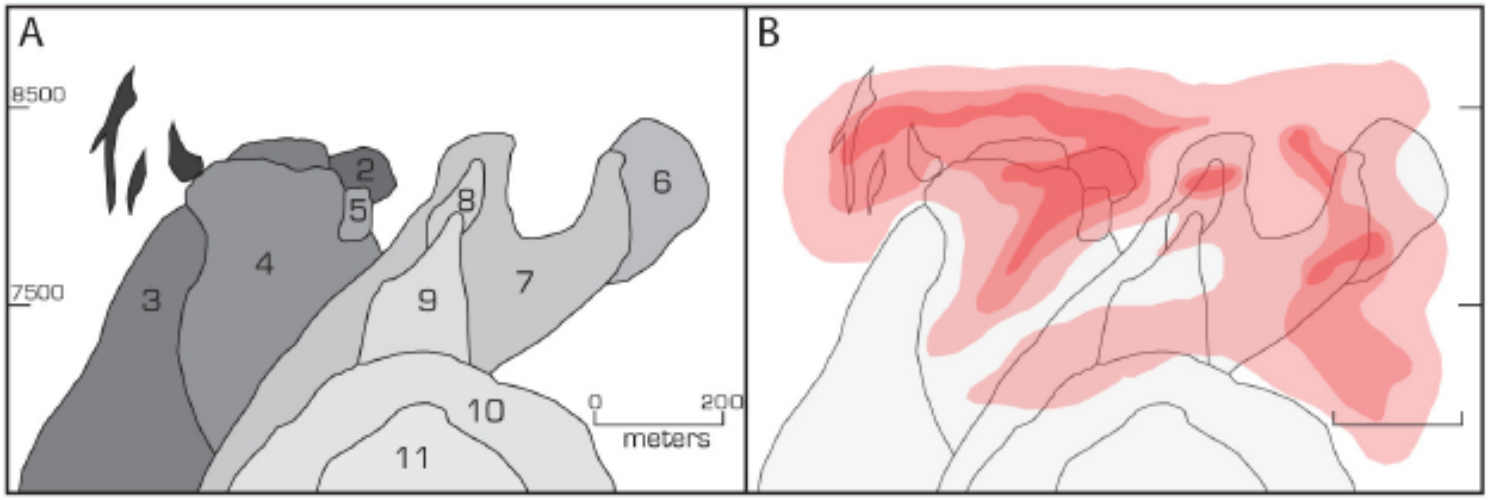

Figure 2. Relationship of multiple intrusions to ore at Henderson. Stocks are shown *A*, Numbered in order of age. Ore tenor is shown. *B*, in successively deeper shades of red, >0.1 percent, >0.3 percent, and >0.5 percent MoS_2. After figure 14 in Carten and others (1988). The earliest stock (the Phantom) does not appear in this cross-section.

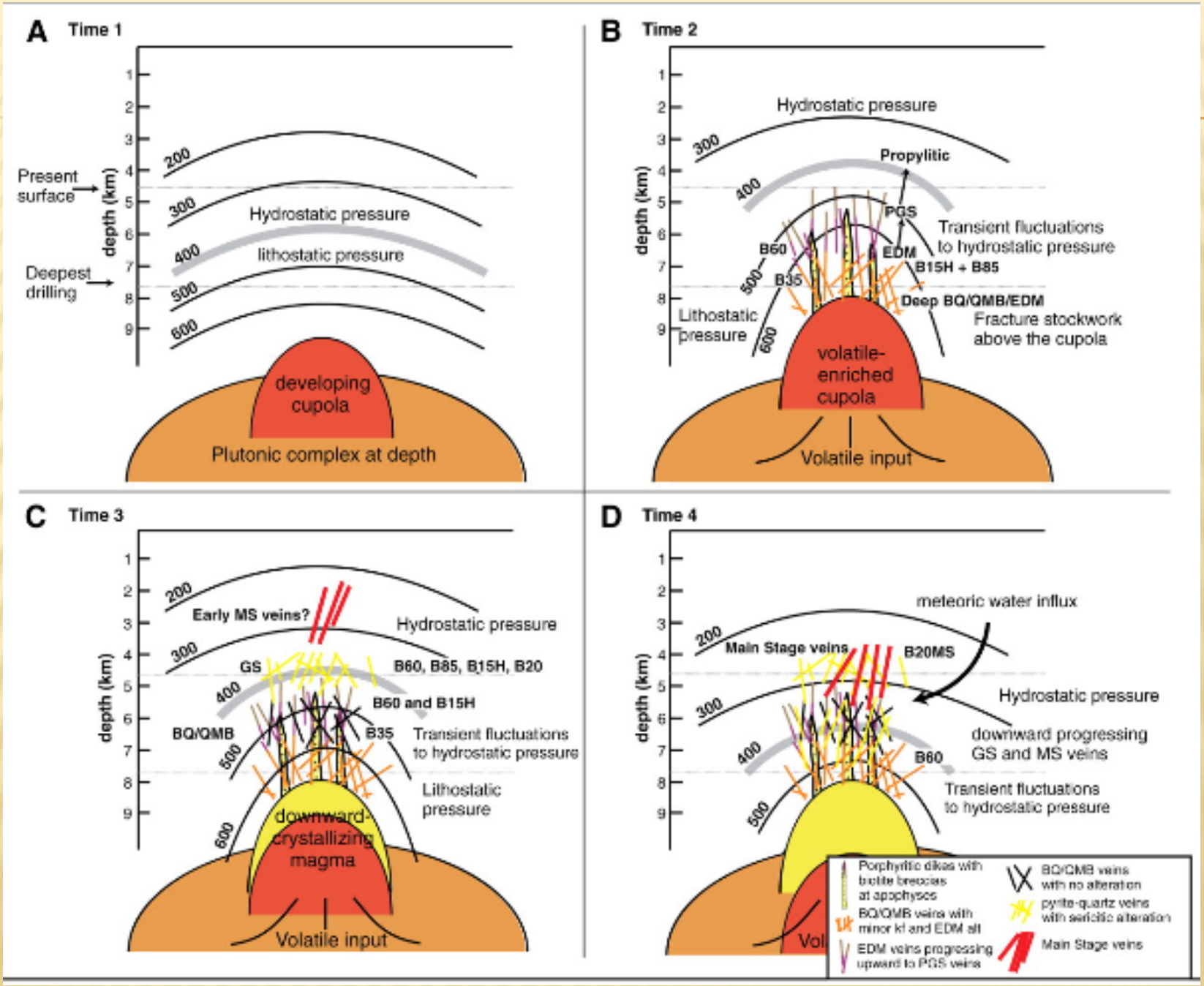
A
Time 1
depth (km)
Present surface
Deepest drilling
200
300
400
500
600
Hydrostatic pressure
lithostatic pressure
developing cupola
Plutonic complex at depth
B
Time 2
Hydrostatic pressure
Propylitic
PGS
Transient fluctuations to hydrostatic pressure
B60
EDM
B15H + B85
B35
Deep BQ/QMB/EDM
Fracture stockwork above the cupola
Lithostatic pressure
volatile-enriched cupola
Volatile input
C
Time 3
Early MS veins?
Hydrostatic pressure
GS
B60, B85, B15H, B20
B60 and B15H
BQ/QMB
B35
Transient fluctuations to hydrostatic pressure
Lithostatic pressure
downward-crystallizing magma
Volatile input
D
Time 4
meteoric water influx
Main Stage veins
B20MS
Hydrostatic pressure
downward progressing GS and MS veins
B60
Transient fluctuations to hydrostatic pressure
Porphyritic dikes with biotite breccias at apophyses
BQ/QMB veins with minor kf and EDM alt
EDM veins progressing upward to PGS veins
BQ/QMB veins with no alteration
pyrite-quartz veins with sericitic alteration
Main Stage veins

COLLUVIAL REE

Colluvial Xenotime and Monazite

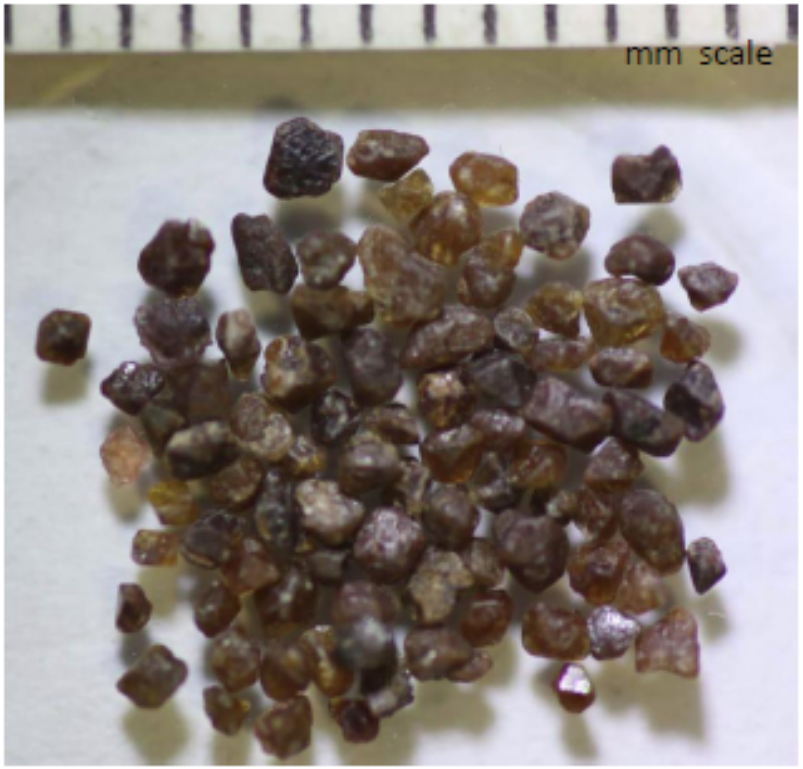

Xenotime

Monazite

Serra Verde, Goiás, Brazil

Colluvial REE Deposits

One of the interesting sources for independent REE and Y mineralization can be in large volume colluvial deposits derived from weathered granite or metamorphic rocks. In some occurrences heavy mineral accumulations can represent several percent of the colluvium.

Heavy minerals may include liberated coarse-grained xenotime and monazite that are readily amenable to well established physical processing techniques without resorting to grinding.

An example of this scenario under current exploration by Mining Ventures of Brazil is the Serra Verde occurrence of Northern Goiás, Brazil.

COLLUVIAL REE

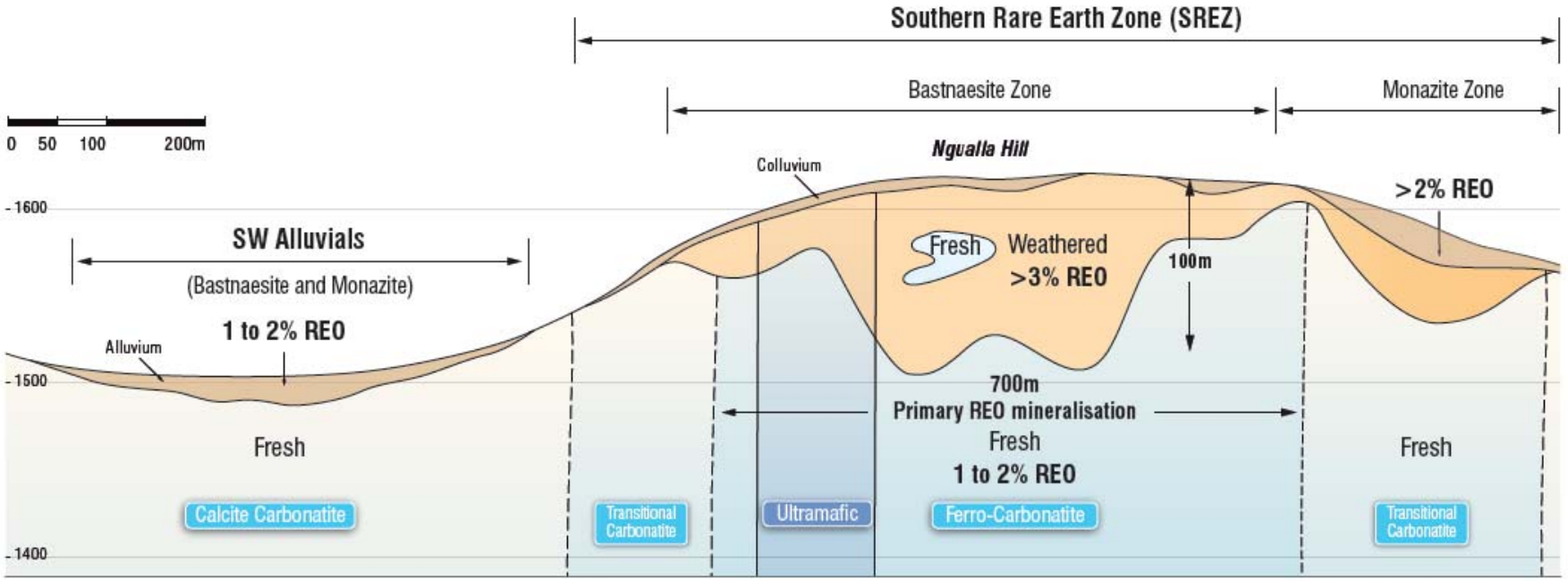

Figure 1: Cross section of Ngualla Hill showing bastneasite zone.

http://content.stockpr.com/peakresources/media/cb0ead90dcba68198a149dafcba9ccfd.pdf

RESIDUAL/LATERITE

- Stratiform phosphate residual
- Ion adsorption clays/laterite/bauxite
- Supergene

RESIDUAL/LATERITE

- Jianghua, China with 0.012 Mt @ 0.035% total rare earth oxides or TREO)
- Mt. Weld, Australia (23.94 Mt @ 7.9% rare earth oxides or REO)
- Araxa, Brazil (6.34 Mt @ 5% TREO)
- Tantalus, Madagascar (1.5 Mt @ 0.8% REO)
- Ngulla, Tanzania (40 Mt @ 4.07% REO)

Ionic Clay Deposits, SE China

T. Tagaki, Geological Survey of Japan

About 0.5 percent TREO in a readily leached form in laterite formed on “tin” granites in southern China. Many of these deposits are enriched in HREE.

A significant source of REE, especially HREE, but resources are rapidly being depleted. Mining of these deposits in South China by undercapitalized small operators is environmentally problematic.

USGS


Ion-Adsorbed Clays
Xunwu Longnan District, Jiangxi Province, China

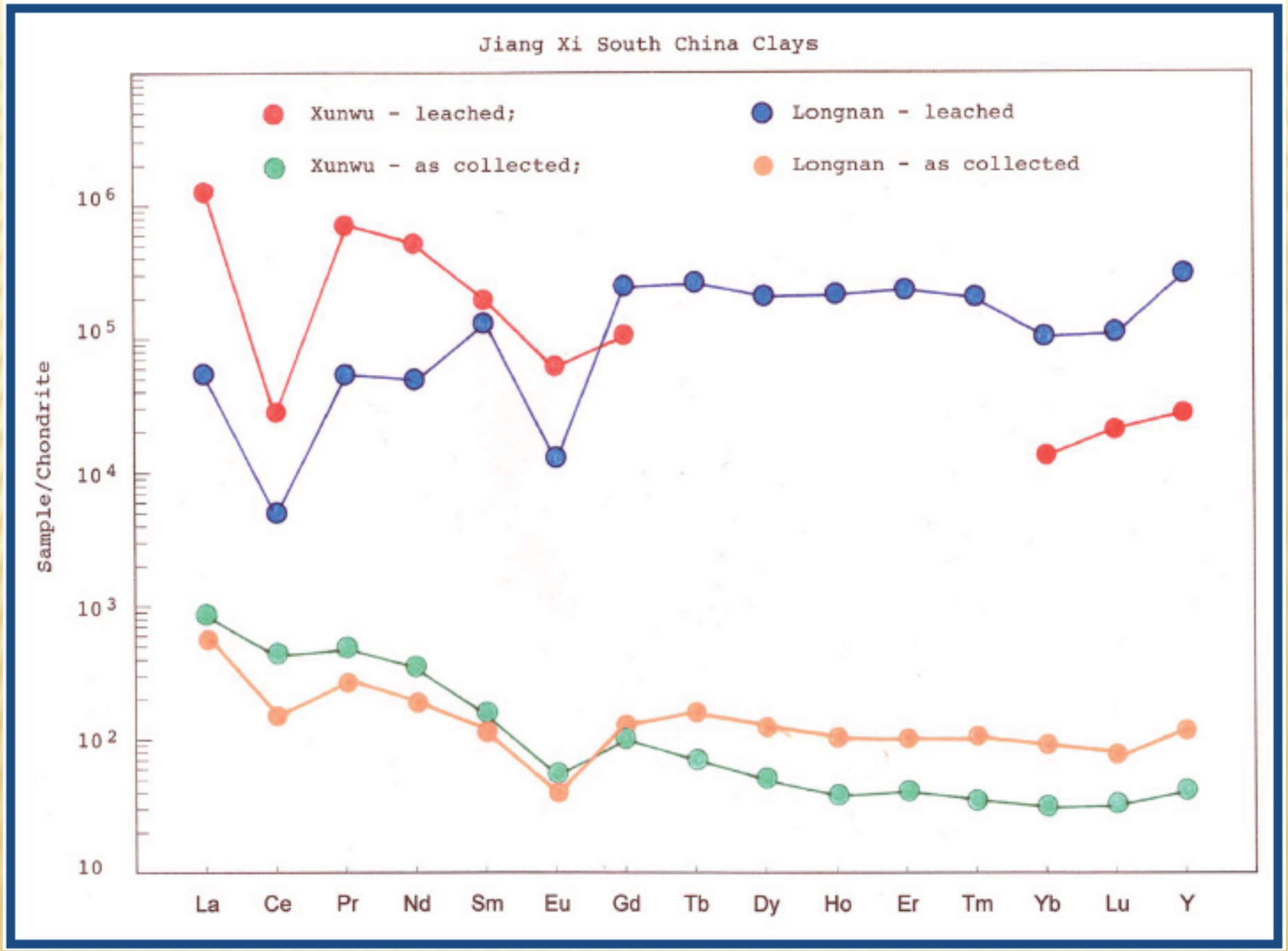
Jiang Xi South China Clays
Xunwu - leached;
Longnan - leached
Xunwu - as collected;
Longnan - as collected
Sample/Chondrite
10^6
10^5
10^4
10^3
10^2
10
La
Ce
Pr
Nd
Sm
Eu
Gd
Tb
Dy
Ho
Er
Tm
Yb
Lu
Y

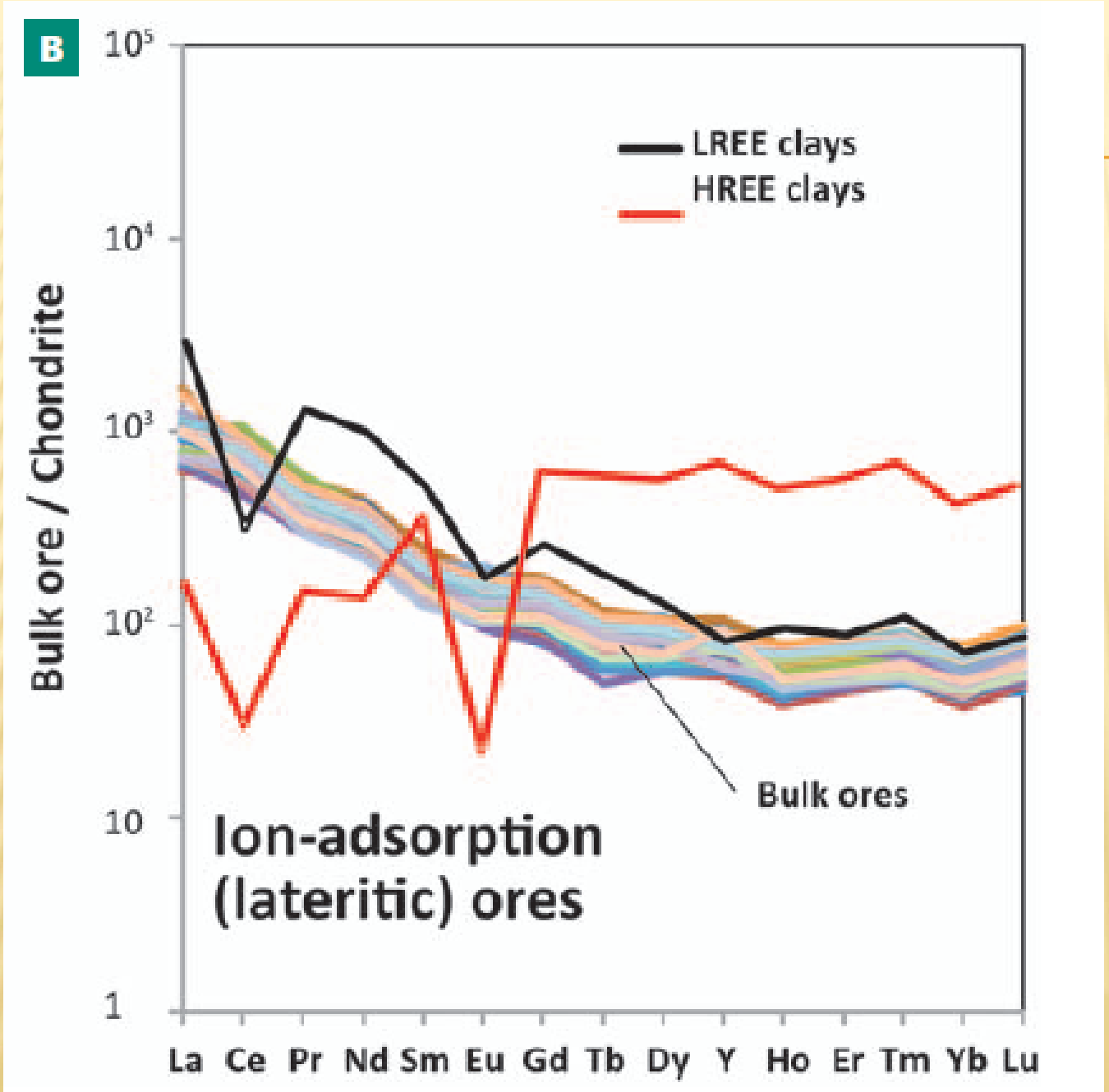

KYNICKY ET AL., 2012

MOUNT WELD, AUSTRALIA

- 35 km south Laverton, western Australia
- Open pit with a strip ratio of 4.6:1
- Mined June 2008
  - 773,300 tonnes ore at 15.4% REO
  - 2 mill cubic meters of overburden removed
- Ore is stockpiled according to mineralogy and grade

http://www.lynascorp.com/Pages/rare-earths-project.aspx

Mount Weld, Australia With no Topographic Expression

March 10, 1980

Category	Tonnes (Mt)	Grade (% REO)	Tonnes REO
Measured	1.2	15.6	186,000
Indicated	5.0	11.7	583,000
Inferred	1.5	9.8	148,000
Total	7.7	11.9	917,000

- Initial mining completed by Lynas Corporation in June 2008
- 773,000 metric tons of ore mined at an average grade of 15.4% REO
- Monazite, REE-bearing crandallite-group, cerianite, rhabdophane, churchite
- Mt Weld Resource Estimate – Central Lanthanide Deposit

June, 2008

Supergene Monazite
light greenish yellow in ferric iron-rich laterite
Araxá, Brazil
(34-A-3)
(coll. A.N.M. January, 1968)

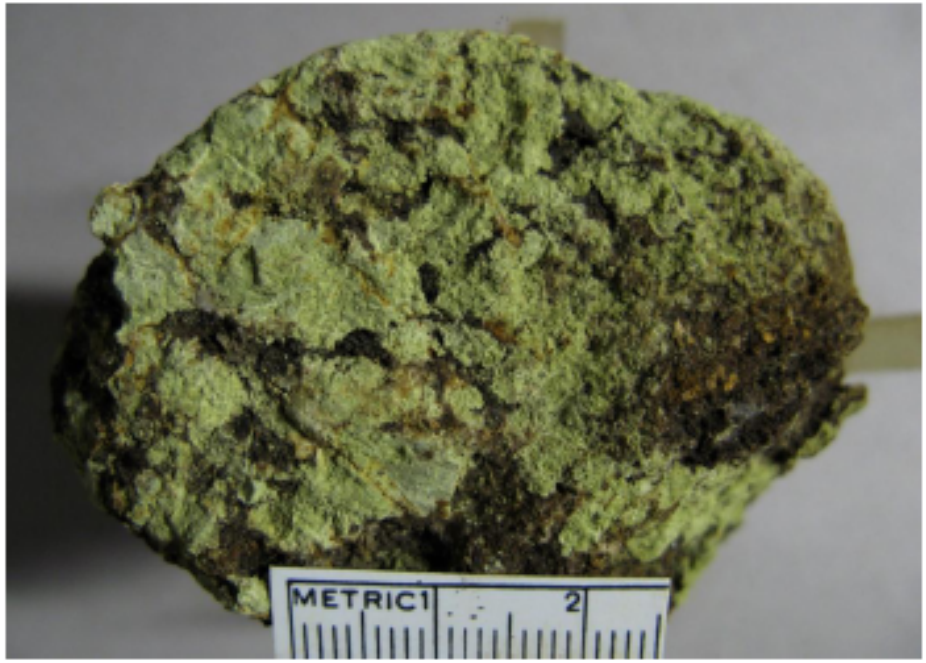

Supergene Monazite
replacing massive apatite mineralization
Araxá, Brazil Furo O-IXMO, 191.25 meters
(12-A-1)

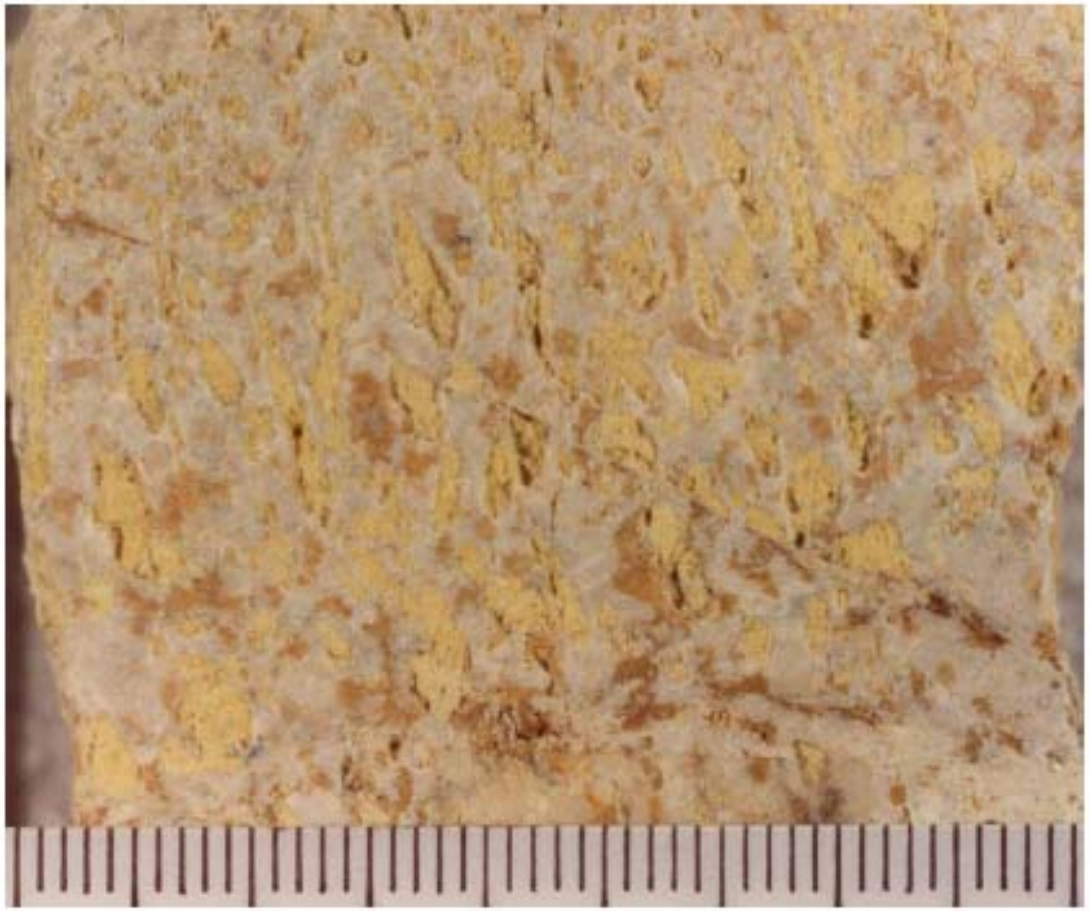

Pseudomorphs of Monazite after Apatite prisms in Carbonatite – Araxá, MG, Brazil

These pseudomorphs are the result of descending water that is enriched in REE from the dissolved primary minerals in the upper level weathered carbonatite. This section of drill core illustrates the leaching of Ca from the apatite and its replacement by REE as a result of the high affinity (partition coefficient) of REE for phosphate.

RESERVES, MOUNT WELD

Rare Earths Oxides	CLD	Duncan Deposit
Lanthanum Oxide	23.88%	24.87%
Cerium Oxide	47.55%	39.38%
Praseodymium Oxide	5.16%	4.75%
Neodymium Oxide	18.13%	17.89%
Samarium Oxide	2.44%	2.83%
Europium Oxide	0.53%	0.77%
Gadolinium Oxide	1.09%	1.99%
Terbium Oxide	0.09%	0.26%
Dysprosium Oxide	0.25%	1.27%
Holmium Oxide	0.03%	0.19%
Erbium Oxide	0.06%	0.41%
Thulium Oxide	0.01%	0.04%
Ytterbium Oxide	0.03%	0.18%
Lutetium Oxide	0.00%	0.02%
Yttrium Oxide	0.76%	5.17%
Total	**100.00%**	**100.00%**

http://www.lynascorp.com/Pages/rare-earths-project.aspx

The mine is within the Central Lanthanide Deposit (CLD), a Resource of 15.0 million tonnes at 9.8% for 1.5 million tonnes of contained REO

MOUNT WELD STOCKPILES WITH RARE EARTH OXIDE PERCENTAGES

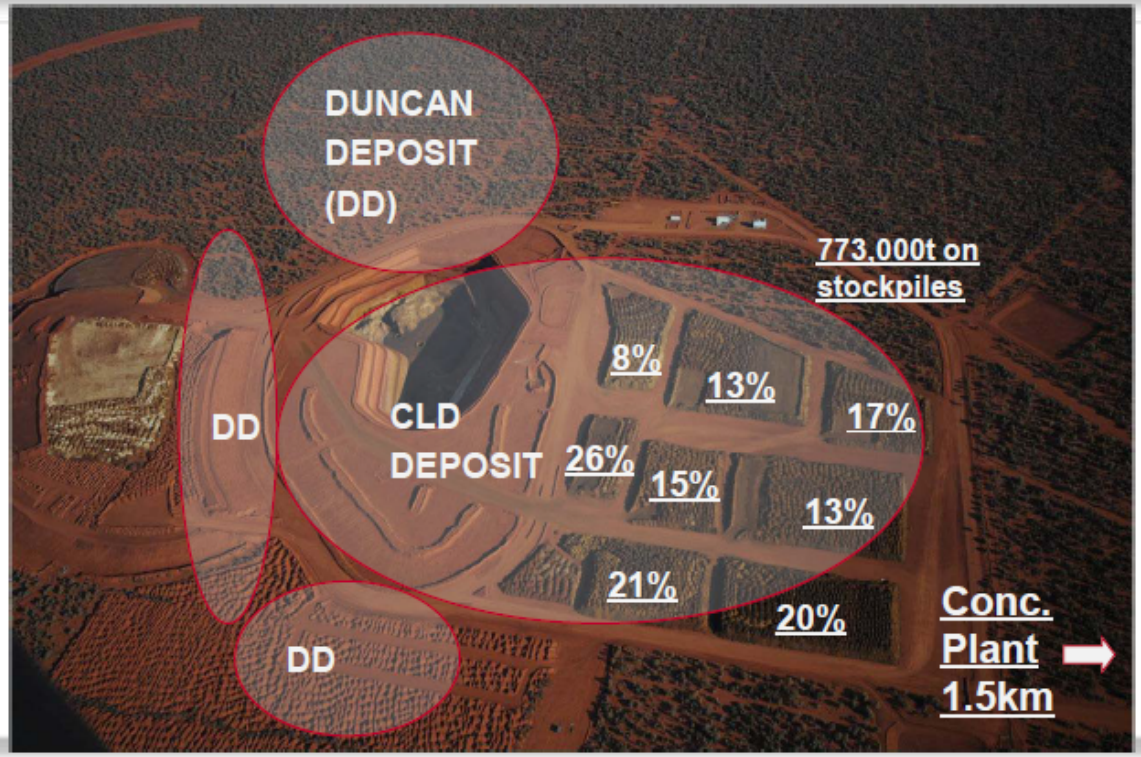

The Duncan deposit is complementary to the current operations at the Central Lanthanide Deposit

CENTRAL LANTHANIDE DEPOSIT AND DUNCAN DEPOSIT RESOURCES

Comparison of REE distribution

REO	CLD (Secondary Monazite)	Duncan (Crandalite)
Lanthanum Oxide	23.88%	24.87%
Cerium Oxide	47.55%	39.38%
Praseodymium Oxide	5.16%	4.75%
Neodymium Oxide	18.13%	17.89%
Samarium Oxide	2.44%	2.83%
Europium Oxide	0.53%	0.77%
Gadolinium Oxide	1.09%	1.99%
Terbium Oxide	0.09%	0.26%
Dysprosium Oxide	**0.25%**	**1.27%**
Holmium Oxide	0.03%	0.19%
Erbium Oxide	0.06%	0.41%
Thulium Oxide	0.01%	0.04%
Ytterbium Oxide	0.03%	0.18%
Lutetium Oxide	0.00%	0.02%
Yttrium Oxide	0.76%	5.17%
Total	**100.00%**	**100.00%**

CLD & Duncan Mineral Resource (2.5% REO cut-off)

Category	Tonnes Mt	Grade % REO	Tonnes (kt) REO
CLD	14.95	9.8	1,465
Duncan	8.99	4.8	432
Total	23.94	7.9	1,891

- Current reserves are 2.08Mt @ 15.5% REO
- Reserve statement expected to be updated in 2012 ahead of Phase 2 mining campaign
- Proven floatable process for the CLD
- Metallurgical test work underway for Duncan

PHOSPHORITE DEPOSITS

Rare Earth Element Minerals & Deposit Types

Group-Mineral	Formula	Carbonatite	Alkaline Intrusion-Related	Placer	Phosphorite
Oxides					
Aeschynite	$(Ln,Ca,Fe)(Ti,Nb)_2(O,OH)_6$		X		
Euxenite	$(Y,Ln,Ca)(Nb,Ta,Ti)_2(O,OH)_6$		X	X	
Fergusonite	$YNbO_4$		X		
Carbonates					
Bastnäsite	$(Ln,Y)CO_3F$	X	X		
Parisite	$Ca(Ln)_2(CO_3)_3F_2$	X	X		
Synchisite	$Ca(Ln,Y)(CO_3)_2F$	X	X		
Tengerite	$Y_2(CO_3)_3 \bullet n(H_2O)$		X		
Phosphates					
Apatite	$(Ca,Ln)_5(PO_4)_3(OH,F,Cl)$	X	X		X
Monazite	$(Ln,Th)PO_4$	X	X	X	
Xenotime	YPO_4		X	X	
Silicates					
Allanite	$(Ln,Y,Ca)_2(Al,Fe^{3+})_2(SiO_4)_3(OH)$		X		
Eudialyte	$Na_4(Ca,Ce)_2(Fe^{2+},Mn^{2+},Y)ZrSi_8O_{22}(OH,Cl)_2$		X		
Thalenite	$Y_2Si_2O_7$		X		
Zircon	$(Zr,Ln)SiO_4$		X	X	

USGS
science for a changing world

Ln: Lanthanide (a.k.a. REE)

PHOSPHORITE DEPOSITS

- Florida, North Carolina
- Phosphoria Formation, Idaho, Montana
- High P_2O_5, 1-40%
- Sedimentary deposits (limestones, muds)
- Apatite, fluorapatite,

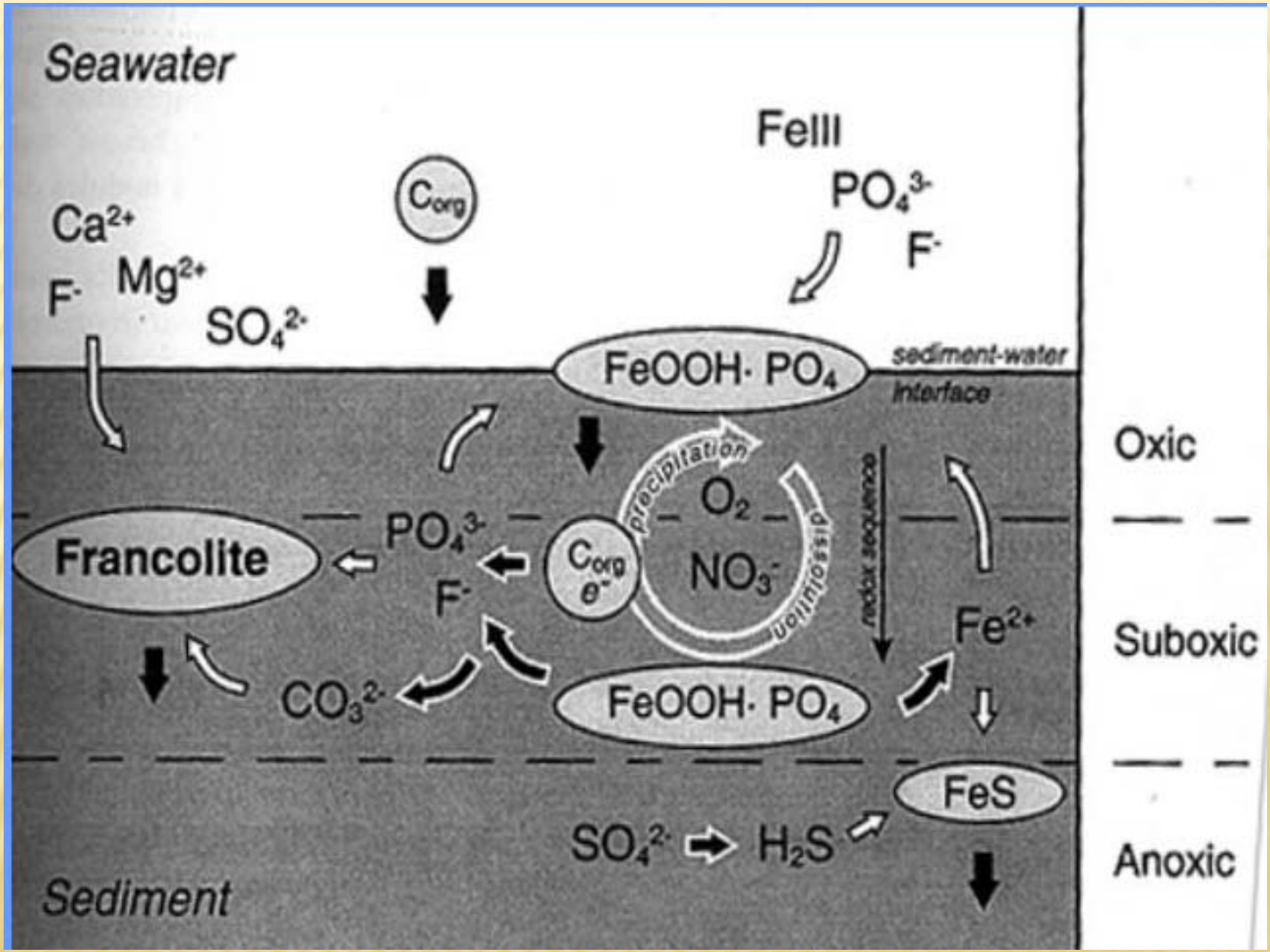
Seawater
FeIII
PO_4^{3-}
F^-
Ca^{2+}
F^-
Mg^{2+}
SO_4^{2-}
C_{org}
$FeOOH \cdot PO_4$
sediment-water interface
Oxic
precipitation
dissolution
redox sequence
O_2
NO_3^-
Francolite
PO_4^{3-}
F^-
C_{org}
θ^-
Fe^{2+}
Suboxic
CO_3^{2-}
$FeOOH \cdot PO_4$
FeS
SO_4^{2-}
H_2S
Anoxic
Sediment

Ancient Phosphorites	Modern/Quat. Phosphorites
• Grainstone phosphorites	Phosphorite nodules
• **Stromatolites (stratiform and columnar Microbial mats)**	Stromatolites are unknown
• A few meters to 100 m thick Phosphorite beds	Scattered on the sea floor
• Both upwelling and non-upwelling regions	Mostly confined to the western margins - **upwelling regions**
• Extensive reworking & **Benthic microbial activity**	**Inorganic processes**

No Modern/Quat. analogs for ancient phosphorites - (Bentor, 1980; Cook, 1994) ??

http://www.ias.ac.in/meetings/annmeet/69am_talks/vprao/img10.html

Stromatolites

Stromatolites are organo-sedimentary deposits produced by sediment trapping, binding and/or precipitation as a result of the growth and metabolc activity of microorganisms, principally Cyanobacteria

(Walter, 1976)

Phosphate Deposits

- Phosphate is mined in Florida (~65 %), North Carolina, Idaho and Utah
- Current potential and past production in Montana and Wyoming
- REE concentrations approach 0.5 %.
- REEs currently are not recovered.
- REEs are part of the waste stream for phosphoric acid production.
- Risks: uranium (radon), selenium

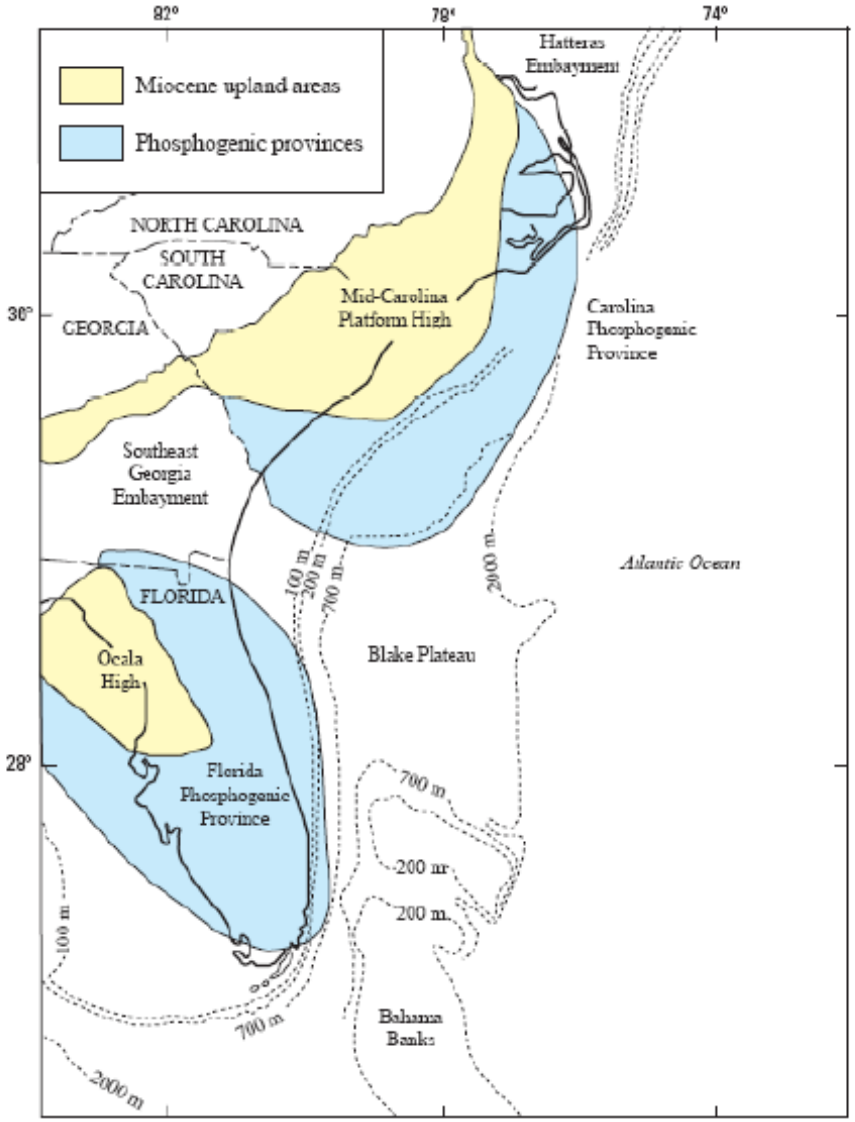

USGS
science for a changing world

MODERN ENVIRONMENTS IN MARINE SEAS

- continental shelves and slopes
  - Peru, Chile, Namibia, South Africa, Baja California
- submarine plateaus, ridges, and banks, such as Blake Plateau off the southeastern US Chatham Rise off New Zealand
- islands, atolls, and within atoll lagoons (guano; Nauru Island)
- mid-plate seamounts

UNCONFORMITY-ASSOCIATED URANIUM DEPOSITS

REE in Uraninites (UO_2)*

Location	Rössing Mine, Namibia	Faraday Mine, Ontario, Canada	Fission Mine, Ontario, Canada	Eldorado Mine, N.W.T., Canada	Collins Bay, Saskatchewan, Canada	Pine Creek Geosyncline, Australia
Geologic Environment	Alaskitic-Granite	Granite Pegmatite	Metamorphic Vein Dike	Hydrothermal Vein Deposit	Unconformity Type Deposit	Unconformity Type Deposit
REE	2.52%	2.89%	1.89%	0.71%	0.13%	0.17%
LREE/HREE	0.41	1.10	1.03	1.15	0.08	0.19

*Fryer, B.J. and Taylor, R.P., 1987, Rare-Earth Element Distributions in Uraninites, Implications of Ore Genesis, Chemical Geology, 63, 101-106. These analyses do not include Y

REE in Uraninite

	Rossing Mine, Namibia	Faraday Mine Ontario, Canada	Fission Mine Ontario, Canada	Eldorado Mine N.W.T., Canada	Collins Bay Saskatchewan. Canada	Pine Creek Geosyncline, Australia
Deposit type	Alaskitic-granite	Granite-pegmatite	Metasomatic vein dyke	Hydrothermal vein deposit	Uncontbrmity-type deposit	Unconformity-type deposit
La (ppm)	1,281	602	652	368	3.9	30
Ce	5,687	8,413	5,692	1,437	50	92
Pr	695	1,317	824	272	14	n.a.
Nd	3,390	7,080	4,374	1,211	83	200
Sm	1,657	2,503	1,454	705	62	214
Eu	n.d.	605	185	298	20	61
Gd	1,849	2,247	1,316	935	202	277
Tb	523	458	301	193	76	83
Dy	4,205	2,869	2,072	958	507	490
Er	2,822	1,766	1,180	389	168	144
Yb	3,060	991	830	347	90	127
TREE (ppm)	**25,163**	**28,856**	**18,872**	**7,115**	**1,276**	**1,741**

Fryer & Taylor (1987)

TYPES OF UNCONFORMITY-ASSOCIATED URANIUM DEPOSITS

- Clay-bound Proterozoic unconformity
- Strata-bound Proterozoic unconformity
- Strata-bound Proterozoic unconformity
- Phanerozoic unconformity-related

Unconformity-associated uranium deposits

- Massive pods, veins and/or disseminated uraninite associated with unconformities between Proterozoic siliciclastic red beds and metamorphic basement that includes graphitic metapelite and radiogenic granite.

Unconformity-associated uranium deposits

- Pitchblende fills extensional features in reactivated fault zones and replaces matrix in sandstone

- One mining district in Canada
  – the Athabasca Basin
  - >30 deposits /prospects
  - most in eastern ¼ of basin
  - produces 1/3 of world's U

World Unconformity-associated U Deposits

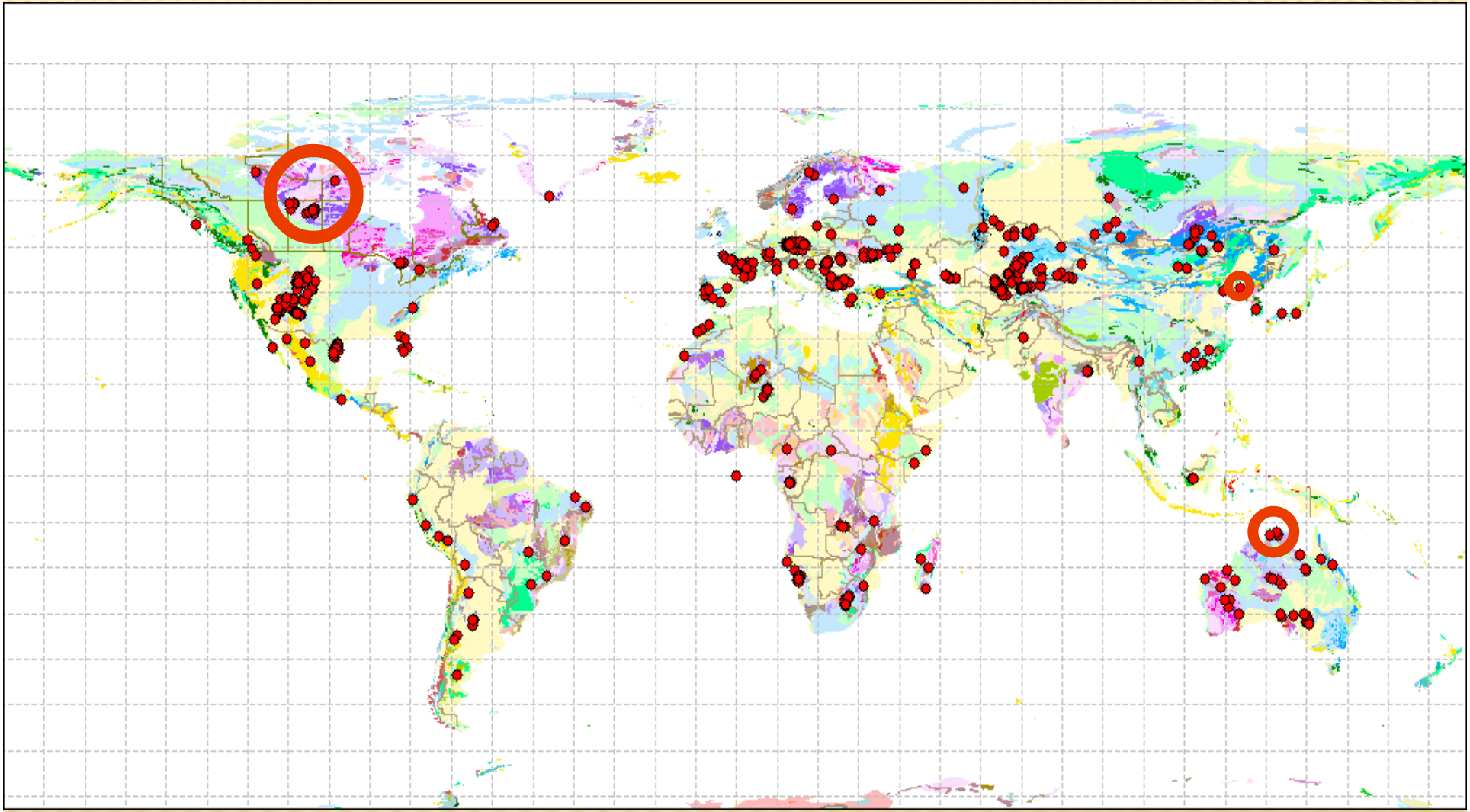

590 Economic / potential U deposits all types >500 Tonnes U @ >0.03% U (IAEA)

One deposit type, two end-member fluid flows

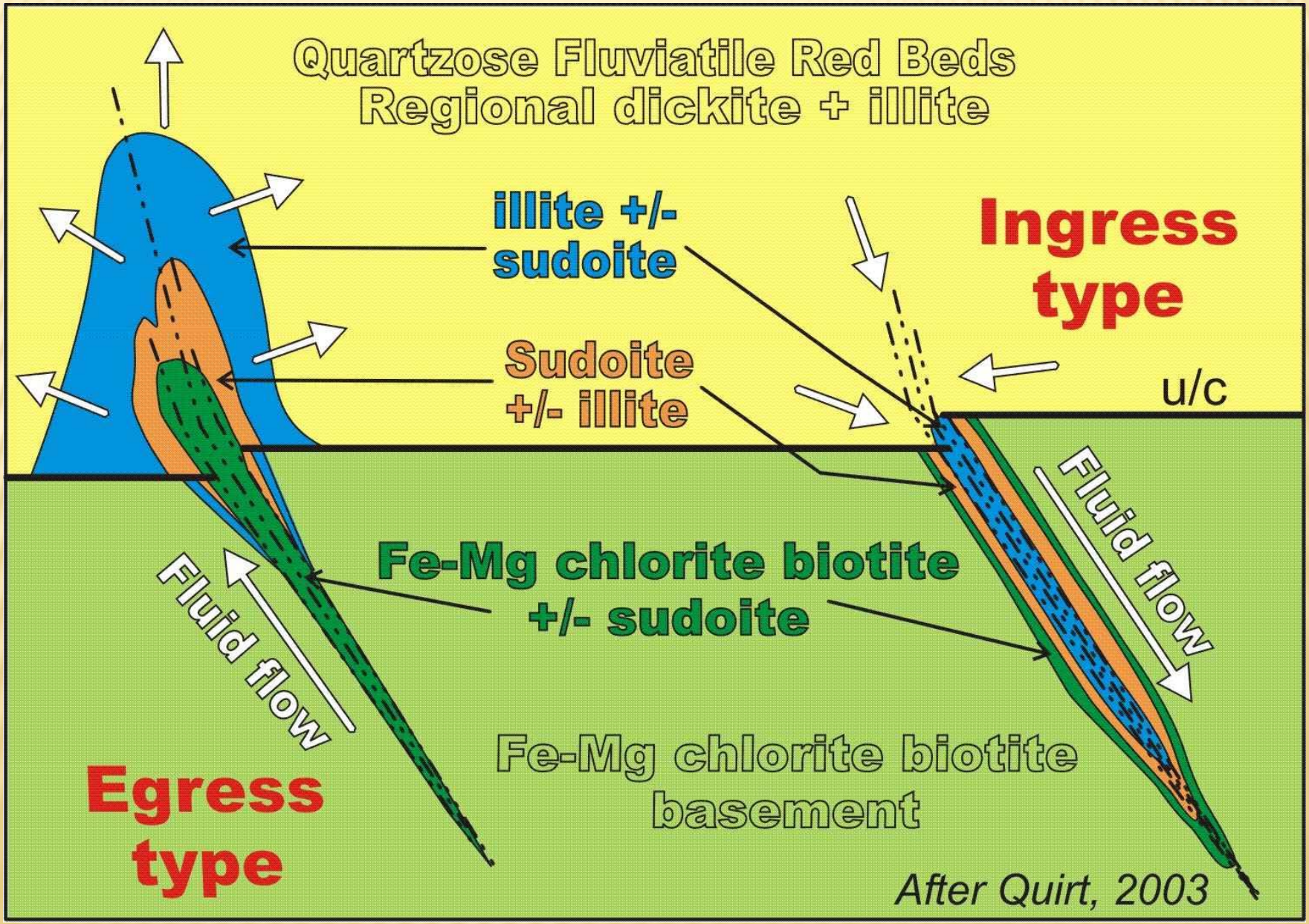

Summary: Unconformity-associated U Deposit Empirical Geological Model

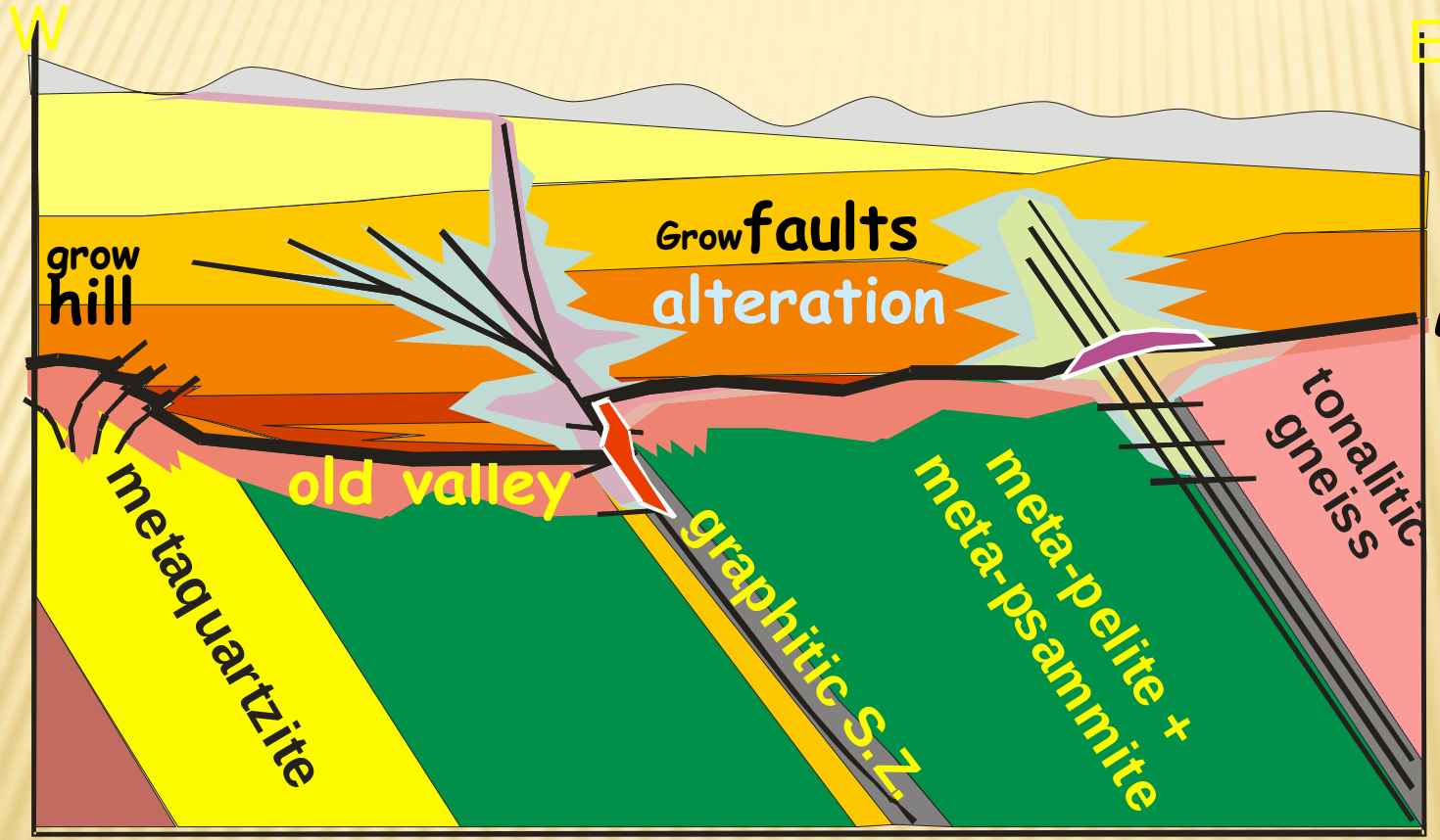

Mono-metallic
- -basement hosted
- -uranium
- -Lower total REE

Poly-metallic
- -"sandstone" hosted
- -U, Ni, Co, Cu, As
- -high total REE

MAJOR UNCONFORMITY TYPE DEPOSITS IN THE WORLD

- Athabasca Basin, Saskatchewan, Canada
- Pine Creek Geosyncline, Northern Territory, Australia

QUARTZ-PEBBLE CONGLOMERATE DEPOSITS

QUARTZ-PEBBLE CONGLOMERATE DEPOSITS

- Upper Archean to Lower Proterozoic age
- consist of detrital ore minerals of uranium and other metals
- pyrite
- Interbedded within siliciclastic sequences containing layers of quartzite and argillite
- mineralized conglomerates.
  - Blind River, uranium and rare earth elements base of the stratigraphic sequence above the unconformity.
  - In the Witwatersrand, uranium in multiple beds dispersed through a thick stratigraphic sequence and is recovered as a by-product of gold production.

QUARTZ-PEBBLE CONGLOMERATE DEPOSITS

- Blind River — Elliot Lake, Ontario, Canada
- Witwatersrand, South Africa

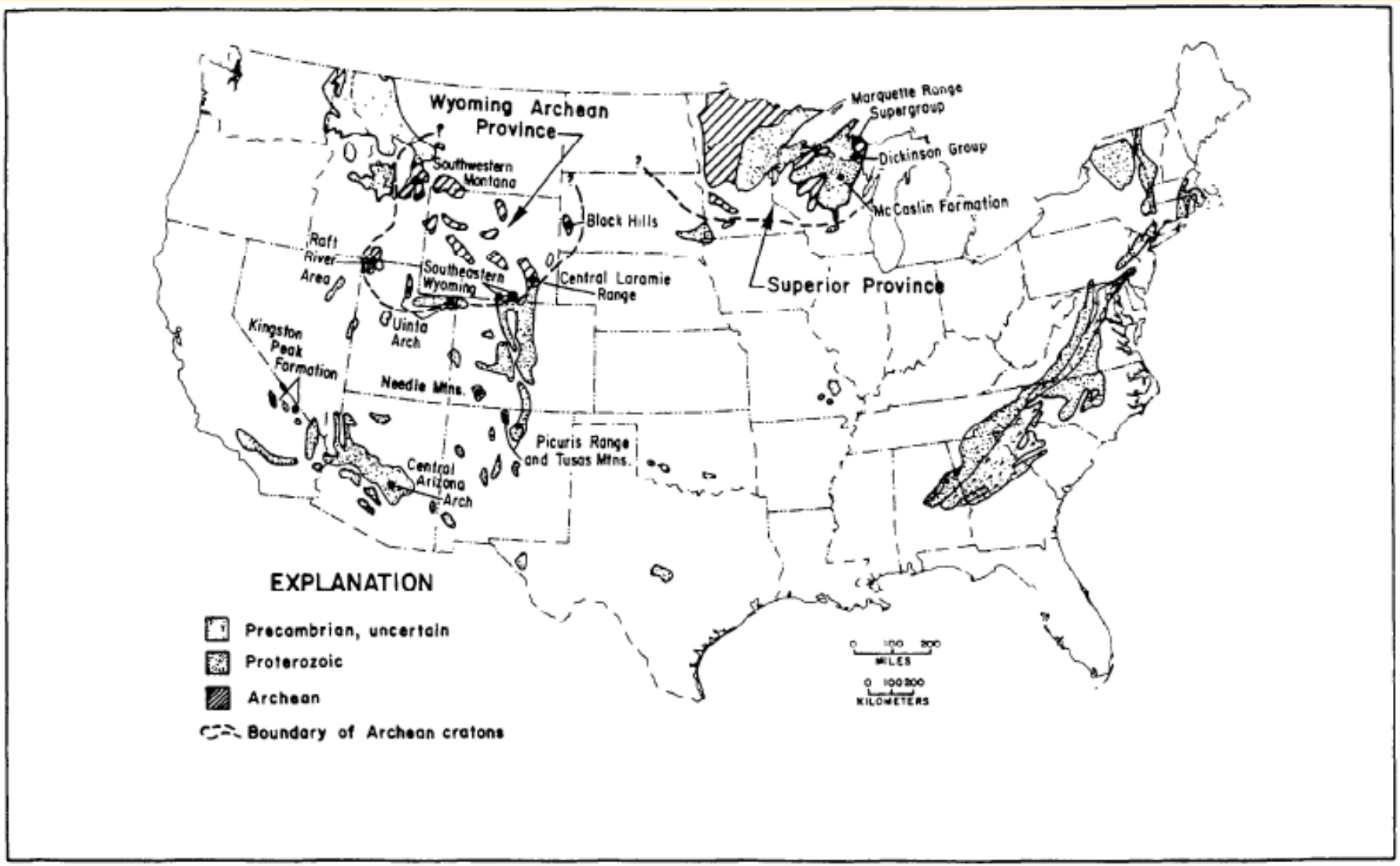

Figure 1. Generalized map of Archean and Proterozoic rocks in the conterminous United States showing specific areas with conglomeratic facies.

SEA FLOOR

- Muds
- Manganese nodules
- Ferromanganese crusts (sea mounts)

Figure 3. Ferromanganese crust coating phosphorite from a Pacfiic seamount.

Figure 1. A cluster of manganese nodules 20 cm in diameter and weighing 25 kg. Photograph courtesy of the German Federal Institute for Geosciences and Natural Resources (BGR).

http://ieeexplore.ieee.org/stamp/stamp.jsp?tp=&arnumber=6107119

SEA FLOOR MUDS

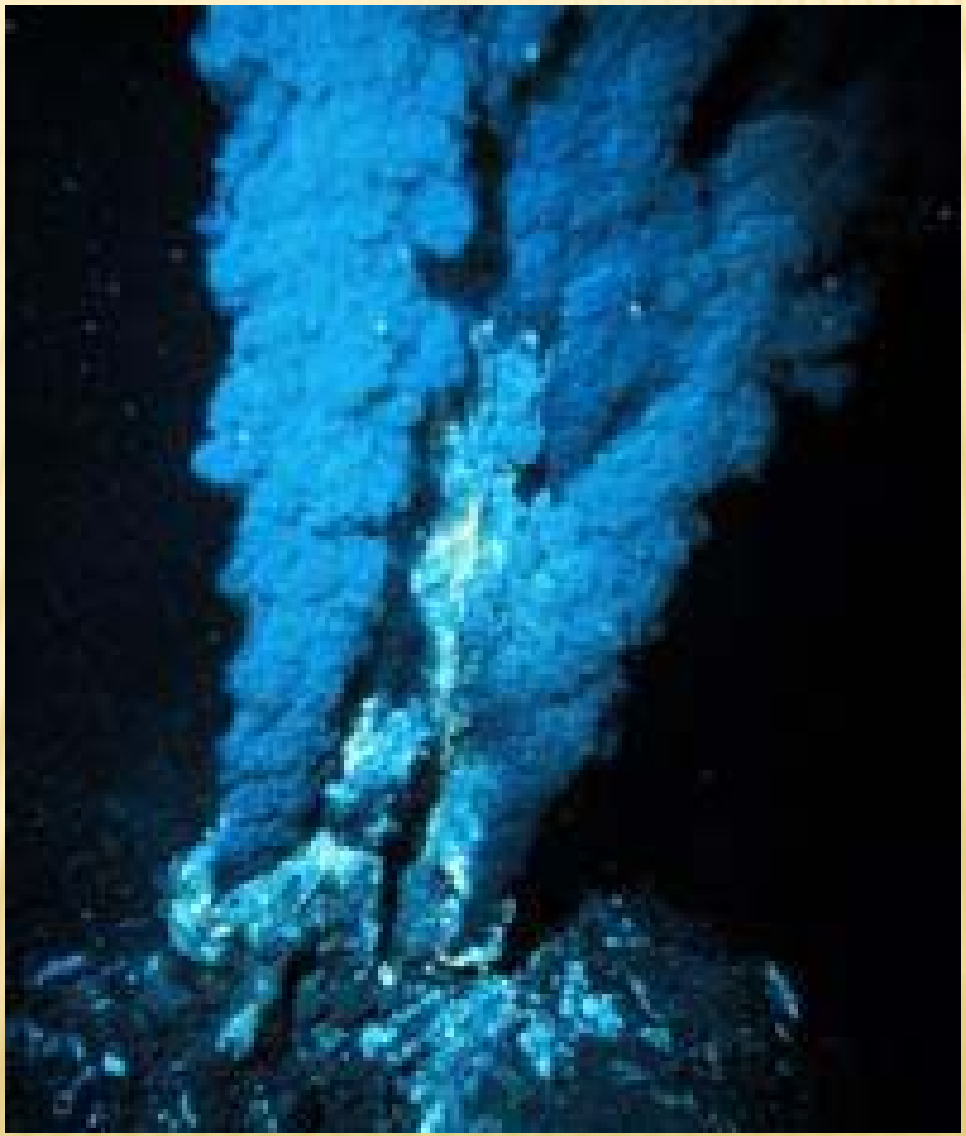

SEA FLOOR MUDS

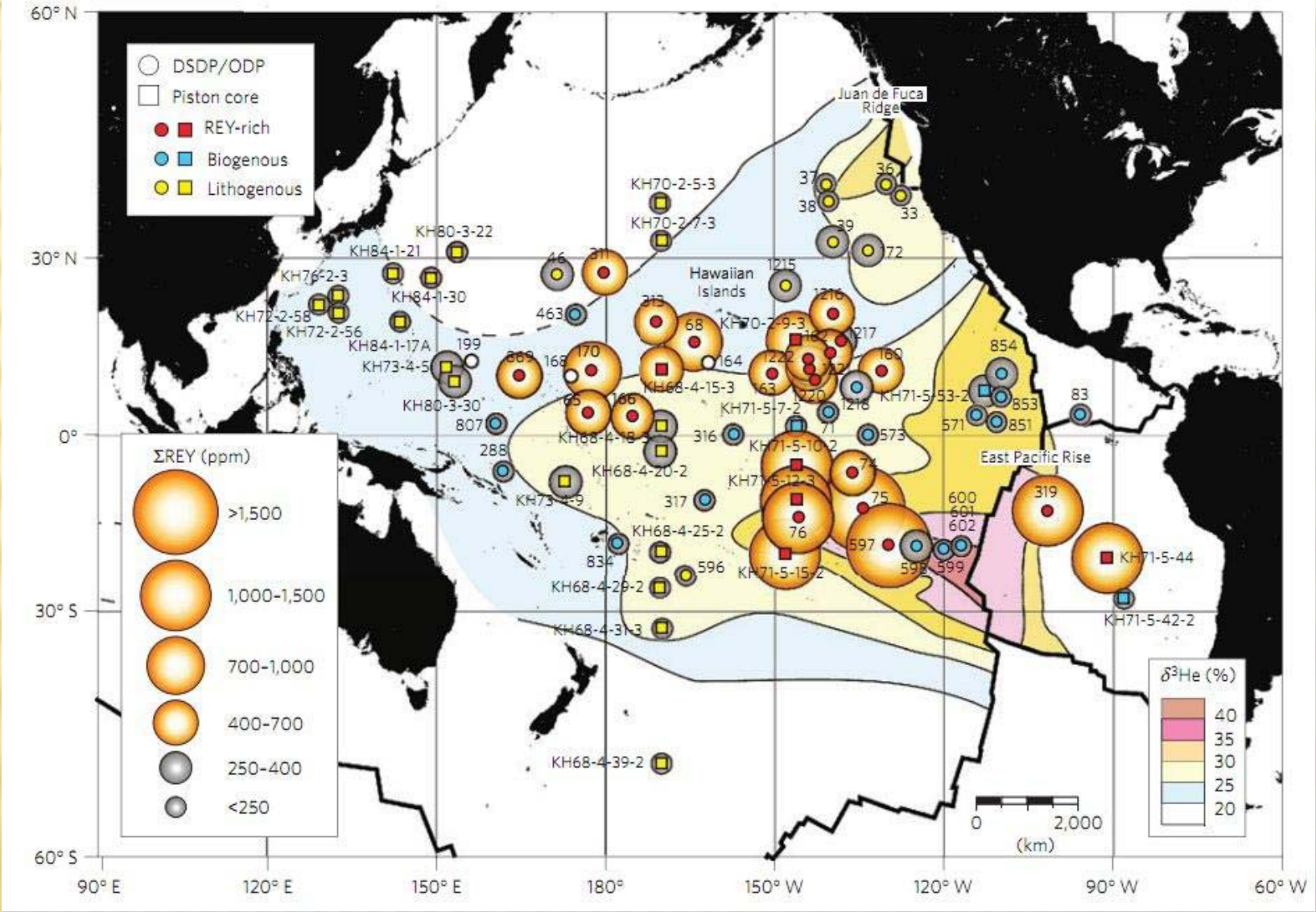

SEA FLOOR MUDS